

---

Theses and Dissertations

---

Fall 2015

# A hydrologic model of Upper Roberts Creek and exploration of the potential impacts of conservation practices

Karl Hoover Brauer  
*University of Iowa*

Copyright 2015 Karl Hoover Brauer

This thesis is available at Iowa Research Online: <https://ir.uiowa.edu/etd/1953>

---

## Recommended Citation

Brauer, Karl Hoover. "A hydrologic model of Upper Roberts Creek and exploration of the potential impacts of conservation practices." MS (Master of Science) thesis, University of Iowa, 2015.  
<https://doi.org/10.17077/etd.elt6os0k>.

---

Follow this and additional works at: <https://ir.uiowa.edu/etd>



Part of the [Civil and Environmental Engineering Commons](#)

A HYDROLOGIC MODEL OF UPPER ROBERTS CREEK AND EXPLORATION OF  
THE POTENTIAL IMPACTS OF CONSERVATION PRACTICES

by

Karl Hoover Brauer

A thesis submitted in partial fulfillment  
of the requirements for the Master of  
Science degree in Civil and Environmental Engineering  
in the Graduate College of  
The University of Iowa

December 2015

Thesis Supervisors: Professor Larry Weber  
Assistant Research Scientist  
Antonio Arenas Amado

Graduate College  
The University of Iowa  
Iowa City, Iowa

CERTIFICATE OF APPROVAL

---

MASTER'S THESIS

---

This is to certify that the Master's thesis of

Karl Hoover Brauer

has been approved by the Examining Committee  
for the thesis requirement for the Master of Science  
degree in Civil and Environmental Engineering at the December 2015  
graduation.

Thesis Committee: \_\_\_\_\_  
Larry Weber, Thesis Supervisor

\_\_\_\_\_  
Antonio Arenas Amado, Thesis Supervisor

\_\_\_\_\_  
A. Allen Bradley, Jr.

## ACKNOWLEDGEMENTS

First and foremost, I would like to thank my advisors Dr. Larry Weber and Dr. Antonio Arenas Amado. Dr. Weber, you were invaluable in your support, advice, and guidance both personally and professionally. Dr. Arenas Amado, your knowledge, patience, and friendship made my success possible.

I would also like to thank the staff and students of IIHR-Hydroscience & Engineering. The friends I have made during my time here have been a constant source of motivation and support. I would especially like to thank Nick Thomas, Chad Drake, Tibebe Ayalew, Daniel Horna-Muñoz, and Kumar Vijay Mishra for the help and encouragement both inside and outside of the office.

Finally, I would like to thank my family. Without your encouragement I would not have started down the path and without your continued support I would not have made it to where I am.

## ABSTRACT

This thesis explores the potential impacts of the implementation of best management practices (BMPs) in Upper Roberts Creek (URC) watershed in northeast Iowa as part of the Iowa Nutrient Research Center (INRC). The INRC was formed in response to the United States Environmental Protection Agency (EPA) requirement that the states along the Mississippi River develop and implement strategies for reducing the nutrient load leaving their states and entering the Gulf of Mexico. The impacts of BMP implementation in URC were evaluated through the use of HydroGeoSphere which was used to develop a three dimensional, coupled surface/subsurface model of the watershed.

The URC model was used to evaluate the hypothetical impacts of the widespread implementation of cover crops on agricultural land within the watershed, the construction of eight Iowa Conservation Enhancement Reserve Program (CREP) style wetlands, and the combination of these two BMPs. Through the comparison of these simplified, hypothetical scenarios to a baseline condition, potential nitrate load reduction estimates were made for each practice or combination of practices. These estimates indicate that neither of the individual practices would be likely to achieve the nitrogen reductions targeted by the EPA and in order to achieve these goals a combination of practices would likely be required.

## PUBLIC ABSTRACT

Excess nutrients in waterways and waterbodies can cause significant problems for the aquatic life which live in them and the people who live nearby. In the Gulf of Mexico each year a large area develops that is devoid of aquatic life, colloquially called the “Dead Zone”. This area is a result of the nutrients which flow from the agricultural Midwest. In an effort to reduce the amount of nutrients flowing out of Iowa into the Gulf of Mexico, this thesis seeks to understand how much of an impact a single watershed plays and what could theoretically be done to ensure more of these nutrients stay on the landscape. The two practices explored in this thesis are the use of cover crops which are grown between fall harvest and spring planting and the construction of new wetlands in the watershed.

## TABLE OF CONTENTS

LIST OF TABLES .....	vii
LIST OF FIGURES .....	ix
CHAPTER 1: INTRODUCTION .....	1
1.1 Motivation and Overview .....	1
1.2 Explanation of Iowa Nutrient Research Center .....	1
1.3 Goals and Objectives .....	2
1.4 Contribution of Thesis .....	4
1.5 The Role of the Upper Roberts Creek Model .....	4
1.6 Chapter Summary .....	4
CHAPTER 2: LITERATURE REVIEW .....	6
2.1 Introduction .....	6
2.2 Hypoxia and Reduction of Nutrient Loading .....	6
2.3 Reduction of Peak Discharges and Improvements in Water Quality .....	8
2.4 Local Water Quality .....	10
2.5 History of Hydrologic Modeling .....	12
2.6 Comparison of Model Types .....	13
2.7 Similar Studies .....	14
2.8 Chapter Summary .....	15
CHAPTER 3: DESCRIPTION OF THE WATERSHED .....	17
3.1 Introduction .....	17
3.2 Hydrology .....	17
3.2.1 Annual Water Cycle .....	18
3.2.2 Monthly Trends in the Water Cycle .....	20
3.2.3 Time of Year for the Occurrence of Peak Discharge .....	21
3.3 Physical Description of the Watershed .....	22
3.3.1 Geology .....	23
3.3.2 Soils .....	24
3.3.3 Topography .....	24
3.3.4 Land Use .....	25
3.3.5 Instrumentation near the Watershed .....	26
3.4 Chapter Summary .....	30
CHAPTER 4: UPPER ROBERTS CREEK MODEL DEVELOPMENT .....	31
4.1 Introduction .....	31
4.2 Selection of HydroGeoSphere and Limitations of the Model .....	31
4.3 Model Construction .....	33
4.3.1 Stream Network and Watershed Boundary .....	33
4.3.2 Surface Grid Development .....	35
4.3.3 Modification of Elevation Data .....	37
4.3.4 Development of Lower Boundary .....	38
4.3.5 Three Dimensional Grid Development .....	39
4.3.6 Model Boundary Conditions .....	40
4.4 Model Properties .....	41
4.4.1 Material Properties .....	41
4.4.2 Overland Flow Properties .....	42

4.4.3	Evapotranspiration Properties .....	43
4.5	Model Inputs .....	46
4.5.1	Rainfall Data .....	46
4.5.2	Potential Evapotranspiration Data.....	46
4.6	Chapter Summary.....	49
CHAPTER 5: UPPER ROBERTS CREEK MODEL CALIBRATION .....		51
5.1	Introduction .....	51
5.2	Development of Initial Conditions.....	51
5.3	Calibration Targets.....	55
5.4	Calibration of Parameters.....	57
5.4.1	Van Genuchten Parameters.....	57
5.4.2	Transpiration Limiting Saturations Parameters .....	62
5.4.3	Tile Layer Hydraulic Conductivity .....	67
5.4.4	Rill Storage .....	73
5.5	Final Parameter Values .....	74
5.6	Chapter Summary.....	76
CHAPTER 6: SIMULATED SCENARIOS.....		78
6.1	Introduction .....	78
6.2	Nitrate Modeling Using HydroGeoSphere.....	79
6.3	Baseline Scenario .....	80
6.4	Cover Crops with No-Till and Strip-Till Practices .....	81
6.5	Nitrate Removal Wetlands .....	86
6.6	Combined Cover Crops with No-Till and Strip-Till Practices and Nitrate Removal Wetlands.....	95
6.7	Chapter Summary.....	99
CHAPTER 7: SUMMARY AND CONCLUSIONS.....		101
7.1	Development of the Upper Roberts Creek Model.....	101
7.2	Calibration of the Upper Roberts Creek Model .....	102
7.3	Use of the Upper Roberts Creek Model .....	103
7.3.1	Simulated Peak Flow and Nitrate Load Reduction from Cover Crops.....	103
7.3.2	Simulated Nitrate Load Reduction from Constructed Wetlands.....	104
7.3.3	Simulated Nitrate Load Reductions from Combined Scenarios.....	104
7.4	Final Remarks .....	105
APPENDIX A: COMPLETE CALIBRATION RESULTS .....		107
APPENDIX B: LEAF AREA INDEX TIME SERIES.....		119
APPENDIX C: ADDITIONAL SCENARIO FIGURES .....		121
REFERENCES .....		132



## LIST OF TABLES

Table 3.1: Soil type composition in URC watershed.....	24
Table 3.2: Land uses in URC watershed by percentage. ....	26
Table 3.3: The periods of record for the instrumentation near URC watershed.....	28
Table 4.1: Summary of ArcGIS functions used to delineate the watershed boundary and the stream network for the URC model. ....	35
Table 4.2: Depths of sublayers in surface soils of three dimensional grid. ....	40
Table 4.3: Soil type and soil properties used in the URC model.....	42
Table 4.4: Land cover types and overland flow properties for the URC model.....	43
Table 4.5: Evaporation parameters for the URC model based on land cover types. ....	44
Table 4.6: Transpiration parameters for the URC model based on land cover types. ....	45
Table 4.7: The accumulated GGD50 and corresponding crop coefficient used to calculate the PET input for the URC model.....	49
Table 5.1: Ratios of hydrologic components used in the calibration and evaluation of the URC model.....	56
Table 5.2: Van Genuchten $\alpha$ and $\beta$ parameters used in the calibration simulations. ....	59
Table 5.3: Results from the calibration of Van Genuchten $\alpha$ and $\beta$ values. ....	62
Table 5.4: TLS values from literature sources.....	64
Table 5.5: TLS value sets used in the calibration process.....	65
Table 5.6: Results from the TLS calibration simulations. ....	66
Table 5.7: Tile spacing and the equivalent hydraulic conductivity used in URC calibration simulations.....	70
Table 5.8: Results from tile spacing simulations.....	71
Table 5.9: Results from the rill storage calibration tests. ....	74
Table 5.10: Final material property values used in URC watershed model. ....	75
Table 5.11: Final overland property values used in URC watershed model. ....	75
Table 5.12: Final evaporation property values used in URC watershed model.....	75
Table 5.13: Final transpiration property values used in URC watershed model. ....	76

Table 6.1: Results from baseline scenario with tile concentration of 25 mg/L. ....	81
Table 6.2: Vertical hydraulic conductivity changes used to account for the increased infiltration from the use of cover crops. ....	83
Table 6.3: Changes to the URC model to account for cover crops and conservation tillage practices. ....	84
Table 6.4: Load reductions from cover crop scenarios. ....	85
Table 6.5: Peak reductions from cover crop scenarios. ....	85
Table 6.6: The individual drainage areas and wetland surface areas for the hypothetical URC wetlands. ....	88
Table 6.7: Storage in the hypothetical wetlands of URC. ....	89
Table 6.8: Wetland efficiency and load reduction calculations for 1 meter wetland scenarios. ....	91
Table 6.9: Wetland efficiency and load reduction calculations for 2 meter wetland scenarios. ....	91
Table 6.10: Calculated annual watershed efficiencies for the wetland scenario simulations. ....	92
Table 6.11: Results from the wetland scenario simulations. ....	93
Table 6.12: Watershed nitrate removal efficiencies for the combined practice scenarios. ....	96
Table 6.13: Results from the combined practice scenarios. ....	97
Table A.1: The calibration ratios and volumetric changes for the Van Genuchten parameter calibration simulations. ....	108
Table A.2: The calibration ratios and volumetric changes for the TLS parameter calibration simulations. ....	111
Table A.3: The calibration ratios and volumetric changes for the different tile layer hydraulic conductivity values tested in the calibration process. ....	114
Table A.4: The calibration ratios and volumetric changes for the two rill storage heights tested. ....	117
Table B.1: LAI for agricultural areas in the URC model. ....	119
Table B.2: LAI for grassy areas in the URC model. ....	120
Table B.3: LAI for forested areas in the URC model. ....	120

## LIST OF FIGURES

Figure 1.1: Conceptual model for the study of URC.....	3
Figure 2.1: The area of the Gulf of Mexico hypoxic zone from 1985 to 2015.....	8
Figure 2.2: Location of gauge used in Roberts Creek monitoring as part of the Big Spring Basin study.....	11
Figure 2.3: The nitrate concentrations and loads at the Roberts Creek gauge from water years 1987 to 1999.....	12
Figure 3.1: URC watershed and its location in Iowa.....	17
Figure 3.2: The location of the Turkey River watershed and the USGS gauge on the Turkey River at Garber, Iowa.....	19
Figure 3.3: Average monthly precipitation for URC.....	20
Figure 3.4: Average monthly discharge for the Turkey River at Garber, Iowa.....	21
Figure 3.5: Annual peak discharge for the Turkey River at Garber, Iowa.....	22
Figure 3.6: Geology of URC.....	23
Figure 3.7: Soil types of URC.....	24
Figure 3.8: Topography of URC watershed.....	25
Figure 3.9: Land uses in URC.....	26
Figure 3.10: Instruments and sensors near URC watershed.....	27
Figure 3.11: Discharge estimates for URC using the Flow Anywhere method.....	29
Figure 4.1: The hydrologic processes HGS is capable of modeling.....	32
Figure 4.2: Watershed outlet point upstream from confluence of URC and Silver Creek.....	34
Figure 4.3: The two dimensional grid developed for the HGS model of URC.....	37
Figure 4.4: The three dimensional grid developed for the HGS model of URC.....	39
Figure 4.5: Rill storage for overland flow.....	43
Figure 4.6: The Nashua, Iowa PET site.....	47
Figure 5.1: Observation wells used in determining the initial conditions for the URC model.....	52

Figure 5.2: USGS groundwater well data for December 15, 2013 to January 15, 2014 .....	53
Figure 5.3: The average depth to the water table for the six observation wells in the URC model .....	54
Figure 5.4: The groundwater response to rainfall in the USGS groundwater well.....	58
Figure 5.5: The groundwater response to rainfall in the IFC groundwater wells.....	58
Figure 5.6: The alternative Van Genuchten $\alpha$ and $\beta$ values which were used for calibration of URC watershed model.....	59
Figure 5.7: The simulated groundwater responses for the original $\alpha$ and $\beta$ values and the three calibration value sets.....	61
Figure 5.8: The simulated groundwater response using $\alpha$ and $\beta$ values from calibration set 3 and the data from the USGS groundwater well.....	61
Figure 5.9: The plot of the water content function with $\theta_{wp}=0.20$ , $\theta_{fc}=0.32$ , $\theta_o=0.76$ , $\theta_{an}=0.90$ , and the transpiration fitting parameter $C_3=2.31 \times 10^{-7}$ .....	64
Figure 5.10: The discharge for 2014 using the TLS values from calibration set 5.....	67
Figure 5.11: Areas within URC watershed requiring drainage tile to achieve full productivity.....	69
Figure 5.12: The discharge for the sixth year of 2014 simulation using the 10 meter tile spacing.....	72
Figure 6.1: Locations of hypothetical conservation practice implementation in URC watershed.....	78
Figure 6.2: Annual cover crop simulation results with tile concentration reduction of 40% to 15mg/L.....	85
Figure 6.3: Cover crop simulation results from June 15 to July 9 with 40% reduction in the tile layer concentration of nitrate.....	86
Figure 6.4: The numbering scheme for the hypothetical wetlands used in the URC model.....	87
Figure 6.5: Annual simulation results from scenario with 2 meter wetland weir and a wetland surface area equal to 2.0% of total wetland drainage area.....	94
Figure 6.6: Simulation results from June 15 to July 9 from scenario with 2 meter wetland weir and a wetland surface area equal to 2.0% of total wetland drainage area.....	94
Figure 6.7: Annual simulation results for scenario with cover crops, 40% reduction in tile layer nitrate concentration, and a wetland surface area equal to 2.0% of the wetland drainage area.....	98

Figure 6.8: Simulation results from June 15 to July 9 for scenario with cover crops, 40% reduction in tile layer nitrate concentration, and a wetland surface area equal to 2.0% of the wetland drainage area. ....	98
Figure C.1: Annual simulation results for scenario with cover crops and 20% reduction in tile nitrate concentration. ....	121
Figure C.2: Simulation results from June 15 to July 9 for scenario with cover crops and 20% reduction in tile nitrate concentration. ....	122
Figure C.3: Annual simulation results for scenario with cover crops and 60% reduction in tile nitrate concentration. ....	122
Figure C.4: Simulation results from June 15 to July 9 for scenario with cover crops and 60% reduction in tile nitrate concentration. ....	123
Figure C.5: Annual simulation results for scenario with 1 meter wetland weir and a surface area equal to 0.5% of the wetland drainage area. ....	123
Figure C.6: Simulation results from June 15 to July 9 for scenario with 1 meter wetland weir and a surface area equal to 0.5% of the wetland drainage area. ....	124
Figure C.7: Annual simulation results for scenario with 1 meter wetland weir and a surface area equal to 2.0% of the wetland drainage area. ....	124
Figure C.8: Simulation results from June 15 to July 9 for scenario with 1 meter wetland weir and a surface area equal to 2.0% of the wetland drainage area. ....	125
Figure C.9: Annual simulation results for scenario with 2 meter wetland weir and a surface area equal to 0.5% of the wetland drainage area. ....	125
Figure C.10: Simulation results from June 15 to July 9 for scenario with 2 meter wetland weir and a surface area equal to 0.5% of the wetland drainage area. ....	126
Figure C.11: Annual simulation results for scenario with cover crops, 20% reduction in tile layer nitrate concentration, and a wetland surface area equal to 0.5% of the wetland drainage area. ....	126
Figure C.12: Simulation results from June 15 to July 9 for scenario with cover crops, 20% reduction in tile layer nitrate concentration, and a wetland surface area equal to 0.5% of the wetland drainage area. ....	127
Figure C.13: Annual simulation results for scenario with cover crops, 20% reduction in tile layer nitrate concentration, and a wetland surface area equal to 2.0% of the wetland drainage area. ....	127
Figure C.14: Simulation results from June 15 to July 9 for scenario with cover crops, 20% reduction in tile layer nitrate concentration, and a wetland surface area equal to 2.0% of the wetland drainage area. ....	128
Figure C.15: Annual simulation results for scenario with cover crops, 40% reduction in tile layer nitrate concentration, and a wetland surface area equal to 0.5% of the wetland drainage area. ....	128

Figure C.16: Simulation results from June 15 to July 9 for scenario with cover crops, 40% reduction in tile layer nitrate concentration, and a wetland surface area equal to 0.5% of the wetland drainage area. ....	129
Figure C.17: Annual simulation results for scenario with cover crops, 60% reduction in tile layer nitrate concentration, and a wetland surface area equal to 0.5% of the wetland drainage area.....	129
Figure C.18: Simulation results from June 15 to July 9 for scenario with cover crops, 60% reduction in tile layer nitrate concentration, and a wetland surface area equal to 0.5% of the wetland drainage area. ....	130
Figure C.19: Annual simulation results for scenario with cover crops, 60% reduction in tile layer nitrate concentration, and a wetland surface area equal to 2.0% of the wetland drainage area.....	130
Figure C.20: Simulation results from June 15 to July 9 for scenario with cover crops, 60% reduction in tile layer nitrate concentration, and a wetland surface area equal to 2.0% of the wetland drainage area. ....	131

## CHAPTER 1: INTRODUCTION

### 1.1 Motivation and Overview

Streams and rivers in the United States are transporting large quantities of nutrients, primarily nitrogen and phosphorus; this problem is most severe in streams and rivers draining Midwestern agricultural land producing corn and soybeans (Malone et al. 2014). The excess of nutrients in the water is not without impacts; communities which rely on rivers and streams for drinking water, such as Des Moines, Iowa, are forced to shoulder the costs of additional water treatment (Des Moines Water Works 2015) while Iowa state parks have issued an annual average of 22 beach warnings over the past 3 years due to toxic algae blooms likely brought on by these nutrients (Iowa Environmental Council 2015). Even greater impacts are felt by ecosystems where these algae blooms sometimes result in hypoxic zones devoid of aquatic life. One of the more notorious hypoxic zones in the United States is in the Gulf of Mexico where the Mississippi River drains into the Gulf (EPA Science Advisory Board 2007). Recognizing the severity of the issue in the Gulf of Mexico, the United States Environmental Protection Agency (EPA), through the Mississippi River/Gulf of Mexico Watershed Nutrient Task Force, issued a Gulf Hypoxia Action Plan in 2008 which required each of the 12 states along the Mississippi River to develop and implement strategies for reducing the nutrient load leaving their state (Mississippi River/Gulf of Mexico Watershed Nutrient Task Force 2008).

### 1.2 Explanation of Iowa Nutrient Research Center

In response to the EPA requirement, a group of agencies consisting of the Iowa Department of Agriculture and Land Stewardship, the Iowa Department of Natural Resources, and the Iowa State University College of Agriculture and Life Sciences developed the Iowa Nutrient Reduction Strategy (Iowa Department of Agriculture and Land Stewardship et al. 2013). This strategy outlines Iowa's plan to reduce the nutrient

discharge from both point sources, such as wastewater treatment plants and manufacturing facilities, and non-point sources, such as farm fields and golf courses. In Iowa, point sources account for 8% of the state nitrogen stream load while non-point sources account for the remaining 92% (Libra et al. 2004). Of these non-point sources, agriculture is the dominant input and output of nitrogen in the state, accounting for over 80% of the total nitrogen (Libra et al. 2004). The total annual nitrogen load from Iowa is approximately 200,000 tons which makes up 20% of the load entering the Gulf of Mexico (Libra et al. 2004).

In addition to the Iowa Nutrient Reduction Strategy, in the spring of 2013 the Iowa Legislature established the Iowa Nutrient Research Center (INRC) to “pursue a science-based approach to nutrient management research” (Iowa Code § 466B.47 2015). The INRC is based at Iowa State University in Ames but research as part of the center is also taking place at the University of Northern Iowa in Cedar Falls and The University of Iowa in Iowa City. INRC projects cover many areas related to nutrients including phosphorus transport in sediments, effectiveness of combined reduction practices, and nutrient trading (Iowa State University College of Agriculture and Life Sciences 2014).

### 1.3 Goals and Objectives

In order to achieve the required nutrient reductions in nutrients in Iowa waters and the Gulf of Mexico, policy makers and officials need to understand the impacts conservation practices may have on those nutrients. Hydrologic models of watersheds can assist those policy makers and officials by allowing for quick and efficient evaluation of the impacts of suggested projects and policy changes. The main goals for this thesis are:

- 1) Develop a hydrologic model for Upper Roberts Creek (URC) which reproduces observed annual water balance ratios.



- 2) Evaluate potential nitrate reduction benefits from the use of cover crops and Conservation Reserve Enhancement Program (CREP)-style wetlands in URC.
- 2) Determine the combinations of conservation strategies and BMPs which may theoretically achieve the Iowa Nutrient Reduction Strategy goal of reducing the nitrogen load from non-point sources by 41%.

The conceptual model for this work is shown in Figure 1.1. There are two main components to this project: the model development and the model application.

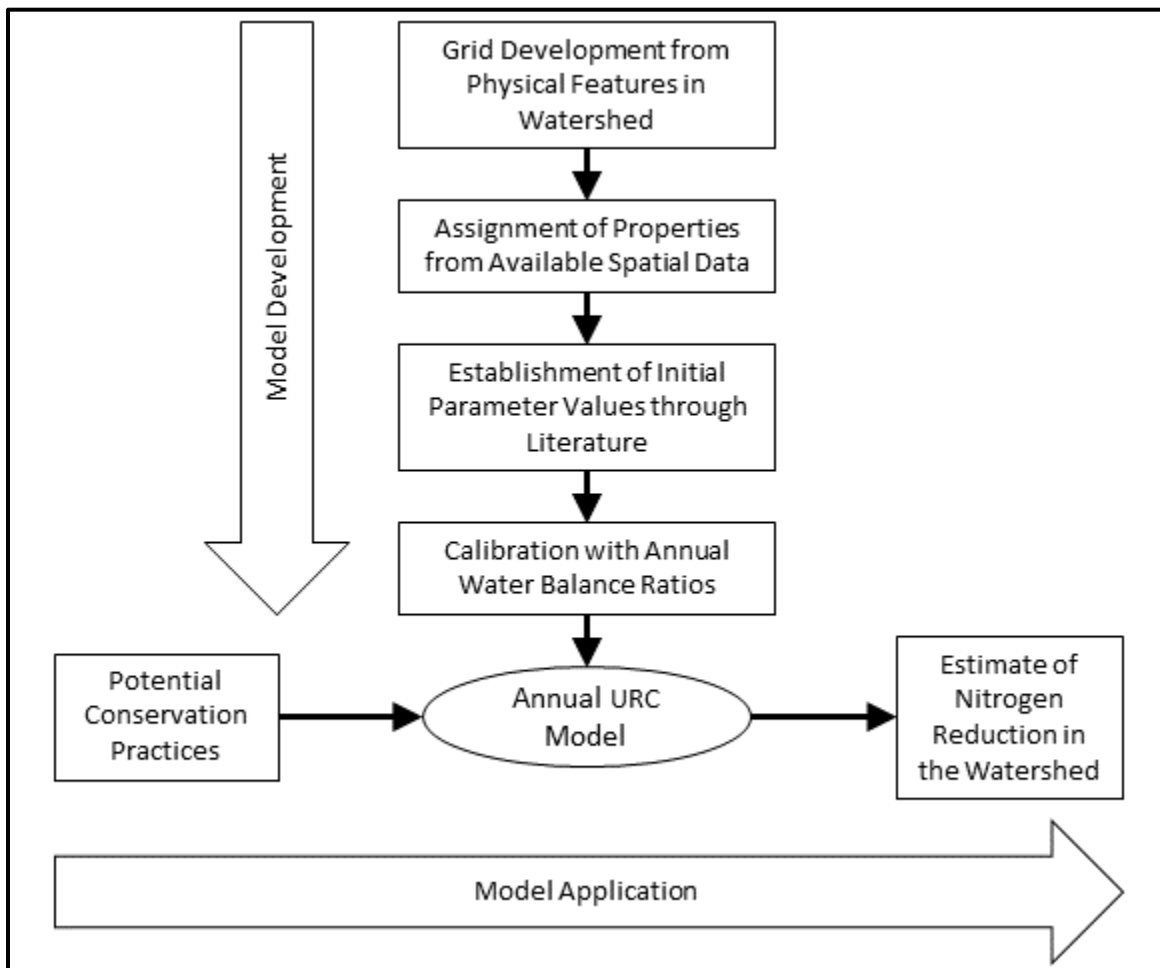


Figure 1.1: Conceptual model for the study of URC. There are two main parts of the study: the model development and the model application.

#### 1.4 Contribution of Thesis

The majority of the work with integrated surface/subsurface models such as the one used in this study has been on small experimental catchments and to a lesser extent, large regional studies; this thesis explores the use of this type of model on a subwatershed scale. Furthermore, it uses this distributed, physically-based model on an ungauged and largely non-instrumented basin which adds complexity to the model development and calibration process. This thesis uses a complex, physically-based model to explore the effectiveness of conservation strategies and BMPs, which is a new application for this type of model.

#### 1.5 The Role of the Upper Roberts Creek Model

This Master's thesis focuses on the development and application of a hydrologic model for URC in northeast Iowa. This research was carried out at IIHR – Hydrosience & Engineering as part of the funding awarded to The University of Iowa by the INRC. Understanding the flow of water is a fundamental step in understanding nutrient travel. The URC model was developed to understand the hydrology of URC watershed within a framework that allowed for the modeling of BMPs. By performing simulations with and without implemented conservation strategies and examining the estimated reduction in nitrate resulting from those strategies, costly field measurements or unnecessary construction can be reduced or avoided.

#### 1.6 Chapter Summary

This chapter outlines the driving factors behind the establishment of the Iowa Nutrient Research Center and the research performed as part of this Master's thesis. In 2008, the EPA issued a report which required the 12 states along the Mississippi River (including Iowa) to develop strategies to reduce the amount of nitrogen and phosphorus which leave their respective states. Out of the Iowa Nutrient Reduction Strategy, was

born the INRC which was tasked with the evaluation of nutrient management practices and other nutrient related research.

This thesis focuses on the development of a hydrologic model of URC as part of the INRC funding provided to IIHR – Hydroscience & Engineering. This model will aid in the understanding of water movement through the watershed and will assist in the comparison of nutrient mitigation strategies.

## CHAPTER 2: LITERATURE REVIEW

### 2.1 Introduction

Flooding and nutrient movement causes damage on local, regional, and national scales. Understanding how to combat flooding and the transport of nutrients can protect Iowa and the nation both financially and ecologically. In the agricultural Midwest, the cost of flooding goes far beyond the infrastructure destroyed. In the 2008 flood it was estimated that the losses in infrastructure and revenue were \$180 million combined (Hicks and Burton 2008). Although this is a large amount of money, the damage to agriculture was even greater at \$2.7 billion (Hicks and Burton 2008). Although no amount of planning and preparation can completely prevent damage caused by flooding, intelligent planning and BMPs can help reduce the extent.

Seemingly small losses of nutrients at the landscape scale can compound and result in large disturbances further downstream. The commercial fishery in the Gulf of Mexico is worth \$650 million annually with sport fishermen contributing another estimated \$1 billion to local economies (Babcock and Kling 2008). Both of these are impacted by changes in the hypoxic zone with larger zones negatively impacting the catches of Brown shrimp, one of the most valuable stocks in the Gulf (Babcock and Kling 2008). Comparatively small investments in properly calibrated hydrologic models can improve our understanding of water flow and can help identify ways to mitigate the damage and reduce associated costs locally and nationally.

### 2.2 Hypoxia and Reduction of Nutrient Loading

Hypoxia is a condition where the dissolved oxygen in the water drops below the level required to support aquatic life; in the Gulf of Mexico that level is 2 mg/L (Mississippi River/Gulf of Mexico Watershed Nutrient Task Force 2008). Over 550 hypoxic zones can be found around the world; two of the more prominent in the United States are the Chesapeake Bay and the Gulf of Mexico (Louisiana Universities Marine

Consortium 2014; Woltemade and Woodward 2008). Of these two, the Gulf of Mexico is the greatest concern for Iowa because runoff and nutrients from Iowa drain into the Gulf of Mexico. Hypoxic conditions are commonly the result of eutrophication brought on by excess nutrients and in the Gulf of Mexico the largest sources of these nutrients are the synthetic and natural fertilizers used in agriculture (Mitsch and Day 2006; Sauer et al. 2008; Woltemade and Woodward 2008).

Since 1985, the Louisiana Universities Marine Consortium has mapped the dissolved oxygen in the Gulf of Mexico to determine the size of the hypoxic, or “dead”, zone. Over the past 5 years, the area of the hypoxic zone has averaged 5,417 square miles which is roughly the size of Connecticut (Louisiana Universities Marine Consortium 2015). In 2008, the Mississippi River/Gulf of Mexico Watershed Nutrient Task Force set a goal of reducing the hypoxic zone to less than 1,931 square miles by 2015.

Unfortunately, this reduction did not materialize and in December 2014 the task force updated the goal to a 20% reduction in nitrogen and phosphorous loading by 2025 and a reduction in hypoxic zone area to less than 1,931 square miles by 2035. Figure 2.1 shows the size of the hypoxic zone for the past 30 years along with the 5 year average and the Mississippi River/Gulf of Mexico Watershed Nutrient Task Force goal.

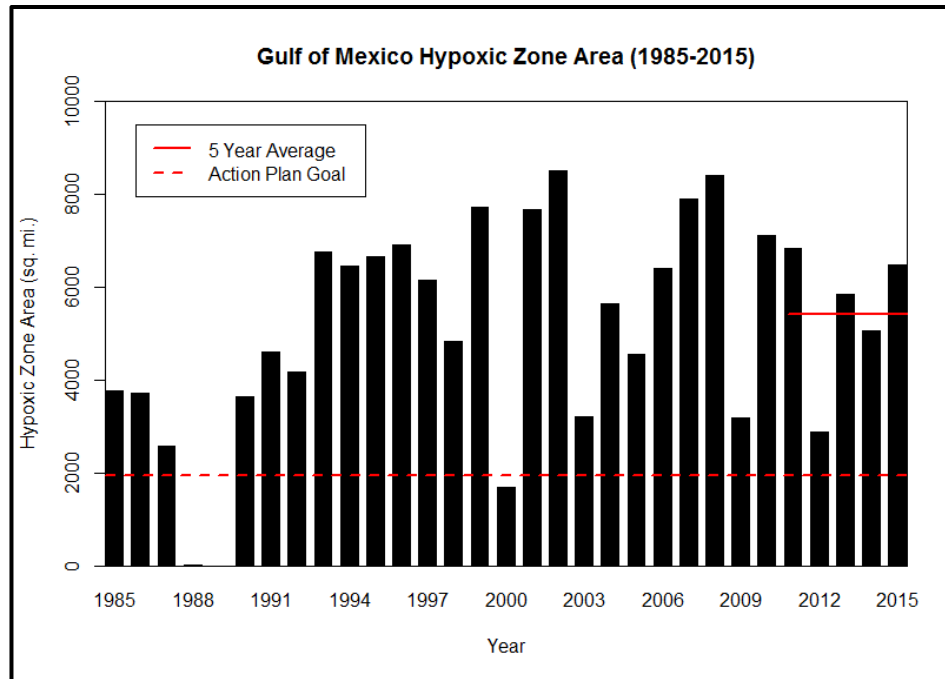


Figure 2.1: The area of the Gulf of Mexico hypoxic zone from 1985 to 2015. The solid red line is the average over the past 5 years and the dashed red line is the goal set by the Mississippi River/Gulf of Mexico Watershed Nutrient Task Force (Louisiana Universities Marine Consortium 2015).

### 2.3 Reduction of Peak Discharges and Improvements in Water Quality

On a local scale, Iowa is impacted more severely by flooding than by eutrophication and hypoxic conditions. Major Midwestern flooding has occurred most recently in 1993, 2008, 2011, and 2013 (Hicks and Burton 2008). The transition from native prairies to agricultural (Babbar-Sebens et al. 2013) and urban environments (Konrad 2003) along with the increasing intensity and frequency of major rainfall events (Min et al. 2011) has increased the intensity, frequency, and associated costs of flooding. Midwestern watersheds are expected to experience 10-20% increases in runoff between 2041 and 2060 which will only add to the existing problem (Melillo et al. 2014). Increasingly, governments and institutions are looking for ways to reduce the impacts of floods and hydrologic modeling allows theories and potential mitigation strategies to be tested before being put into practice, saving both time and money.

One potential tool for reducing peak flows is the reestablishment of wetlands and wetland ecosystems, especially in upland areas. These wetlands store floodwaters which reduces the cumulative runoff from the land surface and downstream flooding (Babbar-Sebens et al. 2013). In addition to increased storage, wetland environments also increase infiltration which reduces total runoff (Babbar-Sebens et al. 2013). Babbar-Sebens et al. (2013) found that the conversion 1.5% of a 162 square mile watershed into 108 wetlands reduced the peak discharge by 6.5 to 19.7% for a storm event. As an additional benefit, wetlands are able to process nitrogen and have been shown to reduce the annual nitrogen export from their drainage area by 32 to 66% (Mitsch and Day 2006)

In addition to wetlands, cover crops can be used as a tool to reduce peak flows and nitrogen export. Cover crops are vegetation planted “to protect and improve soil, crops, or water quality” (Dabney 1998). These crops are grown after the primary crop has been harvested and provide protection for the field from late fall to early spring after which time the cover crop residue provides biomass and organic matter to improve the soil health (Kladivko et al. 2014). Cover crops can be very effective in increasing infiltration, surface roughness, and annual transpiration (Dabney 1998). As a result of these changes to watershed hydrology, cover crops can reduce the peak discharge in a watershed by 7 to 10% (Drake 2014; Klingner 2014).

Much like wetlands, cover crops have an added bonus of reducing nitrogen export. Cover crops take up nitrogen that would otherwise be lost from the landscape through runoff. When the cover crop is tilled into the soil and breaks down, that nitrogen is released back into the soil and can increase the productivity of the field (Varvel et al. 2008). Malone et al. (2014) estimated that the use of cover crops could reduce nitrogen loss by 42.5% in tile drained areas of the Midwest and Kladivko et al. (2014) estimated a 20% reduction in nitrogen load in the Mississippi River if all farms in those same areas implemented cover crops.

## 2.4 Local Water Quality

Water quality is becoming an area of increasing concern in Iowa and around the nation and as a result several studies have been performed looking at different scales of water quality issues around URC.

On a statewide level, Libra et al. (2004) looked at the nutrient balance for all of Iowa from 2000 to 2002. They found that 200,000 tons of nitrogen are discharged from Iowa streams each year with a statewide average yield of 11 lb/ac. 92% of this nitrogen is from non-point sources with agricultural inputs and outputs dominating the balance. Iowa contributes about 20% of the 1 million tons of nitrogen which reaches the Gulf of Mexico each year (Libra et al. 2004).

This same study by Libra et al. (2004) broke down the nutrient balance for larger watersheds in the state. One of these larger watersheds was the Turkey River of which URC is a tributary. In the Turkey River the study estimated the stream load to be 18.1 lb/ac. with an average concentration of 9.0 mg/L and 91.7% of the total stream nitrogen coming from non-point sources (Libra et al. 2004).

Garrett (2012) also examined nitrogen in the Turkey River but the study period was 2004 to 2008. These years were wetter than those explored in the Libra et al. (2004) study and as a result lower concentration and higher load were observed. The average concentration over those years was 6.77 mg/L and the average load was 22.3 lb/ac (Garrett 2012).

On an even more local level, nitrogen in Roberts Creek was monitored from 1987 to 1999 as part of the study of the Big Spring Basin (Liu et al. 2000). The gauge on Roberts Creek drained 70.7 square miles which is approximately twice the size of URC. Figure 2.2 shows the location of the RC02 gauge where measurements were taken along with URC as a reference point.



Over the 13 years of data gathering the average nitrate concentration was 7.37 mg/L and the average load was 10.05 lb/ac (Liu et al. 2000). Figure 2.3 shows the data for each individual water year.

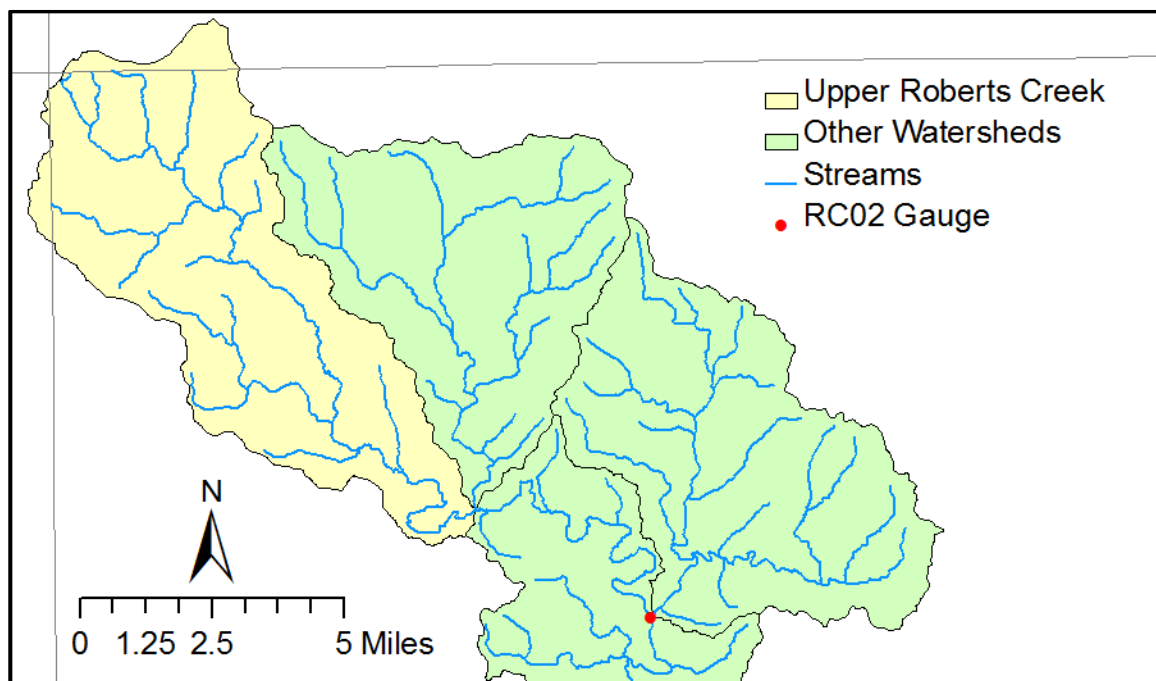


Figure 2.2: Location of gauge used in Roberts Creek monitoring as part of the Big Spring Basin study (Liu et al. 2000). The drainage area of the gauge is approximately twice the drainage area of URC.

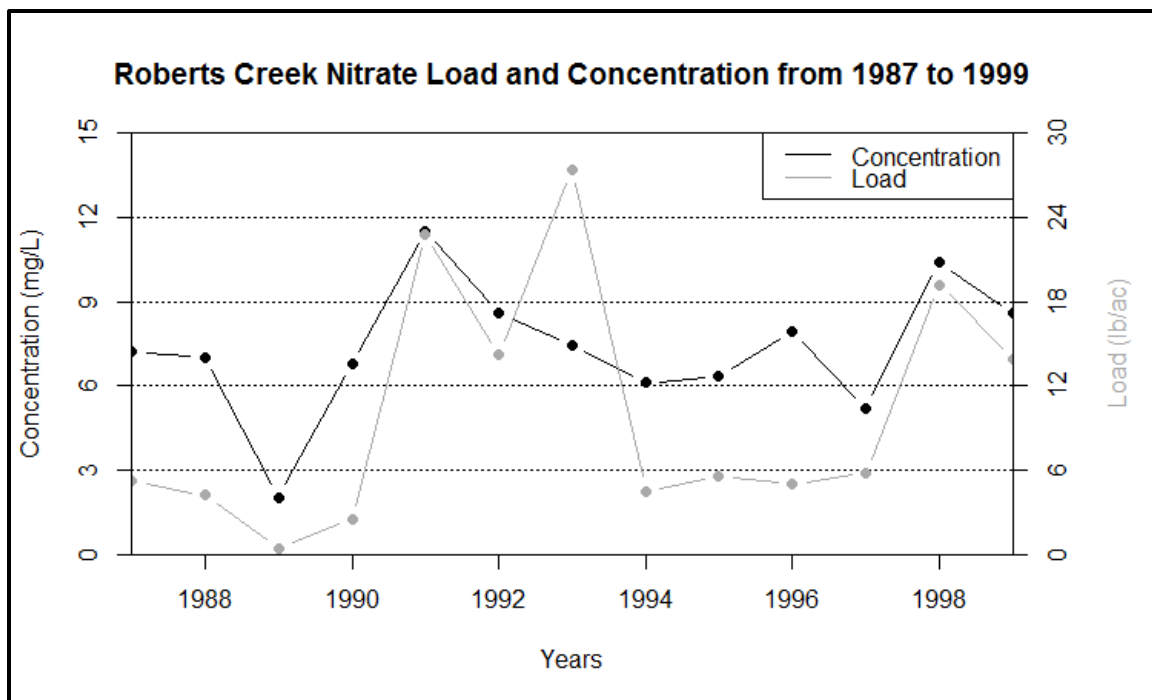


Figure 2.3: The nitrate concentrations and loads at the Roberts Creek gauge from water years 1987 to 1999. The average concentration over this time period was 7.37 mg/L and the average load was 10.05 lb/ac.

## 2.5 History of Hydrologic Modeling

The origins of hydrologic modeling date back to 1850 when Mulvaney developed the rational method. At their most basic, hydrologic models describe how rainwater is distributed within a watershed through evaporation, runoff, or changes in stored water (Penman 1961). Early hydrologic models used mathematical functions to describe single components of the hydrologic cycle using relationships between water, soil, land use, and climate (Singh and Woolhiser 2002). In the 1960s, as computers became more prevalent and powerful, watershed models were developed which could account for virtually all of the hydrologic processes within a watershed (Singh and Woolhiser 2002). Continued increases in computing power have allowed for the development of new hydrologic models and the refinement of older models to produce more accurate simulations and results. Recent advances, including the use of remotely sensed data and geographic

information systems, have continued to push hydrologic modeling capabilities (Singh and Woolhiser 2002).

## 2.6 Comparison of Model Types

There are two main types of numerical models: lumped, conceptual models and distributed, physically-based models (Refsgaard and Knudsen 1996). Lumped, conceptual models use simplified mathematical equations to describe the relationships between the hydrologic components while ignoring the spatial variability in watershed parameters such as vegetation, soil, and topography (Islam 2011). In these models, a single set of parameters is selected for the whole watershed or large sections of it; although in the latter case the model is sometimes referred to as a semi-distributed model (Meselhe et al. 2004). These simplifications can result in reduced simulation times and fewer required model inputs but more hydrometeorological data is required for accurate calibration (Abbott et al. 1986).

On the other hand, distributed, physically-based models are rooted in the principles of physics along with energy and water fluxes (Islam 2011). They take into account the spatial variability of the watershed by assigning characteristics at each point in the grid on which they solve their equations (Leavesley 1994). Distributed, physically-based models do not require as much hydrometeorological data to calibrate the model (Abbott et al. 1986) but they do require significant amounts of localized data for inputs such as soil type, land use, topography, and soil moisture (Refsgaard and Knudsen 1996). As computational power, remote sensing, data collection, and databases have improved, the use of distributed, physically-based models has become more widespread; a trend which will likely continue with further advancements in these areas (Meselhe et al. 2004).

## 2.7 Similar Studies

HydroGeoSphere (HGS) is a widely respected coupled surface/subsurface, distributed, physically-based hydrologic modeling software which has been in use since 2002 (Brunner and Simmons 2012). In HGS, the surface flow is represented in two dimensions through the diffusion wave approximation of the Saint Venant equation and the subsurface flow is modeled in three dimensions through the Richards' equation for unsaturated-saturated subsurface flow (Aquanty Inc. 2013). In fully integrated mode, HGS is capable of partitioning precipitation into all of the main components of the hydrologic cycle (Brunner and Simmons 2012).

HGS is not the only such model with these capabilities which has been developed in recent years. InHM and MODHMS are just two other examples of similar models which have been tested and used in similar roles (Jones et al. 2008). The increasing use of these types of models has meant that they have been used in situations involving similarly sized watersheds, similar land uses, and similar drainage conditions but generally without the overlap of all three. As such there is no direct comparison to the study of URC.

Jones et al. (2008) used the modeling software InHM to develop a surface/subsurface model of Laurel Creek watershed in Ontario, Canada which is roughly 30 mi<sup>2</sup>. This study explored the feasibility of using surface/subsurface, distributed, physically-based hydrologic modeling software in a watershed of this size. Up until this point most of the studies using this kind of software were on small, experimental catchments. Jones et al. (2008) found that the application of these types of models was feasible at this and larger watershed scales.

Li et al. (2008) did explore the use of HGS at a larger scale. In this study, the Duffins Creek watershed in Ontario, Canada was modeled for almost an entire year. Duffins Creek watershed is approximately three times the size of URC watershed. This study showed that physically-based modeling can simulate the observed hydrograph response over several seasons (Li et al. 2008).

Brookfield and Wilson (2015) take the next step in size increase with their HGS model of the Lower Republican River Basin in Kansas which is 4,000 mi<sup>2</sup>. Although this work focuses primarily on modeling groundwater, it occurs in a predominantly agricultural area which makes it similar to URC.

The study by De Schepper et al. (2015) takes place on a very small scale but it explores the modeling of tile drainage which is prevalent in URC and throughout Iowa. De Schepper et al. (2015) found that HGS was capable of simulating tile drainage through a variety of means but that when dealing with large models the most reasonable method for their representation was through the use of “high-conductivity porous medium layer”. This approach was taken when modeling tile drainage in URC.

## 2.8 Chapter Summary

Understanding flooding and nutrient transport on a local level is crucial to understanding how to protect Iowa and the nation. One of the major national environmental concerns is the hypoxic zone in the Gulf of Mexico. This zone exists at least in part because of eutrophication brought on by runoff laden with natural and synthetic fertilizers from Midwestern corn and soybean producing states, including Iowa. On a more local level, devastating floods have hit the Midwest in four of the last 25 years. Major flooding is increasing along with the intensity and frequency of major rainfall events which has been exacerbated by the transition from native land cover to agricultural and urban environments. The reestablishment of wetlands and the use of cover crops on agricultural lands could help reduce the peak flows and nutrient transport.

Hydrologic modeling can help describe the impact conservation practices, such as wetlands and cover crops, may have on peak flow reduction and nutrient transport. Hydrologic modeling began with the rational method in 1850 and by the 1960s had developed into full watershed models. Today, there are two main types of models. Lumped, conceptual models simplify the mathematical equations describing hydrologic

relationships and use a single set of parameters to describe the watershed characteristics. Distributed, physically-based models use equations based on the principles of physics along with energy and water fluxes to describe watershed behavior and account for the spatial variability of the landscape by ascribing parameters for the physical characteristics at each point in the watershed.

HGS is a distributed, physically-based modeling software which has been in use since 2002. This software has been used in many different applications including some similar to this study of URC watershed and it is well respected in the academic community.

## CHAPTER 3: DESCRIPTION OF THE WATERSHED

### 3.1 Introduction

Having a thorough understanding of the hydraulic and physical attributes of the area is important when developing a model to ensure that the model fits within the known environment. This chapter will review what is known about the hydrology near URC watershed as well as the physical characteristics which are so crucial to understanding the behavior of the watershed and developing the model.

### 3.2 Hydrology

URC is located in northeast Iowa near Postville (See Figure 3.1). The watershed is 35.2 mi<sup>2</sup> and is defined by the twelve digit hydrologic unit code (HUC 12) 070600040402. The watershed is primarily in Clayton County but there are also small portions in Fayette and Allamakee Counties. URC drains from the northwest to southeast and flows into Roberts Creek before joining the Turkey River approximately 19.4 miles downstream of the URC watershed outlet.

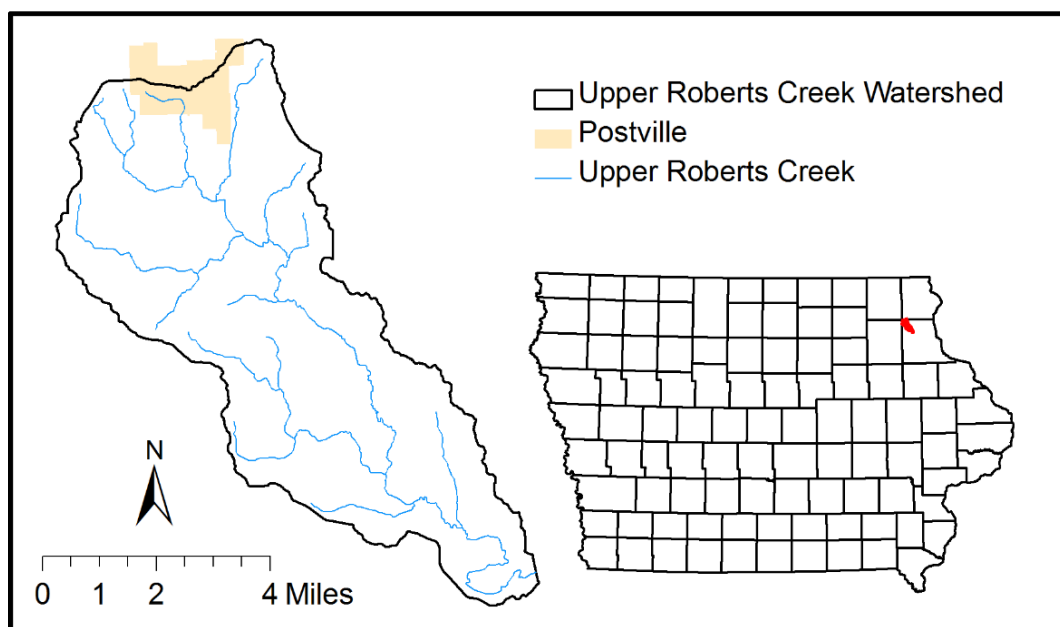


Figure 3.1: URC watershed (HUC 070600040402) and its location in Iowa. The watershed drains 35.2 mi<sup>2</sup>.

### 3.2.1 Annual Water Cycle

The annual water balance consists of one major input, precipitation, and two major outputs, evapotranspiration and discharge. Each of the outputs can be further subdivided, evapotranspiration into evaporation and transpiration and discharge into overland flow (runoff) and baseflow. When considering the annual water cycle, long term trends are often the most informative and from the long term perspective it is often assumed that there is no annual change in the storage of water within the watershed (Calder 1993); this assumption will be made in URC.

Quantifying each of the inputs and outputs in URC is difficult because of a lack of data and instrumentation in the watershed. However, URC is a tributary of the Turkey River and the Turkey River has been studied extensively and is well monitored. The characteristics of the Turkey River and URC are similar in terms of land use and soil type allowing the hydrology of the Turkey River to be used as a proxy for URC in some cases where there is no direct measurement in URC. The nearest United States Geological Survey (USGS) gauge downstream of URC is on the Turkey River at Garber, Iowa (USGS 05412500); this site was used for analysis of flow trends as there was no measurement of URC specifically (Figure 3.2).



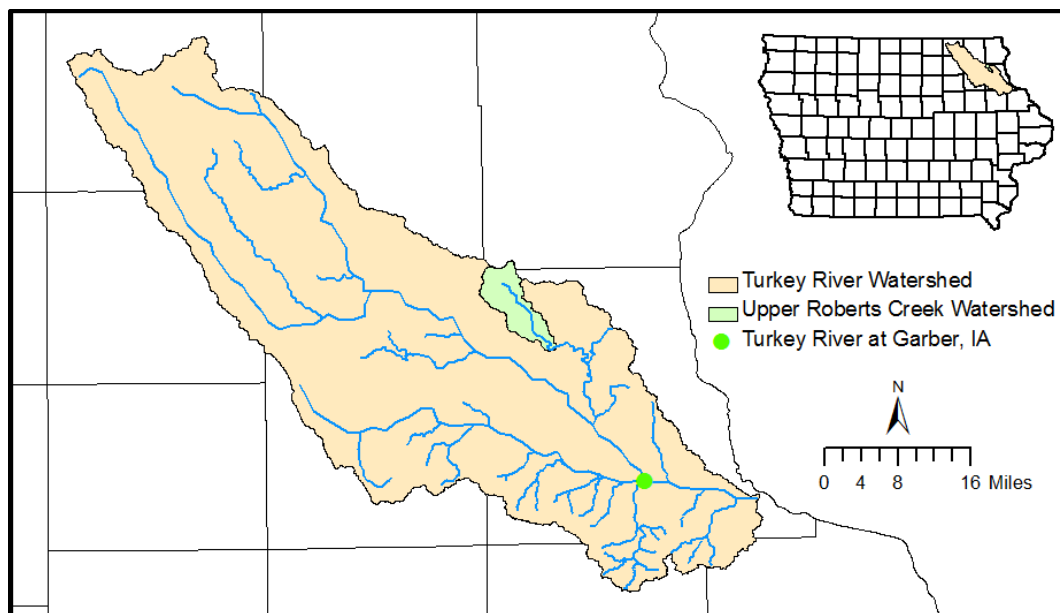


Figure 3.2: The location of the Turkey River watershed and the USGS gauge on the Turkey River at Garber, Iowa (USGS 05412500). URC is within the Turkey River watershed.

The average annual precipitation for URC watershed between 1981 and 2010 was approximately 35.6 inches (PRISM Climate Group and Oregon State University 2004). Although there are no direct measurements of evapotranspiration for URC, both McDonald (1961) and Hoyt (1936) found that the average evapotranspiration to precipitation ratio to be approximately 0.75 (26.7 inches) on the Mississippi River above Keokuk, Iowa. More recently, Schilling et al. (2008) looked at the annual water balance for the Raccoon River near Des Moines, Iowa and found the evapotranspiration to precipitation ratio to be 0.76. Sanford and Selnick (2013) developed a regression using climate and land cover to estimate evapotranspiration across the conterminous United States; based on their equations, the evapotranspiration to precipitation ratio for URC should be 0.65.

The 30% (10.7 inches) of the rainfall that does not leave URC watershed as evapotranspiration exits as discharge either from baseflow or overland flow. Schilling and Libra (2003) looked at the baseflow in Iowa streams and found that in the Turkey

River between 1940 and 2000 baseflow averaged 56.1% of the total discharge. Assuming the same percentage for URC, 6.0 inches of the annual precipitation becomes baseflow and the remaining 4.7 inches makes up the overland flow component. The portion of rainfall that becomes baseflow may not leave the watershed the same year it arrives as precipitation since it takes time to infiltrate into the soil and then exfiltrate into stream network, but under the assumption that there is no change in water stored in the watershed, an average of 6.0 inches of water reaches the stream network and is discharged from the watershed as baseflow each year.

### 3.2.2 Monthly Trends in the Water Cycle

The precipitation for URC varies throughout the year (Figure 3.3). The majority of the rainfall occurs in the spring and summer months with 51.7% falling in the four months of May through August. The precipitation is lowest in December, January, and February and the precipitation that falls this time is often in the form of snow which melts in the spring as the weather warms up.

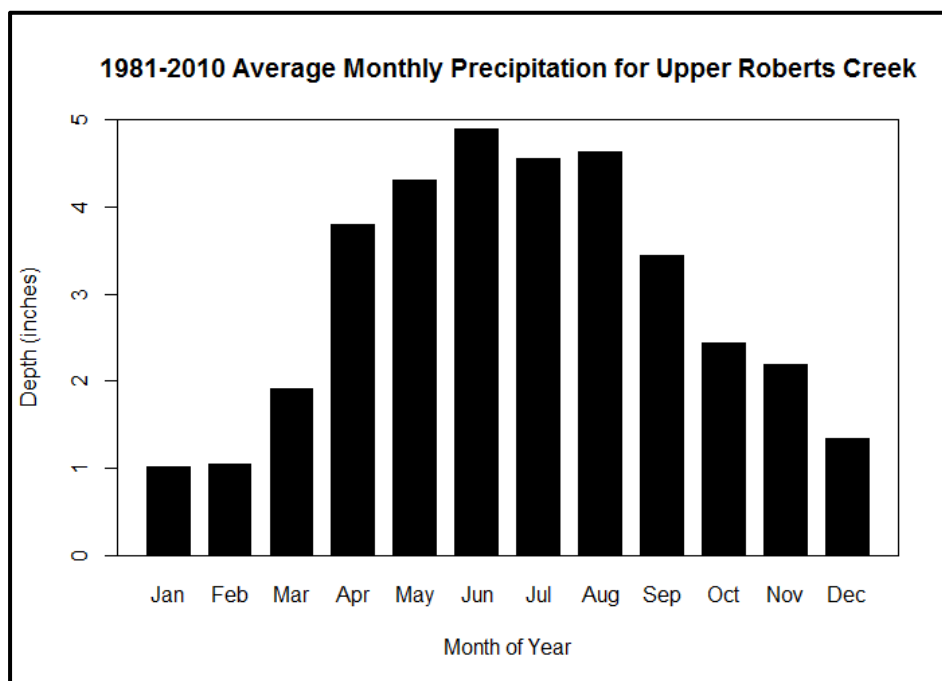


Figure 3.3: Average monthly precipitation for URC. This plot shows the average monthly precipitation (in inches) for URC over the 30 year period from 1981-2010 (PRISM Climate Group and Oregon State University 2004).

The discharge of the Turkey River at Garber, Iowa shows the result of the delayed snowmelt (Figure 3.4). Assuming that the discharge of URC exhibits a similar pattern, it can be seen that the greatest discharge occurs from March through June which is two months earlier than the peak in precipitation. The discharge during these four months makes up 54.4% of the annual volume. Decreases in discharge can be observed in July and August in spite of high rainfall totals; this is likely because of increased evapotranspiration from the elevated summer temperatures and maturation of agricultural crops.

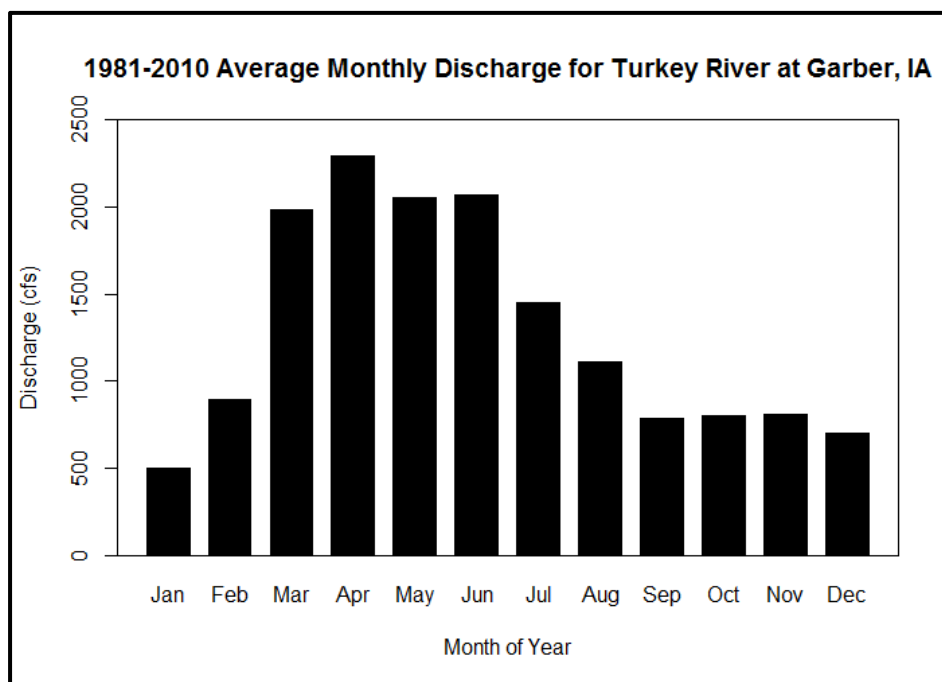


Figure 3.4: Average monthly discharge for the Turkey River at Garber, Iowa (USGS 05412500). This plot shows the average monthly discharge (in cubic feet per second) over the 30 year period from 1981-2010 (United States Geological Survey 2015).

### 3.2.3 Time of Year for the Occurrence of Peak Discharge

On top of knowing when the majority of the discharge occurs, it is also important to know when the peak discharges occur. Figure 3.5 shows the maximum annual peak flows for the USGS site on the Turkey River at Garber, Iowa for the available 96 years of records dating back to 1902. The majority of the annual maximums occur during the

March through June period of high discharge but with higher concentrations on the ends of that period in either March or June. The concentration of annual maximum peak discharge in March is likely the result of snowmelt while the concentration in June is likely the result of heavy rains (Bradley et al. 2015). Also, the June peaks tend to be higher than those in March signifying that they likely occurred during flood events.

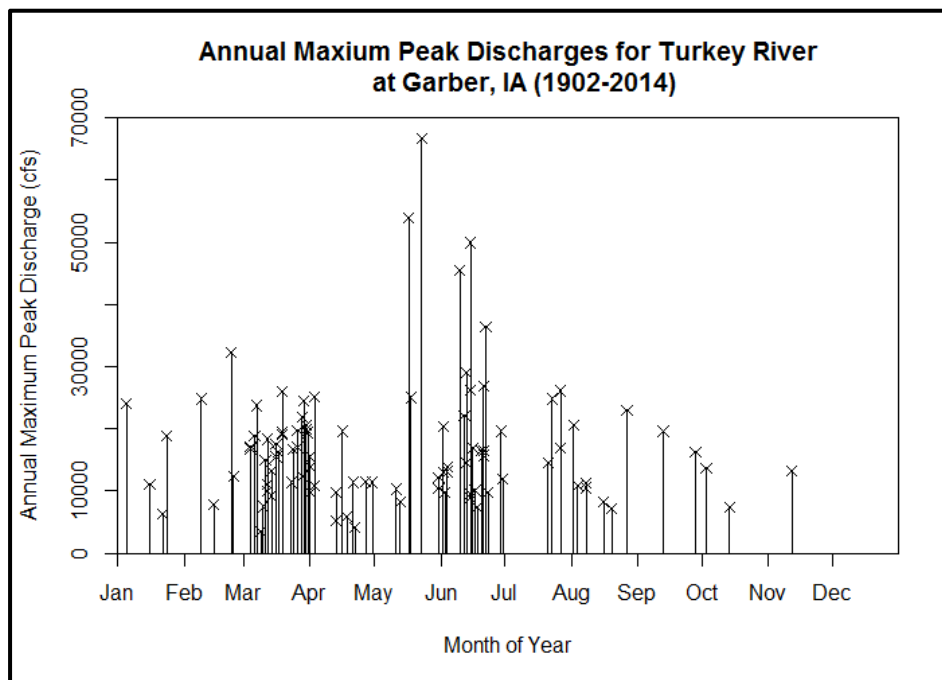


Figure 3.5: Annual peak discharge for the Turkey River at Garber, Iowa (USGS 05412500). This plot shows the annual maximum peak discharge for 96 years of data recorded from 1902 to 2014 (United States Geological Survey 2015).

### 3.3 Physical Description of the Watershed

Although precipitation plays a big role in determining discharge from a watershed, the physical characteristics of the land and soil play an important part as well. This section discusses the physical description of URC and the instrumentation found nearby. These characteristics and the instrumentation near the watershed are crucial for the development of a hydrologic model.

### 3.3.1 Geology

URC is in the Iowa landform region classified as the Paleozoic Plateau (Liu et al. 2000; Rowden et al. 1995). The Paleozoic Plateau is characterized by narrow valleys and an absence of glacial deposits in much of the region. Sedimentary rocks such as shallow limestone and karst formations are common in the region and can result in sinkholes, caves, and springs (Liu et al. 2000; Rowden et al. 1995). The Paleozoic Plateau extends east to the Mississippi River where rock layers resistant to erosion result in bluffs, rapids, and waterfalls (Prior and Iowa Department of Natural Resources 1991).

Figure 3.6 shows the depth to bedrock and the sinkholes and karst formations found in URC watershed. The depth from the surface to the bedrock is fairly shallow through most of the watershed with one deep band along the western edge. The majority of the watershed is made up of karst formations and there have been two sinkholes recorded in the watershed; one in the very southern portion of the watershed and one on the western side.

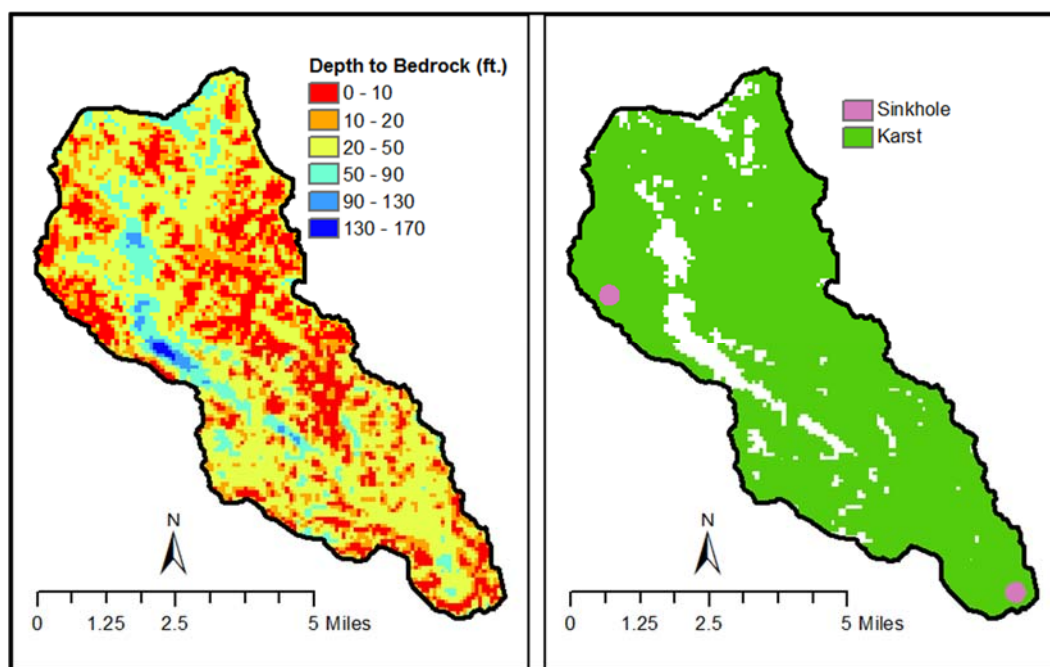


Figure 3.6: Geology of URC. Left: Depth from the surface to the bedrock in feet. Right: Prevalence of karst formations and the two sinkholes in the watershed (Iowa Department of Natural Resources and Iowa Geological Survey 2003-2014).

### 3.3.2 Soils

There are four general soil types found in URC watershed but the overwhelming majority of the watershed is made up of silt loam (Figure 3.7 and Table 3.1). Silt loam is generally considered to be a very good agricultural soil that drains well and has good porosity.

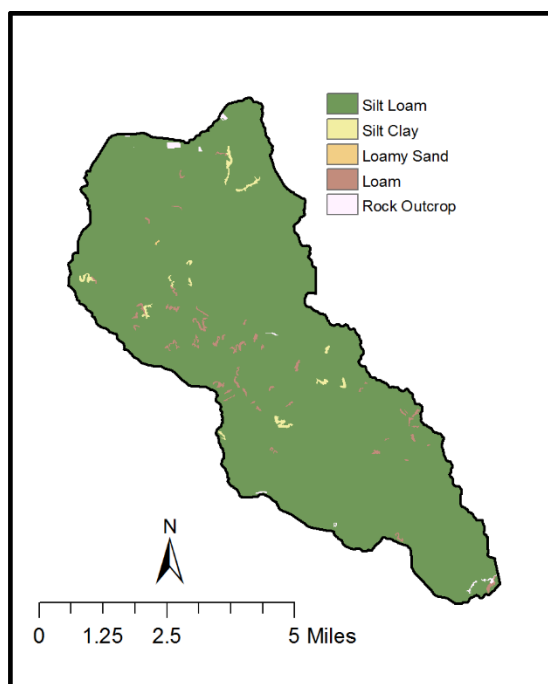


Figure 3.7: Soil types of URC. URC watershed is made up almost entirely of silt loam (Iowa Department of Natural Resources and Iowa Geological Survey 2003-2014).

Table 3.1: Soil type composition in URC watershed.

<b>Soil Type</b>	<b>Percent of Watershed Area</b>
Silt Loam	98.10
Loam	1.03
Silt Clay	0.61
Rock Outcrop	0.26
Loamy Sand	0.01

### 3.3.3 Topography

URC watershed has fairly typical topography for the Paleozoic Plateau. The elevation ranges from 1262 feet above mean sea level (MSL) to 936 feet above MSL

which results in a total relief of 326 feet (Iowa Department of Natural Resources and Iowa Geological Survey 2003-2014). The terrain in the watershed is heavily sloped in some areas, especially near the watershed outlet. The land slopes in the watershed range from near 0% within the stream to a high of 22%. The area-weighted average land slope for the entire watershed is 7.5%. Figure 3.8 shows both the elevation and the land slope for URC.

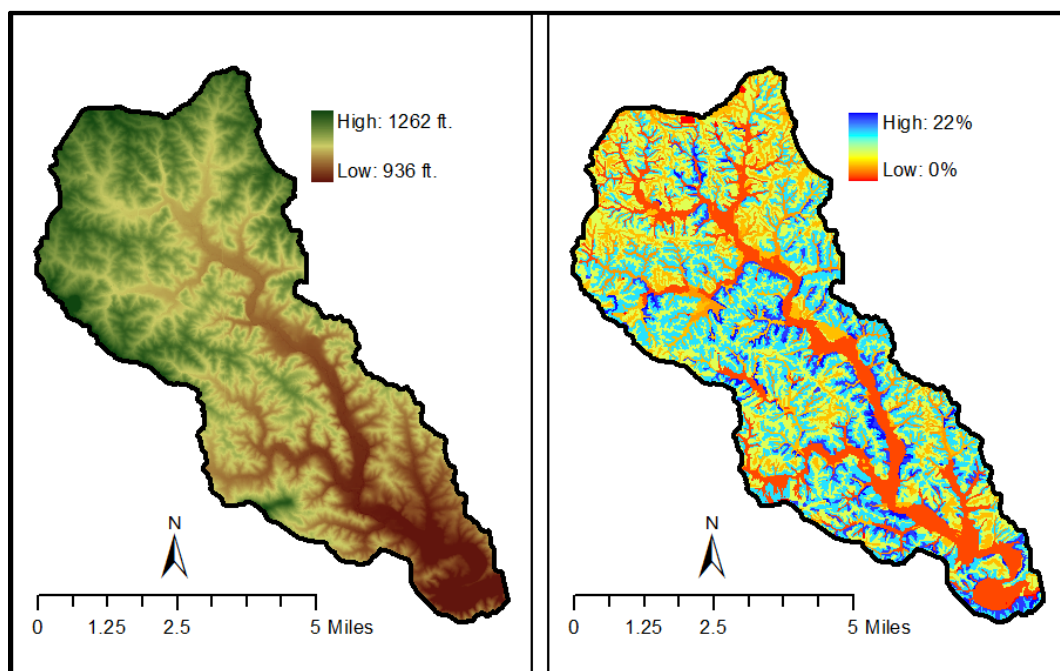


Figure 3.8: Topography of URC watershed. Left: Surface elevation in feet. Right: Percent slope of the land (Iowa Department of Natural Resources and Iowa Geological Survey 2003-2014).

### 3.3.4 Land Use

The primary land use in URC watershed is agriculture. Cultivated crops make up the largest portion of the watershed at 76% and pasture is the third most common land use at 8%; combined, agriculture accounts for 84% of the total land in the watershed (Fry et al. 2011). Five percent of the watershed is developed land and is mostly located in the northern part of the watershed in and around Postville. The proportions of different cultivated crops in the watershed are unknown but in 2014 71.0% of cultivated acreage in

Clayton County was planted with corn, 25.8% with soybeans, and 3.2% with oats (USDA 2014). Figure 3.9 shows the location of each land use and Table 3.2 shows the percentages of total area dedicated to each land use.

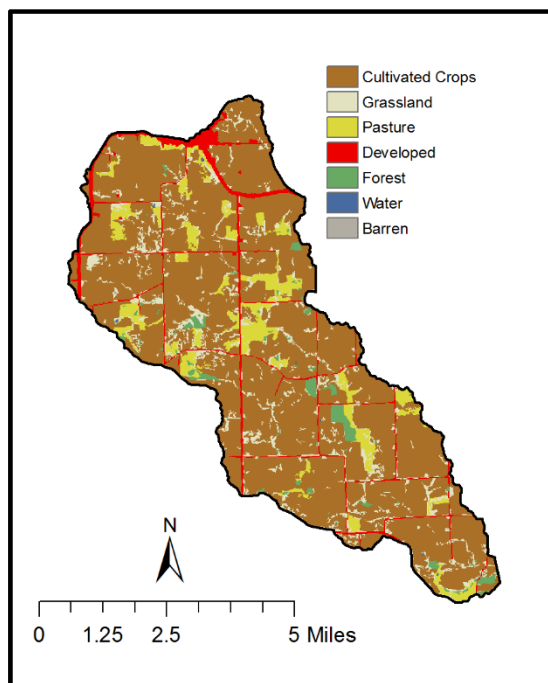


Figure 3.9: Land uses in URC. Cultivated crops make up 76% of the watershed and total agriculture accounts for 84% (Fry et al. 2011).

Table 3.2: Land uses in URC watershed by percentage.

Land Use	Percent of Watershed Area
Cultivated Crops	75.93
Grassland	8.50
Pasture	8.15
Developed	5.24
Forest	2.11
Water	0.05
Barren	0.03

### 3.3.5 Instrumentation near the Watershed

There are no instruments in URC watershed to measure streamflow, precipitation, or current conditions but there are some instruments nearby which can be used to



approximate what is occurring in URC (Figure 3.10). Two of the instruments near the watershed are currently out of service: a USGS Groundwater Well near Eldorado, Iowa (USGS 430203091501201) about 10 miles away which reported the depth from the surface to the water table and a soil moisture sensor (NASA 0033) which was in place for the IFloodS experiment. The instruments currently in operation are the Iowa Flood Center (IFC) stream sensor which measures stream height on Roberts Creek near Elkader, Iowa (IFC RBRTSCR01), a USGS stream gauge on the Turkey River at Spillville (USGS 05411600), and a new USGS stream gauge on Otter Creek at Elgin, Iowa (USGS 05411900). The IFC stream sensor is collocated with an IIHR – Hydroscience & Engineering water quality station (IIHR WQS0018).

In addition to these six instruments, there are also five IFC rainfall and soil moisture/temperature gauges located in Otter Creek (IFC RGS0043, IFC RGS0044, IFC RGS0045, IFC RGS0046, IFC RGS0047). These rainfall and soil moisture gauges were installed in the last two years and are all still in operation. Table 3.3 shows the period of record for the eleven nearby instruments and gauges.

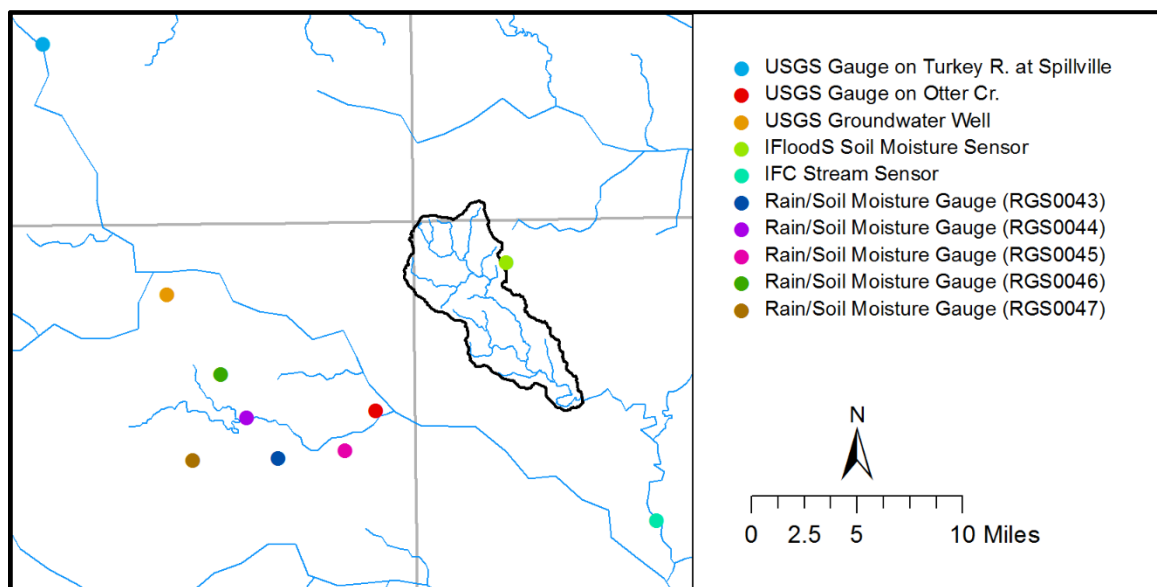


Figure 3.10: Instruments and sensors near URC watershed. None of the sensors are located in the watershed but they are close to it and can offer some insight into the conditions in URC watershed (Iowa Department of Natural Resources and Iowa Geological Survey 2003-2014).

Table 3.3: The periods of record for the instrumentation near URC watershed.

<b>Instrument/Gauge</b>	<b>Period of Record</b>
USGS Gauge on Turkey River at Spillville	4/6/1956 – Current (Missing: 10/1/1973 to 9/30/1977 and 10/1/1991 to 4/5/2010)
USGS Gauge on Otter Creek	3/27/2014 – Current
USGS Groundwater Well near Eldorado (USGS 430203091501201)	1/23/2009 – 10/17/2014
IFloodS Soil Moisture Sensor (NASA 0033)	4/2/2013 – 7/16/2013
IFC Stream Sensor on Roberts Creek	12/14/2011 – Current
IIHR Water Quality Station on Roberts Creek	2/16/2015 – Current
IFC Rain/Soil Moisture Gauge (RGS0043; renamed RGS0027 in 2015)	5/15/2014 – Current
IFC Rain/Soil Moisture Gauge (RGS0044)	5/15/2014 – Current
IFC Rain/Soil Moisture Gauge (RGS0045)	4/19/2014 – Current
IFC Rain/Soil Moisture Gauge (RGS0046)	9/25/2014 – Current
IFC Rain/Soil Moisture Gauge (RGS0047)	5/15/2014 – Current

The nearby USGS stream gauges provide an opportunity to estimate the daily mean discharge for URC using the Flow Anywhere method found in the USGS report *Computing Daily Mean Streamflow at Ungaged Locations in Iowa by using the Flow Anywhere and Flow Duration Curve Transfer Statistical Methods* (Linhart et al. 2012). The Flow Anywhere method uses the known discharge at a gauge location and the drainage areas of the gauge location and the ungauged location to estimate the discharge at the ungauged location. Based on hydrologic and statistical analysis, Iowa has been divided into three different regions and a regional regression equation has been developed for each region. URC is in aggregated region one where the regional regression equation for estimating daily mean streamflow at an ungauged location is:

$$Q_u = 1.06 \frac{DA_u^{1.20}}{DA_r} \times Q_r^{0.979}$$

where,

$Q_u$  = Daily mean streamflow at the ungauged location

$DA_u$  = Drainage area at the ungauged location in the ungauged watershed

$DA_r$  = Drainage area at the reference stream gauge

$Q_r$  = Daily mean streamflow at the reference stream gauge

USGS gauges on the Turkey River at Spillville and on Otter Creek at Elgin were used to estimate the discharge at URC because they are closest in size and proximity to URC. The gauge on the Turkey River at Spillville is approximately 20 miles from URC and has a drainage area of 177 mi<sup>2</sup>. The gauge on Otter Creek is approximately 5 miles away and has a drainage area of 46.2 mi<sup>2</sup>. The Flow Anywhere method is valid from October 1, 1977 to the present. Figure 3.11 shows the estimated discharge for URC for each of the reference gauges and their periods of record.

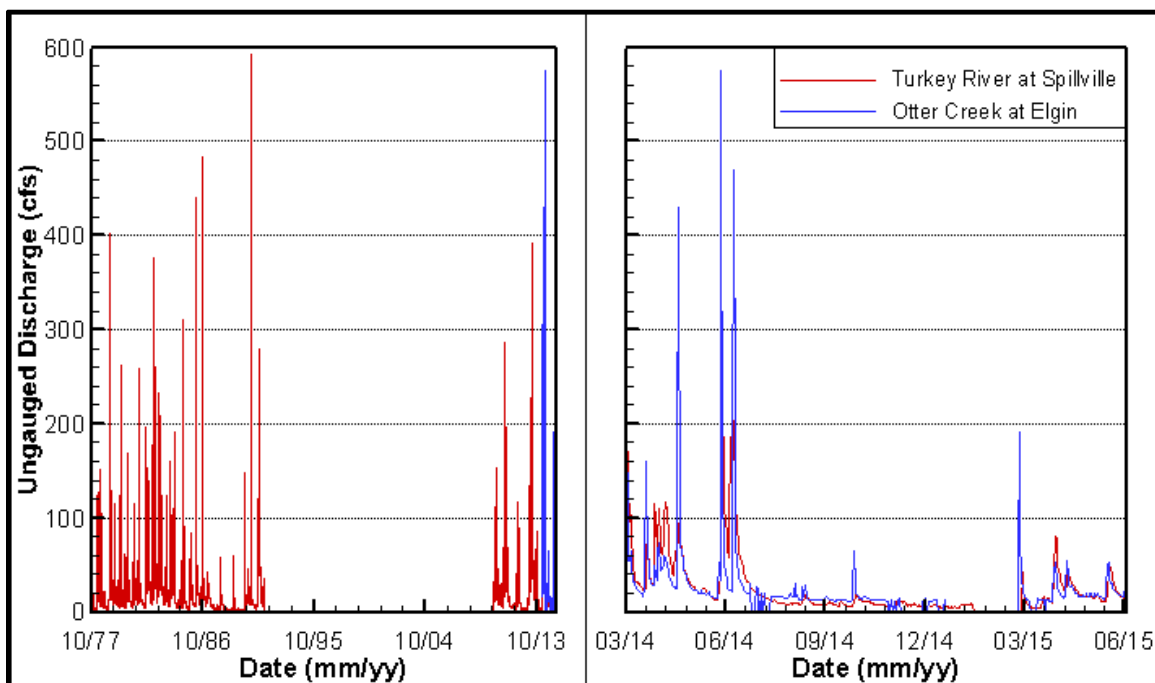


Figure 3.11: Discharge estimates for URC using the Flow Anywhere method. Left: Discharge estimates from 10/1/1977. Right: Discharge estimates from 3/27/2014. The reference gauges used for the estimates were the USGS stream gauges on the Turkey River at Spillville, Iowa (USGS 05411600) and on Otter Creek at Elgin, Iowa (USGS 05411900).

### 3.4 Chapter Summary

This chapter describes some of the hydrologic and physical characteristics of URC watershed. URC watershed (HUC 070600040402) drains 35.2 mi<sup>2</sup> in northeast Iowa. On average, 35.6 inches of rain falls in the watershed each year with the majority between May and August. Due to snowmelt and the lack of vegetation to take up the moisture early in the year, the majority of the annual discharge occurs between March and June. As expected, the annual peak discharges occur during this period as well but are commonly on either end; in March due to snowmelt and in June due to heavy rainfall.

URC watershed is located in the Paleozoic Plateau landform region of Iowa and exhibits many of the attributes characteristic to this region including shallow sedimentary rocks. These rocks are also indicative of karst subsurface formations which are found across most of the watershed. Sinkholes are common in karst areas and two sinkholes have been found in the watershed. The soil in URC watershed is predominantly silt loam which is a very good agricultural soil. The dominant land use in the watershed is agriculture, specifically cultivated crops with approximately 70% of that area planted with corn. There are no instruments or measuring devices for streamflow, precipitation, or current conditions in the watershed but there are eleven nearby instruments and gauges which were used in the model development discussed in the next chapter.

## CHAPTER 4: UPPER ROBERTS CREEK MODEL DEVELOPMENT

### 4.1 Introduction

This chapter summarizes the development of the URC hydrologic model. The URC hydrologic model uses the modeling software HGS which was developed by R. Therrien and E.A. Sudicky at the University of Waterloo in Waterloo, Ontario, Canada (Brunner and Simmons 2012). The general procedure for the development of the model involved the use of ESRI ArcGIS to prepare the geographic information for import into Pointwise Gridgen, Version 15.18. Gridgen was then used to generate an unstructured, triangular grid for the model. The unstructured grid was processed using MATLAB into a format where it could be imported into Grid Builder, Revision 33 where it was further processed into an HGS readable form. These HGS readable grids were combined with the land use and land cover datasets discussed in Chapter 3 to develop a HGS model of URC.

### 4.2 Selection of HydroGeoSphere and Limitations of the Model

HGS can be classified as a mathematical, fully integrated, physically-based, surface/subsurface model (Brunner and Simmons 2012). This means that it uses mathematical expressions to represent the physical processes observed in the natural environment. Those mathematical expressions are based on physical parameters which can be measured in nature. Unlike in lumped parameter models, parameters in physically-based models these are not grouped together as representative values but remain distributed throughout the model as they appear on the landscape. HGS links the surface and the subsurface together forming a complete picture of what is happening in the watershed. Figure 4.1 illustrates the different hydrologic processes HGS is capable of modeling. This type of model especially excels at long term simulations and simulations under unsaturated conditions because it integrates the surface and the subsurface into a single model.

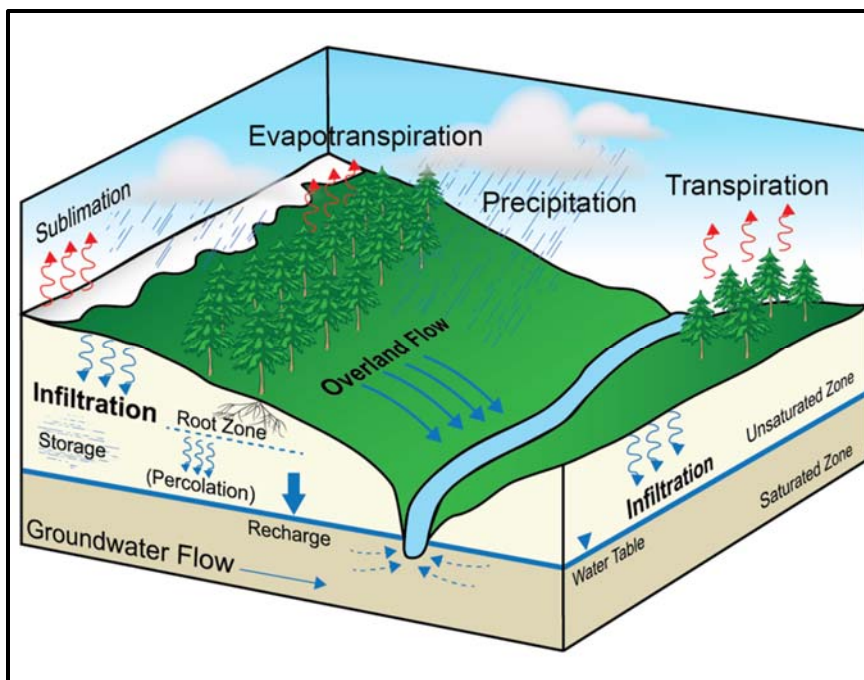


Figure 4.1: The hydrologic processes HGS is capable of modeling. (IIHR - Hydroscience & Engineering/University of Iowa 2014)

Like any modeling software, HGS has both positive and negative aspects that needed to be considered before it is selected to model URC. The most important aspect of HGS is the fully integrated mode in which it simulates water flow. This allows HGS to partition rainfall in a physically based manner and accurately balance all the components of the hydrologic cycle; these components can be easily compared to measured field data. Additionally, the spatial scale of HGS is quite flexible and it has been used at a variety of spatial scales from the field scale verification of the study performed by Abdul (1985) to the larger watershed and regional scales (Goderniaux et al. 2009; Li et al. 2008). It is also very flexible in its capabilities and is able to handle additional aspects such as fractures and mass transport, the latter of which was used to explore the transport of nitrates in URC.

One of the major drawbacks of distributed, physically-based modeling software such as HGS is that they are computationally expensive meaning that simulations can take a considerable amount of time. HGS is no exception but through the use of the high

performance computing systems at the University of Iowa and a parallelized Linux based version of the code, the computation times remained reasonable.

### 4.3 Model Construction

There are two main categories of components used in the construction of the URC model: physical components, such as the land use, soil type, elevation data, and stream network, and input components, such as rainfall and potential evapotranspiration (PET).

#### 4.3.1 Stream Network and Watershed Boundary

The stream network and watershed boundary are key parts of any hydrologic model. To identify and delineate the stream network and the watershed boundary, an initial starting point was needed. The Natural Resource Conservation Service (NRCS) has developed a dataset for all twelve digit hydrologic units in Iowa. Although the accuracy of this dataset was not sufficient for modeling purposes, it provided a starting point and a general view which could be compared to the finished product.

The delineation of the watershed boundary and the stream network use very similar processes. First, the 1 meter digital elevation model (DEM) for the area surrounding URC was obtained from the IFC. Once this data was loaded into ArcGIS, the following commands were used to delineate the watershed: fill sinks, flow direction, flow accumulation, snap to pour point, watershed, and from raster to polygon. A description of each command is shown in Table 4.1. The pour point, or watershed outlet, which was used to delineate the model was about 500 feet upstream of the confluence of URC and Silver Creek (Figure 4.3). This point was selected because it was near a roadway which was higher than the surrounding area and created a outlet as the stream was contained under the overpass. Also of note, when the watershed was converted from a raster to a polygon, the polygon was simplified to smooth the rough edges of the raster which was useful for the generation of the grid.

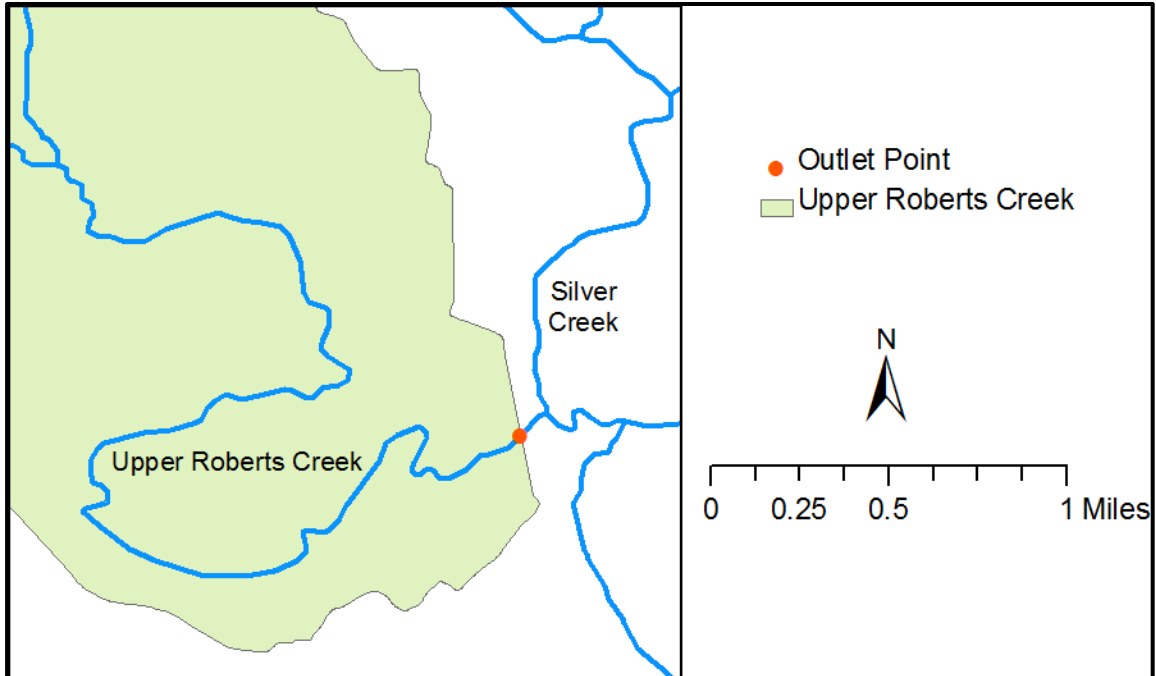


Figure 4.2: Watershed outlet point upstream from confluence of URC and Silver Creek. The outlet point for the watershed boundary was positioned approximately 500 feet upstream from the confluence.

The delineation of the stream network required fewer steps and in most cases the processed data from the watershed delineation could be used again. The commands for the delineation of the stream network were fill sinks, flow direction, and flow accumulation. At this point, the stream network could be identified with a threshold value indicating where streams would form. It was determined that any area greater than 160 acres ( $0.25 \text{ mi}^2$ ) which drained through a single point would be identified as part of the stream network. This identified stream network was then examined against the elevation data and minor manual modifications to the stream network were made to ensure the stream centerline was located in the areas of lowest elevation especially in places where the stream passes under a roadway which often led to anomalies in the delineated stream.



Table 4.1: Summary of ArcGIS functions used to delineate the watershed boundary and the stream network for the URC model.

<b>ArcGIS Function</b>	<b>Used For Watershed Delineation</b>	<b>Used For Stream Network Delineation</b>	<b>Description</b>
Fill Sinks	X	X	Fills in the depressional areas in the DEM.
Flow Direction	X	X	Determines the direction of flow in the filled DEM from higher elevation to lower elevation.
Flow Accumulation	X	X	Determines how much area drains through each cell in the filled raster according to the flow direction raster.
Snap to Pour Point	X		Attaches the pour point or watershed outlet to the nearby point with the highest flow accumulation value.
Watershed	X		Delineates the watershed which drains through the pour point according the flow direction raster.

#### 4.3.2 Surface Grid Development

The grid used in the URC model was an unstructured, triangular grid developed using Pointwise Gridgen Version 15.18. Gridgen automatically developed the grid based on both external and internal parameters which controlled the grid area and the size of the grid cells. Four controlling boundaries were used during the grid generation: the watershed boundary, the stream centerlines, the roadways, and the town limits of Postville, Iowa.

The stream centerlines, roadways, and town limits of Postville were all located within the watershed boundary. These internal boundaries were selected because of their importance to the model and the topography of the watershed. The stream centerline was selected because it is important for grid points to fall within the stream to ensure

continuous flow of water and prevent artificial ponding along the stream. The roadways were used because in agricultural landscapes like those found in Iowa, the roadways are major obstructions controlling and directing the flow of water. The town limits of Postville define the boundary between two distinct areas of the watershed: the agricultural region which makes up the majority of the watershed and the more developed area around Postville.

The grid cell size was controlled by the nodal spacing assigned to the controlling boundaries and the Gridgen growth parameters. The nodal spacing was set at 40 meters along the stream centerline and 200 meters along the watershed boundary. For the roadways and the town limits of Postville the spacing was variable; the nodes near the stream centerline were separated by approximately 40 meters but the spacing increased to a maximum of 200 meters as the distance from the stream centerline increased. The grid which was initially created by Gridgen was improved by relaxing and refining the arrangement of grid cells in each section while visually evaluating the grid for elements which were likely to cause numerical problems due to elongation or groups of eight or more elements sharing single node. The final result is a two dimensional, unstructured, triangular grid with 12,300 nodes and 24,316 elements (Figure 4.3). The average grid cell is 0.93 acres while the maximum and minimum within the grid are 6.07 and 0.04 acres respectively. This grid was exported from Gridgen and run through a MATLAB script developed at IIHR which converted it to a format which could be read by Gridbuilder, Revision 33 and from there it was exported as a HGS readable file.

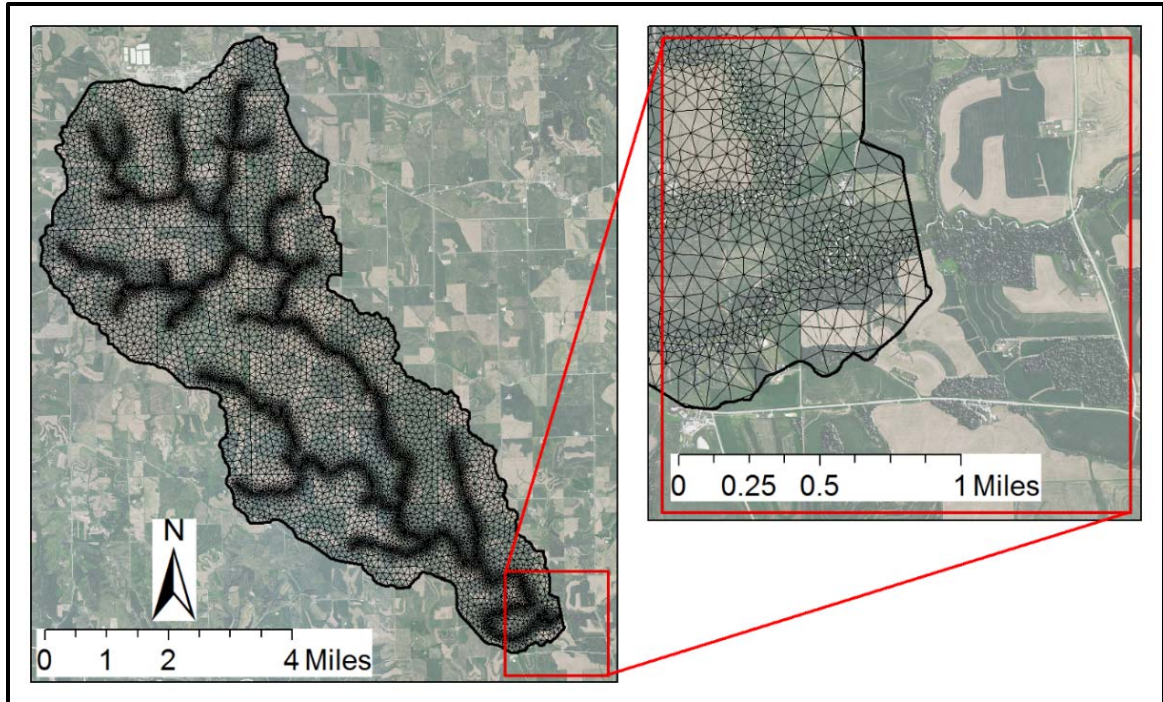


Figure 4.3: The two dimensional grid developed for the HGS model of URC. The grid exhibits higher resolution near the stream centerline.

#### 4.3.3 Modification of Elevation Data

In order to achieve adequate simulation times and performance, the newly created grid was tested using surface simulations, without infiltration, to ensure water was able to flow out the watershed with minimal ponding. For the simulations, a short intense rainfall event was followed by a long drainage period with no evapotranspiration so any ponding locations in the watershed could be identified. These areas of ponding were individually examined to determine if the ponding was realistic or if it was due to a grid artifact. In most cases, the ponding was the result of the grid structure lacking the detail to account for small drainage pathways and when this was the case, the elevation at the location of ponding or a nearby node was modified to ensure drainage similar to the natural environment.

Modifications were also made to the elevations along the stream centerline. Prior to modifications, there was significant ponding within the stream centerline itself because the 40 meter nodal resolution along the stream centerline could not capture all

topographic features. The ponding was especially apparent at bends in the stream and at confluences within the stream network. To remedy this, points spaced every 8 meters along the centerline were extracted along with their elevations. The points for each reach in the stream were run through another MATLAB script which fit a curve through the points. The curves which could be fit were linear, quadratic, or cubic polynomials. In addition to those three curve fits, the stream reaches could be broken into smaller sections within the script and a quadratic polynomial would be fit to each section. Once an appropriate fit was selected, the script would assign a new elevation to each point based on the fitted curves. The points with their new elevations were imported into ArcGIS and a raster was created from the buffered points where each buffered section had the new elevation. The new streamline raster was merged into the existing DEM to create a new elevation raster for the model that would ensure streamflow throughout the watershed.

#### 4.3.4 Development of Lower Boundary

The lower impermeable boundary for the model was defined by the bedrock which was determined from the *Iowa Bedrock Surface Elevation* dataset produced by the Iowa Geological Survey (IGS) (Iowa Department of Natural Resources and Iowa Geological Survey 2003-2014). The bedrock data is in raster format with 110 meter resolution and is based on the well log information found in the IGS GeoSam library and Iowa Department of Transportation well logs.

One of the issues in using such a coarse dataset in the URC model was that in some areas, especially near the stream, the bedrock dataset indicated that the bedrock elevation was higher than the known surface elevation. To prevent this, the lower boundary in the model was defined to be whichever was lower, the bedrock elevation or 2 meters below the surface. The end result was a lower boundary which extended from 2 meters (6.6 feet) below the surface at spots near the stream to a maximum of 53.5 meters (175.6 feet).

### 4.3.5 Three Dimensional Grid Development

With the top and the bottom boundaries for the model established, the full three dimensional grid for the model was created. There are three main layer types which were created within the model: the sub-tile soils, the drainage tile, and the surface soils. Figure 4.4 shows the three dimensional grid.

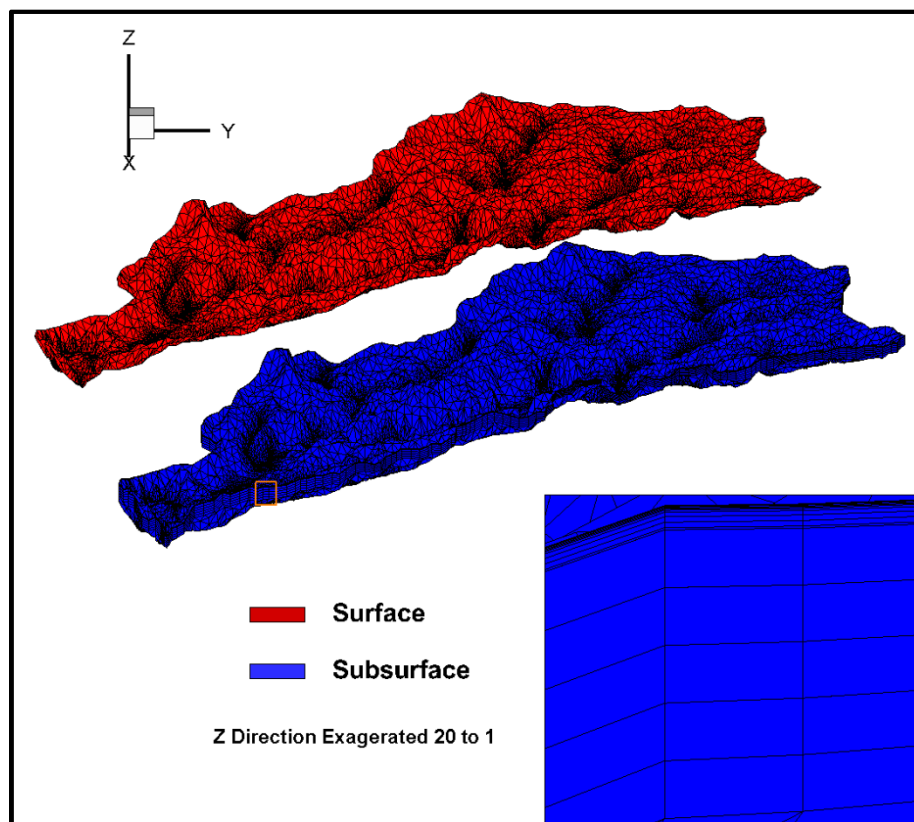


Figure 4.4: The three dimensional grid developed for the HGS model of URC. The grid is more refined near the surface.

From the lower boundary of the model to a depth of 1.1 meters below the surface three evenly spaced nodal sublayers were assigned which created four element layers. Above the sub-tile layers is found a tile layer which is 10 centimeters in depth going from 1.1 meters below the surface to 1.0 meters below the surface. This layer was included to model the behavior of drainage tiles which are very prevalent in the agricultural areas of Iowa. It extends over the whole watershed and modifications to the hydraulic properties

of this layer were used to simulate the behavior of drainage tiles. In simulations where the tile layer was not active, this layer was assigned the same properties as the layers above and below it. The surface soils were modeled from 1.0 meter below the surface to the surface by using eight nodal sublayers. The layers were spaced to ensure a more refined grid near the surface and to match the soil moisture data gathered by the IFC which is measured at 2 inches below the surface, 4 inches below the surface, 8 inches below the surface, and 20 inches below the surface (Table 4.2). As a whole, the three dimensional grid is made up of 15 nodal layers and 14 elemental layers which contain a total of 184,500 nodes and 340,424 elements.

Table 4.2: Depths of sublayers in surface soils of three dimensional grid.

<b>Sublayer Number</b>	<b>Depth to Layer (cm)</b>	<b>Depth to Layer (in)</b>	<b>Approximately IFC Soil Moisture Measurement Depth</b>
1	2.5	0.98	
2	5.0	1.97	X
3	10.0	3.94	X
4	15.0	5.91	
5	20.0	7.87	X
6	30.0	11.81	
7	50.0	19.69	X
8	75.0	29.53	
9	100.0	39.37	

#### 4.3.6 Model Boundary Conditions

The boundary conditions for the model are defined as Neumann specified flux boundary at the surface to apply rainfall and evapotranspiration and a critical depth outflow at the watershed outlet defined from the stream centerline node out two nodes in either direction along the watershed boundary for a total of five critical depth nodes. The remaining boundaries including the bottom and lateral subsurface boundaries were assigned no flow conditions. The surface and subsurface domains are coupled using dual

node surface/subsurface coupling which estimates the domain exchange through differences in head at the overlapping nodes.

#### 4.4 Model Properties

The properties used within the model fall into three main categories: material properties which are applied beneath the surface of the model, overland flow properties which are applied to the surface of the model, and evapotranspiration properties which are applied above the surface, at the surface, or below the surface depending on the component of evapotranspiration. Each of these categories will be discussed in more detail in the following sections.

##### 4.4.1 Material Properties

The material properties are assigned to the three dimensional subsurface elements to simulate the different soil and geologic parameters found within the model. The hydraulic conductivity, porosity, and the Van Genuchten parameters ( $\alpha$  and  $\beta$ ) for saturation-pressure and relative permeability are assigned to the three dimensional elements throughout the model based on the soil type found at the centroid of each element. The soil above and below the tile layer were assigned the properties of the soil type at the surface based on the SSURGO soil data which was gathered from the Iowa Department of Natural Resources and Iowa Geological Survey (2003-2014) website. In simulations that incorporated the impacts of drainage tile, the tile layer elements were assigned separate values which will be discussed in the following chapter. The streambed was assigned a different soil type from what the SSURGO data indicated in order to better represent the expected sandy stream bottom and to ensure connectivity between the stream and the tile layer. The horizontal hydraulic properties associated with each soil type are assigned from the *ROSETTA Class Average Hydraulic Parameters* (Schaap et al. 2001) with the exception of silt loam soil which had been calibrated in previous simulations by Thomas (2015). The hydraulic conductivity was modeled as anisotropic

with the vertical hydraulic conductivity assigned to be one order of magnitude greater the horizontal hydraulic conductivity. This anisotropy was used to account for macropores and preferential pathways for water movement in the soil (De Schepper et al. 2015).

Table 4.3 contains the soil classes found in the model and the corresponding soil properties.

Table 4.3: Soil type and soil properties used in the URC model. These are based on the *ROSETTA Class Average Hydraulic Parameters* (Schaap et al. 2001).

Soil Type	Horizontal Hydraulic Conductivity (m/s)	Porosity	$\alpha$	$\beta$
Silt Loam	$2.11 \times 10^{-6}$	0.439	1.88	3.17
Silt Clay	$1.11 \times 10^{-6}$	0.481	1.62	1.32
Loamy Sand	$4.43 \times 10^{-6}$	0.387	2.67	1.45
Loam	$1.39 \times 10^{-6}$	0.399	1.11	1.47
Rock Outcrop	$1.60 \times 10^{-6}$	0.400	2.70	4.00
Tile	$1.00 \times 10^{-3}$	0.399	3.48	1.75
Stream	$1.20 \times 10^{-3}$	0.440		

#### 4.4.2 Overland Flow Properties

Overland flow properties are assigned to the two dimensional elements on the surface of the model based on the land use at the centroid of each two dimensional element. These properties control the flow of water along the surface and the flow of water into the subsurface; they include Manning roughness coefficients in the  $x$  and  $y$  directions, the rill storage height, and the coupling length between the surface and the subsurface. The rill storage height is the depth of water which must be present on the surface before lateral surface flow is able to occur (Figure 4.5). The land use was assigned based on the 2006 National Land Cover Database (NLCD) and the land cover types were simplified into seven main categories (Fry et al. 2011). The overland flow properties for each land type were assigned based on work by Chow (1959) and Mattocks



and Forbes (2008). Table 4.4 contains the seven land cover types used in the model along with the assigned overland flow properties for each land cover type.

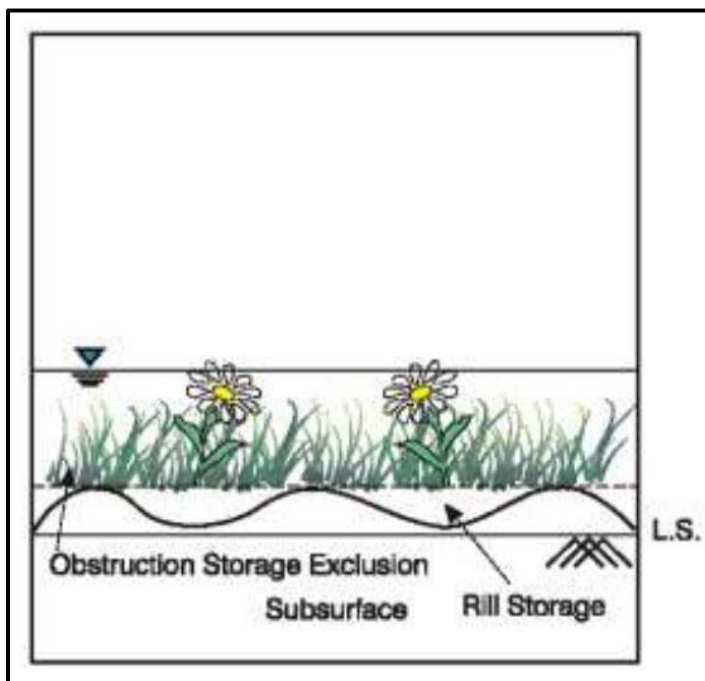


Figure 4.5: Rill storage for overland flow. Rill storage is the amount of storage which must be overcome before lateral surface flow is allowed to occur (Aquanty Inc. 2013).

Table 4.4: Land cover types and overland flow properties for the URC model.

Land Cover Type	X and Y Friction	Rill Storage	Coupling Length
Agricultural	0.07	0.002	0.01
Grass	0.07	0.002	0.01
Forest	0.12	0.002	0.01
Developed	0.10	0.002	0.01
Wet Areas	0.05	0.002	0.01
Stream	0.03	0.002	0.01
Overland (Other)	0.08	0.002	0.01

#### 4.4.3 Evapotranspiration Properties

The evapotranspiration properties in the model are assigned to two dimensional elements at the surface and three dimensional elements below the surface. These properties control how water leaves the model through evapotranspiration based on the

land cover type. Once again, the land cover was based on the 2006 NLCD but instead of using seven main categories, only 5 were used. The areas classified as wet areas or stream were combined into a signal category, the few locations categorized as overland were reassigned as part of the crop group which is the dominant classification in the watershed.

The evaporation component of evapotranspiration is reported as three different types of evaporation based on where the water leaves the model. Canopy evaporation accounts for evaporation from interception storage, surface evaporation is evaporation from a free surface such as a pond or puddle, and subsurface evaporation arises from the subsurface layers close to the surface and can draw water from below the surface up to the specified evaporation depth. The evaporation parameters used to set up the model were selected from literature sources. The evaporation depth, evaporation limiting saturation, and initial interception storage came from Sciuto and Diekkruger (2010) and the evaporation limiting saturations came from Li et al. (2008). The evaporation parameters used in the model are summarized in Table 4.5.

Table 4.5: Evaporation parameters for the URC model based on land cover types.

Land Cover Type	Evaporation Depth	Evaporation Limiting Saturations		Canopy Storage Parameter	Initial Interception Storage
		Minimum	Maximum		
Agricultural	0.2	0.30	0.40	0.00005	0.0
Grass	0.2	0.30	0.40	0.00005	0.0
Forest	0.2	0.30	0.40	0.00005	0.0
Developed	0.2	0.30	0.40	0.00005	0.0
Stream	0.0	0.20	0.32	0.0	0.0

The transpiration portion of evapotranspiration occurs in the subsurface. Root depths are assigned to each land cover type and transpiration is allowed to remove water from the surface down to that depth based on the soil saturation. The initial transpiration

parameter values were selected from literature sources but were later modified through model calibration; the root depth is from Breuer et al. (2003), the transpiration limiting saturation (TLS) values are from Sciuto and Diekkruger (2010), and the transpiration fitting parameters are from Li et al. (2008). The transpiration parameters which are used in the model are summarized in Table 4.6.

Table 4.6: Transpiration parameters for the URC model based on land cover types.

Land Cover Type	Root Depth	TLS Values				Transpiration Fitting Parameters		
		Wilting Point	Field Capacity	Oxic Limit	Anoxic Limit	C1	C2	C3
Agricultural	1.43	0.30	0.40	0.85	0.97	0.31	0.2	$2.31 \times 10^{-7}$
Grass	0.93	0.30	0.40	0.85	0.97	0.31	0.2	$2.31 \times 10^{-7}$
Forest	2.00	0.30	0.40	0.85	0.97	0.31	0.2	$2.31 \times 10^{-7}$
Developed	0.50	0.30	0.40	0.85	0.97	0.31	0.2	$2.31 \times 10^{-7}$
Stream	0.00	0.29	0.30	0.31	0.32	0.00	1.0	0.0

The leaf area index (LAI) is the primary control of the partitioning of evapotranspiration into evaporation and transpiration. The LAI values which were included as part of the evapotranspiration properties came from a variety of sources because there was no single source which could adequately cover all land cover types. The LAI values for the agricultural lands came from Kim et al. (2012), Asner et al. (2003) provided values for grassy areas, Breuer et al. (2003) provided information for forested lands, and the value for the developed area was assigned based on previous HGS models developed by Thomas (2015). The only remaining land cover type was the stream which was assigned a LAI of 0 since there are no leaves or canopy originating from the stream (Li et al. 2008).

## 4.5 Model Inputs

In addition to the model parameters, the model also required inputs for the period of interest. The two primary types of inputs are rainfall data and PET data. Details of these two model input types and how the data was gathered will be discussed in the following sections.

### 4.5.1 Rainfall Data

Rainfall is the primary driver of hydrologic systems and as such, it is the key input in any hydrologic model (Price et al. 2014; Schuurmans and Bierkens 2007). As mentioned in Chapter 3, there are no rain gauges in URC watershed and the gauge nearest the watershed is 15 miles away in Calmar, Iowa (COOP: 131126). Due to the high spatial variability of rainfall, this gauge may not provide accurate rainfall data for URC (Price et al. 2014). There are however 5 nearby rainfall gauges in Otter Creek which is about 4 miles from URC. These gauges have information starting in the middle of April 2014, before the heavy rainfall period of May to August. These gauges have the advantage of reporting rainfall amounts in 15 minute intervals which is important because the temporal resolution of rainfall can play a major factor in the accuracy of a model (De Schepper et al. 2015; Krajewski et al. 1991; Wang et al. 2009). For these reasons, it was decided that the rainfall input would be the data from the Otter Creek gauges with Calmar data filling in information from before the gauges were operational. For the time period where the Otter Creek rainfall gauges were operational, the arithmetic average rainfall from all five gauges was used as the model input.

### 4.5.2 Potential Evapotranspiration Data

Evapotranspiration is the secondary driver for hydrologic models. When using HGS, a PET is input into the model and, based on the land use and evapotranspiration parameters discussed earlier in this chapter, an evapotranspiration value is assigned and applied to the appropriate elements.

In Iowa, there are two good sources for PET data. There is the Iowa State University AgClimate (ISUAG) network and the Iowa State University Soil Moisture (ISUSM) network. The ISUAG network is an older system which was put in place in late 1980s and removed in 2014. When the ISUAG network was removed, some of the sites were converted to the new ISUSM network. One of the sites which was transitioned from the old network to the new network was at Nashua, Iowa which is about 50 miles away from URC watershed (Figure 4.6). The PET from the Nashua site was used in the URC model. It contains data from 1/1/1988 to 4/17/2014 as part of the ISUAG network (ISUAG A135879) and from 6/30/2013 to the present as part of the ISUSM network (ISUSM NASI4). During the period of overlap between the data sets, the ISUSM data was selected instead of the ISUAG data.

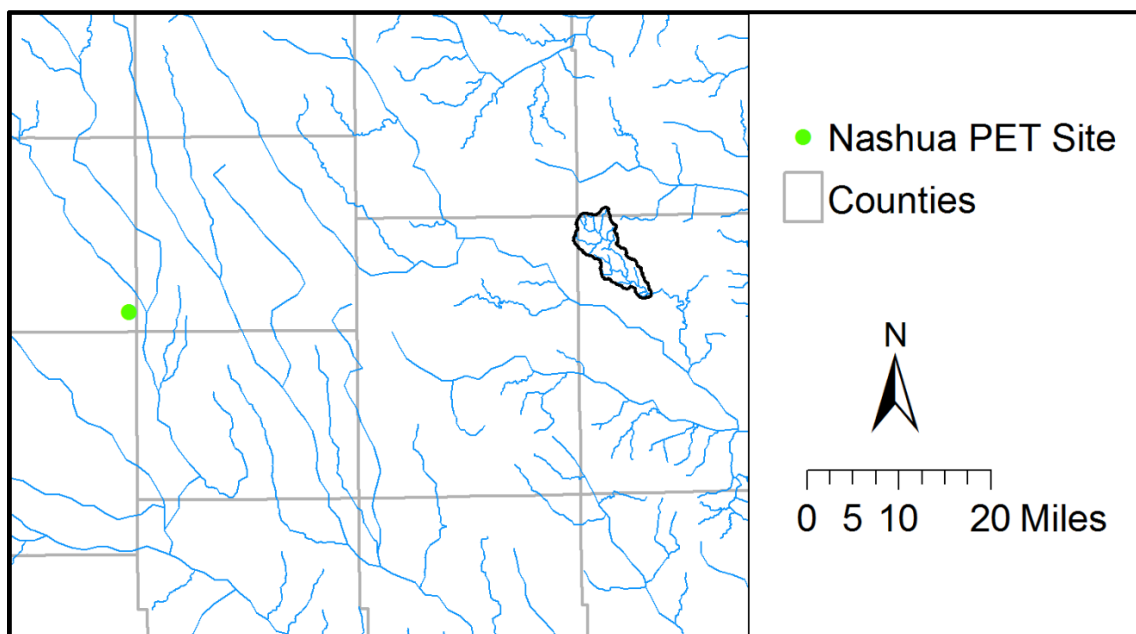


Figure 4.6: The Nashua, Iowa PET site. This site was part of the Iowa State University (ISU) AgClimate network and was transitioned to the new ISU Soil Moisture network.

PET is calculated with the assumption that the evaporation is occurring from a fully mature alfalfa field (High Plains Regional Climate Center 2015); this differs from URC where most of the land is used for row crop agriculture, with corn making up 71.0%

and soybeans 25.8% of that land (USDA 2014). To account for the difference in evapotranspiration between these two vegetation types, a crop coefficient was used to adjust the PET with the form:

$$PET_{Adj} = K_c \times PET_0$$

where,

$PET_{Adj}$  = PET after it has been adjusted by the crop coefficient

$K_c$  = Crop coefficient which varies depending on the expected stage of development for the crop

$PET_0$  = Reference PET from the site at Nashua

The High Plains Regional Climate Center (2015) has compiled the crop maturity, in accumulated growing degree days with a minimum temperature of 50 degrees Fahrenheit (GDD50), and the corresponding crop coefficient for a variety of Midwestern crops. As mentioned previously, corn is the dominant crop type in URC and the coefficient series for typical corn was selected to adjust the PET in the URC model. GDD50 data was available along with the PET information from the Nashua, Iowa climate site. The accumulated GDD50 and crop coefficients for corn are shown in Table 4.7.

Table 4.7: The accumulated GDD50 and corresponding crop coefficient used to calculate the PET input for the URC model (High Plains Regional Climate Center 2015). The crop coefficient series selected is for corn which is the primary land cover in the watershed.

<b>GDD50</b>	<b>Crop Coefficient (<math>K_c</math>)</b>
0	0.10
240	0.18
360	0.35
480	0.51
600	0.69
720	0.88
840	1.01
960	1.10
1200	1.10
1440	1.10
1680	1.10
1920	1.10
2160	0.98
2400	0.60
2450	0.10

#### 4.6 Chapter Summary

The fully integrated, physically based, surface/subsurface modeling software HGS was used to develop the hydrologic model of URC. A two dimensional surface grid of the watershed was developed using Gridgen Version 15.18. This grid was projected from the surface downward at varying intervals to a lower boundary which was determined from the bedrock elevation data. The grid layers were more refined near the surface to quickly account for changes occurring due to rainfall and evapotranspiration.

Once the grid was developed, properties were assigned to the model. Material properties were assigned to the subsurface with three main regions, the surface soil layers which extends from the surface to 1.0 meters below the surface, the tile layer which extends 10 centimeters further and sub-tile soil layers. The properties in the surface soil and sub-tile soil layers were assigned based on SSURGO soil data. In simulations incorporating the impacts of drainage tile, a tile layer which separated the two was

assigned properties which simulated the flow through drainage tiles. Overland flow and evapotranspiration properties were assigned to the model based on the land cover from the NLCD 2006.

The two main model inputs are precipitation and PET. Precipitation inputs were gathered from averaged rainfall from the IFC gauges in the Otter Creek watershed. For time periods where there was no IFC data available, the hourly rainfall from a rain gauge at Calmar, Iowa was used. The PET inputs were gathered from ISUAG and ISUSM sites located at Nashua, Iowa and adjusted with a crop coefficient to more accurately represent URC.



## CHAPTER 5: UPPER ROBERTS CREEK MODEL CALIBRATION

### 5.1 Introduction

Although distributed, physically-based models can be calibrated using a shorter hydrometeorological record than lumped, conceptual models, they do still require calibration (Abbott et al. 1986). This calibration ensures that the model is correctly describing what is physically occurring in the watershed. A common calibration method is to run the model for a time period with known model inputs, such as rainfall and PET, and outputs, such as streamflow. Using the known inputs, a simulation is performed and the results are compared to the known outputs. Model parameters are then adjusted and the process is repeated until the simulated results are at an acceptable level of agreement with the measured data. This chapter discusses the calibration process for URC and the final parameters used in the model.

### 5.2 Development of Initial Conditions

One of the most important aspects of model calibration is ensuring that the initial conditions used in the model are accurate and reasonable (Seck et al. 2015). The best way to identify the initial conditions for a model would be to collect data for the entire watershed and form a complete picture at a single moment in time (Perez 2011). Realistically, the time and effort required to gather this amount of data is not feasible and an alternative method of developing initial conditions must be used. Perez (2011) outlines several different options for initial condition development such as running a simulation using long term average inputs until a steady state condition is achieved, draining the model from a fully saturated state until the modeled outflow matches the observed outflow, and using meteorological data to force the model until the simulated heads are consistent between years.

For the URC model, the initial condition was achieved by starting from a fully saturated state and draining the watershed without any additional rainfall but with an

applied PET rate of 0.864 millimeters per day ( $1 \times 10^{-8}$  meters per second) which is approximately the average for the month of May near URC. Throughout the simulation, the average depth to water table in the watershed was monitored in six observation wells (Figure 5.1). The initial condition was found when the average depth to water table in those six observation wells was approximately equal to the depth observed in early January 2014 at the USGS groundwater well near Eldorado, Iowa (USGS 430203091501201, Figure 3.10). Figure 5.2, from the USGS National Water Information System, shows the measured depth from the surface to the water table in that well from December 15, 2013 to January 15, 2014. The depth to water table on January 1, 2014 was 16.25 feet (4.95 meters).

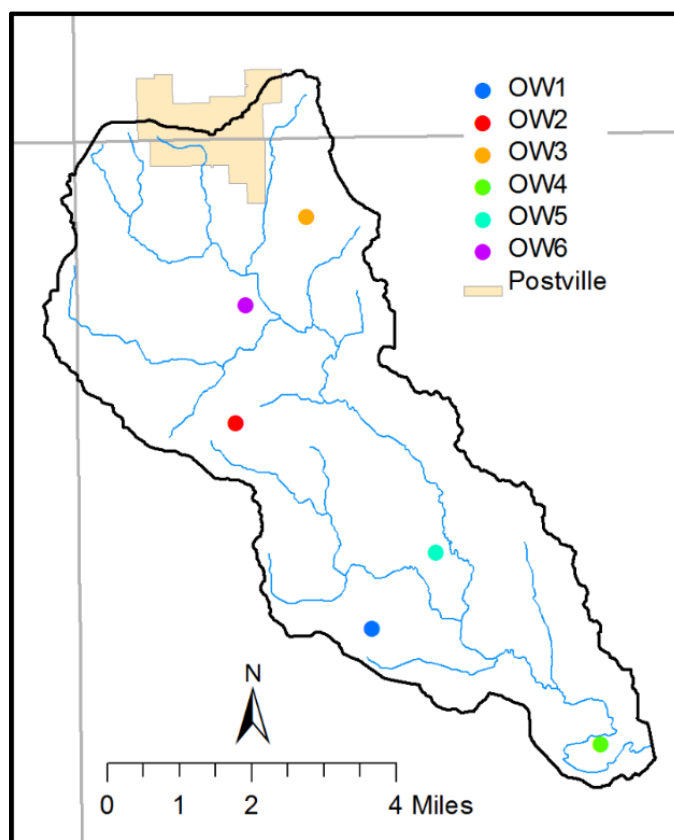


Figure 5.1: Observation wells used in determining the initial conditions for the URC model. The average of the six wells was compared to the nearby USGS groundwater well.

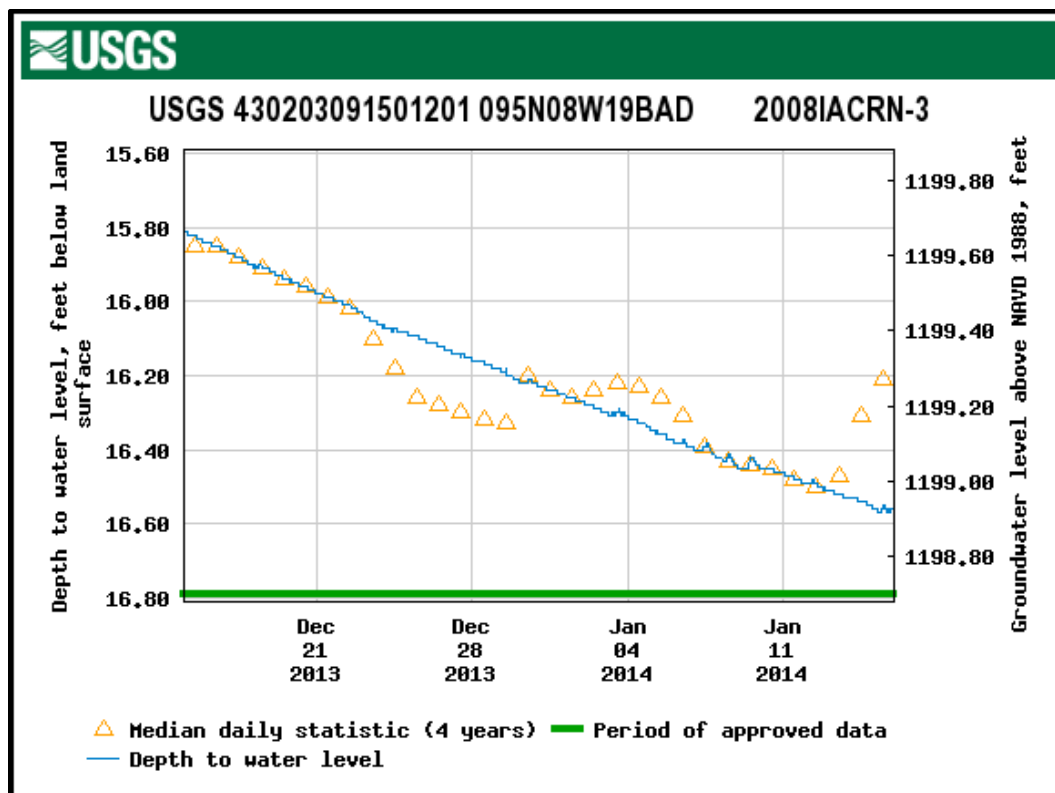


Figure 5.2: USGS groundwater well data (USGS 430203091501201) for December 15, 2013 to January 15, 2014. The depth to water table on January 1, 2014 16.25 feet (4.95 meters) (United States Geological Survey 2015).

HGS produced output files approximately every 30 days throughout the simulation; these output files were used to calculate the average depth to the water table among those six observation wells for the duration of the simulation (Figure 5.3). The output files from 181 days of simulation time were selected as the initial condition, at which point the average depth to water table among the six observation wells was 4.46 meters. Although this is not as deep as the 4.95 meters observed from the USGS groundwater well data, it was thought to be accurate because the USGS observation well was located on a high point near a road whereas the simulation observation wells were scattered on upland, lowland, and side slope areas.

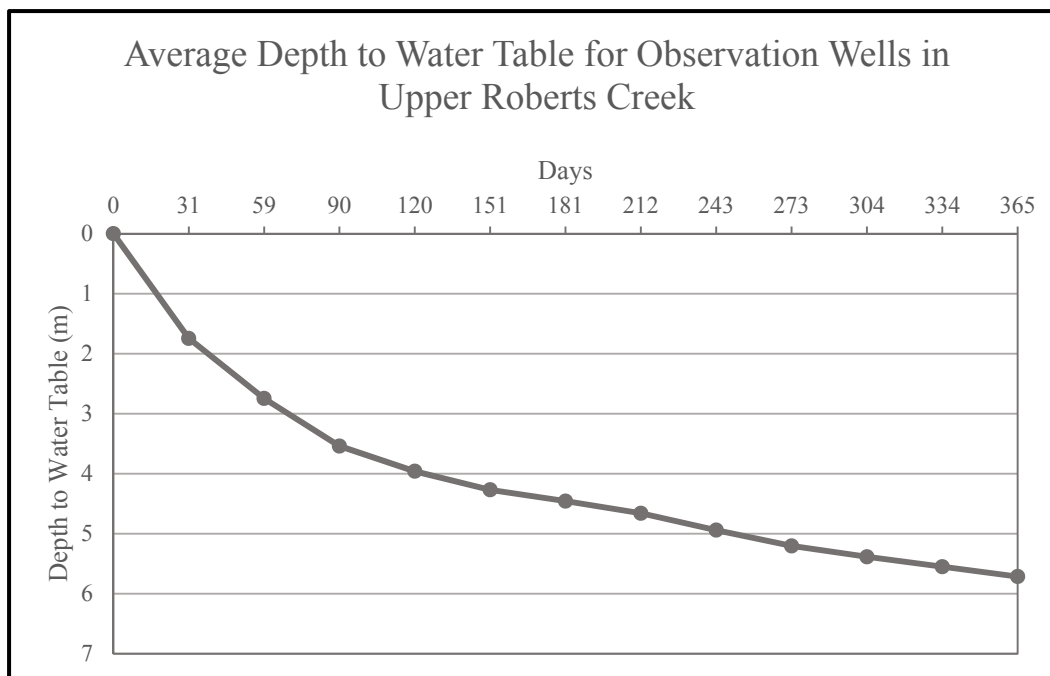


Figure 5.3: The average depth to the water table for the six observation wells in the URC model. The output files from the day 181 data point were used as the initial condition for model simulations.

Although this initial condition proved to be a suitable starting point, the results from simulations run from this point still exhibited the impacts of initialization. To minimize these impacts, the calibration simulations were run for multiple years with 2014 data applied for each simulated year and the volumetric year-on-year changes were analyzed for the main components of the hydrologic cycle. Each additional year of simulated time brought the simulations closer to a converged pseudo steady state and a 1% change threshold for the calibration ratios was used as the benchmark for determining when the simulations were converged (Ajami et al. 2015). Not all calibration simulations achieved a pseudo steady state and most of the calibration simulations used the outputs of previous simulations as the initial condition in order to avoid using the drained initial condition and the lengthy simulation times required to achieve a pseudo steady state from that point. The simulation with the final parameter values did converge to the pseudo steady state.

### 5.3 Calibration Targets

The calibration process requires targets which are used to evaluate the quality of the results and the impact of changes made during the calibration process. Calibration targets can vary depending on the type of model being developed. In the case of the URC model, annual simulations were the primary focus and therefore annual baselines needed to be developed to look at the impacts of changes in the watershed. From an annual perspective, it is informative to look at the ratios between components of the hydrologic cycle.

The ratios used in the URC model evaluation and calibration process were total discharge to precipitation ( $Q/P$ ), evapotranspiration to precipitation ( $ET/P$ ), evaporation to evapotranspiration ( $E/ET$ ), transpiration to evapotranspiration ( $T/ET$ ), baseflow to total discharge ( $Q_b/Q$ ), and total discharge to estimated total discharge based on the USGS gauges on Otter Creek at Elgin, Iowa and the Turkey River at Spillville, Iowa ( $Q/Q_r$ ). The estimated total discharges based on Otter Creek at Elgin, Iowa and the Turkey River at Spillville, Iowa were determined using the Flow Anywhere method for regional regression as discussed in Chapter 3 (Linhart et al. 2012).

The targets for these ratios were found in literature and the values are shown in Table 5.1. When evaluating the existing literature for these ratios, studies performed in Iowa or in Midwestern, agriculturally dominated landscapes were given preference but in some cases ratios from other locations were used. There are no literature sources cited for the  $Q/Q_r$  ratio but it ideally would be 1 which would show that the modeled flow is equal to the estimated flow. In reality, this value could have significant variation since  $Q_r$  is itself an estimate and for this reason the  $Q/Q_r$  ratio was primarily used to identify major issues with the model. The USGS gauge on Otter Creek at Elgin began operation on March 27, 2014 so when calculating  $Q/Q_r$  for Otter Creek the simulated discharge from this date to the end of the year was used. When calculating the ratios, the model precipitation input was used because HGS does not directly output precipitation.

Table 5.1: Ratios of hydrologic components used in the calibration and evaluation of the URC model. Q is total flow, P is precipitation, ET is evapotranspiration, E is evaporation, T is transpiration,  $Q_b$  is base flow, and  $Q_r$  is the estimated flow based on the Flow Anywhere method for regional regression streamflow estimation.

<b>Ratio</b>	<b>Target Value</b>	<b>Literature Values</b>	<b>Literature Sources</b>
Q/P	0.25	0.24 0.27 0.24	Schilling et al. (2008) McDonald (1961) Hoyt (1936)
ET/P	0.75	0.76 0.73 0.76	Schilling et al. (2008) McDonald (1961) Hoyt (1936)
E/ET	0.30	0.26, 0.33 0.35, 0.23	Kang et al. (2003) Wang et al. (2013)
T/ET	0.70	0.74, 0.67 0.65, 0.77 0.61±0.15	Kang et al. (2003) Wang et al. (2013) Schlesinger and Jasechko (2014)
$Q_b/Q$	0.55	0.56 0.45-0.66	Schilling et al. (2008); Schilling and Libra (2003) Schilling (2005)
$Q/Q_r$	1.0		

To further test the accuracy of these target ratios, the ratios for nearby Otter Creek were calculated for 2014 based the measured discharge at the USGS gauge and the average precipitation from the five IFC rainfall gauges within the watershed. For the period of the year where before the USGS gauge was operational a baseflow of 15 cfs was assigned and rainfall data from Calmar, Iowa was used for the portion of the year before the IFC rainfall gauges were operational. The baseflow was calculated from the USGS gauge data using the USGS HYSEP code. Based on this measured data, the discharge to precipitation ratio for Otter Creek in 2014 was 0.301, the evapotranspiration to precipitation ratio was 0.699, and the baseflow to total discharge ratio was 0.615. The similarity between these measured ratios from nearby Otter Creek and the values selected from literature suggests that the target ratios chosen are reasonable for URC.

## 5.4 Calibration of Parameters

Once an acceptable initial condition and the calibration target ratios were established, the calibration of the model could begin. The calibration process involved running the model from the initial condition and evaluating the results after each simulated year. The simulation results were also compared to the previous simulation year results to determine if a pseudo steady state had been achieved. In addition to comparing the ratios from the simulation to the ratio targets, the average daily simulated discharge was visually compared to the estimated discharges to ensure the simulated timing of events was reasonable. Based on those comparisons, parameters were adjusted within the model to improve the accuracy. The parameters which were explored and adjusted were the Van Genuchten  $\alpha$  and  $\beta$  values, the TLS parameters, the hydraulic conductivity of the tile layer, and the rill storage height. The model was improved throughout the calibration process with each calibration step building upon the previous with the exception of the rill storage height and the hydraulic conductivity of the tile layer which were run separately with the best of each combining to form the final parameter values.

### 5.4.1 Van Genuchten Parameters

The Van Genuchten parameters  $\alpha$  and  $\beta$  are used to predict the saturation of soils under partially saturated conditions (Van Genuchten 1980). Due to their impact on the partial saturation of soils, the Van Genuchten parameters were used to calibrate the response observed in groundwater wells following storm events.

It was observed that the USGS and IFC groundwater wells near URC exhibited very quick changes in water level following a storm, much quicker than would be expected for water infiltrating from the surface (Figure 5.4 and Figure 5.5). It was determined that the quick response was likely due to water flowing into the well from the capillary zone just above the water table. The addition of a small amount of water to this

zone can increase the saturation in this region enough to cause it to become fully saturated and push water into the groundwater well (Gillham 1984).

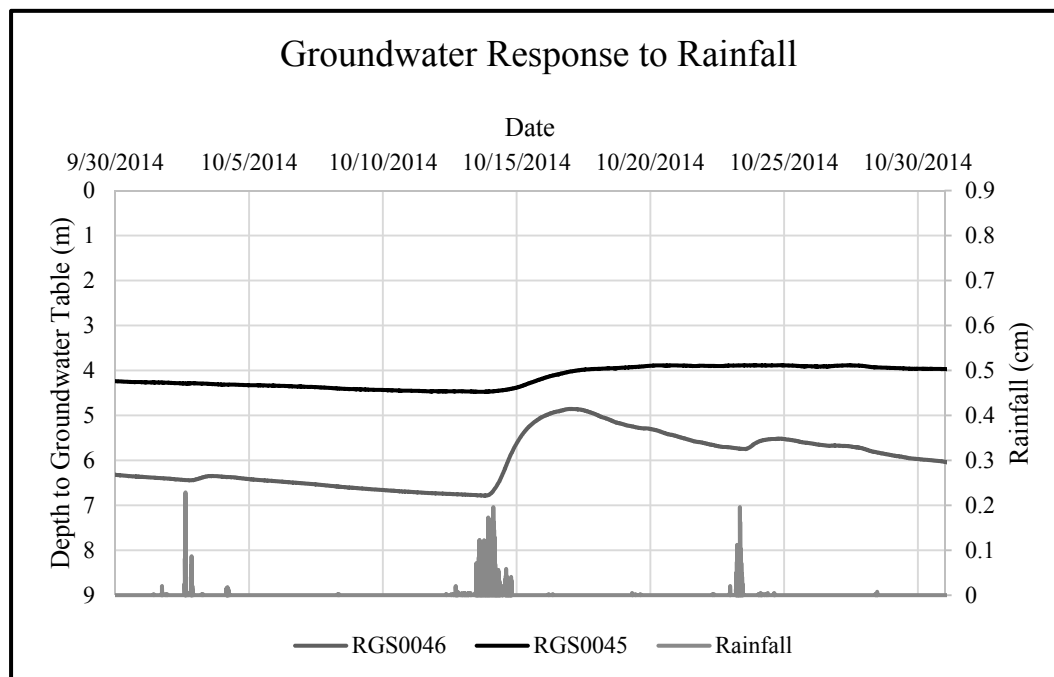


Figure 5.4: The groundwater response to rainfall in the USGS groundwater well (USGS 430203091501201).

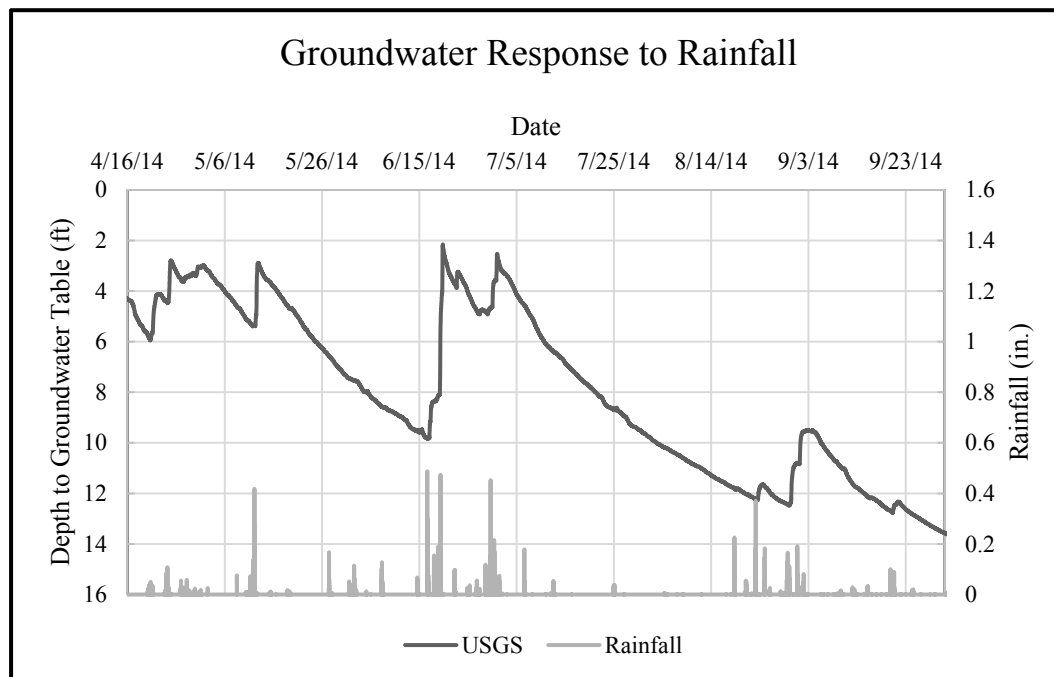


Figure 5.5: The groundwater response to rainfall in the IFC groundwater wells (IFC RGS0045 and IFC RGS0046).



Using the original  $\alpha$  and  $\beta$  values for silt loam there was very little soil near full saturation. To better represent the quick change in groundwater observed following storm events, three new sets of  $\alpha$  and  $\beta$  values were selected all of which resulted in a larger capillary fringe. These  $\alpha$  and  $\beta$  values are shown in Table 5.2 and the plots of the soil saturation are shown in Figure 5.6.

Table 5.2: Van Genuchten  $\alpha$  and  $\beta$  parameters used in the calibration simulations.

Van Genuchten Parameter	$\alpha$	$\beta$
Original	1.88	3.17
Calibration Set 1	0.25	4.50
Calibration Set 2	0.30	3.90
Calibration Set 3	0.41	2.80

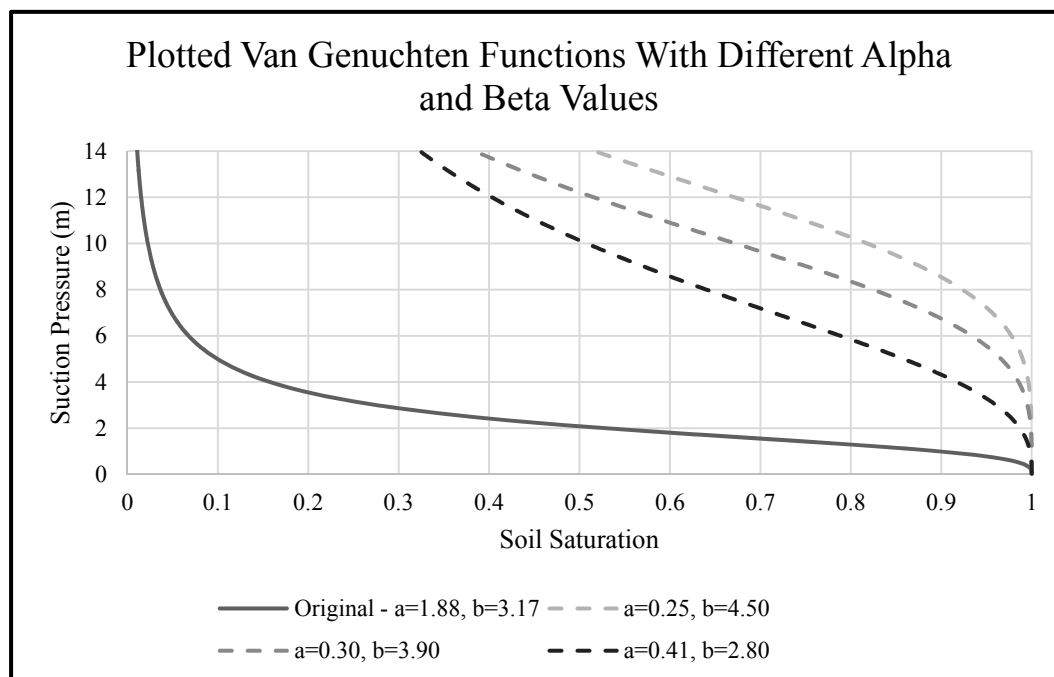


Figure 5.6: The alternative Van Genuchten  $\alpha$  and  $\beta$  values which were used for calibration of URC watershed model.

Using these new  $\alpha$  and  $\beta$  values, simulations were run to examine which calibration ratios most closely matched the target values. The different  $\alpha$  and  $\beta$  values

showed quite different responses. The groundwater response were Thiessen polygon weighted at the six observation wells in the watershed and the watershed average was compared to the groundwater response at the USGS well.

Figure 5.7 compares the results from the different calibration sets with each other. From this figure it can be seen that the groundwater response in the original value set responds with quick peaks but without the slow decline in water table observed in the USGS well. The simulated results with calibration sets 1 and 2 are very similar owing to the fact that several of the observation wells experienced full saturation during the simulation. This full saturation is not observed in the USGS well nor would it be expected over this time period.

Figure 5.8 compares the results with the third set of calibration values to the observed response at the USGS well. This third set of values was determined to most accurately represent the observations from the USGS well. The magnitude of the groundwater response was less than observed in the USGS groundwater well but since the simulated results were averaged over the entire watershed instead of at a single location it was not expected to achieve identical magnitudes. The results shown in these figures are from the first year of simulated data.

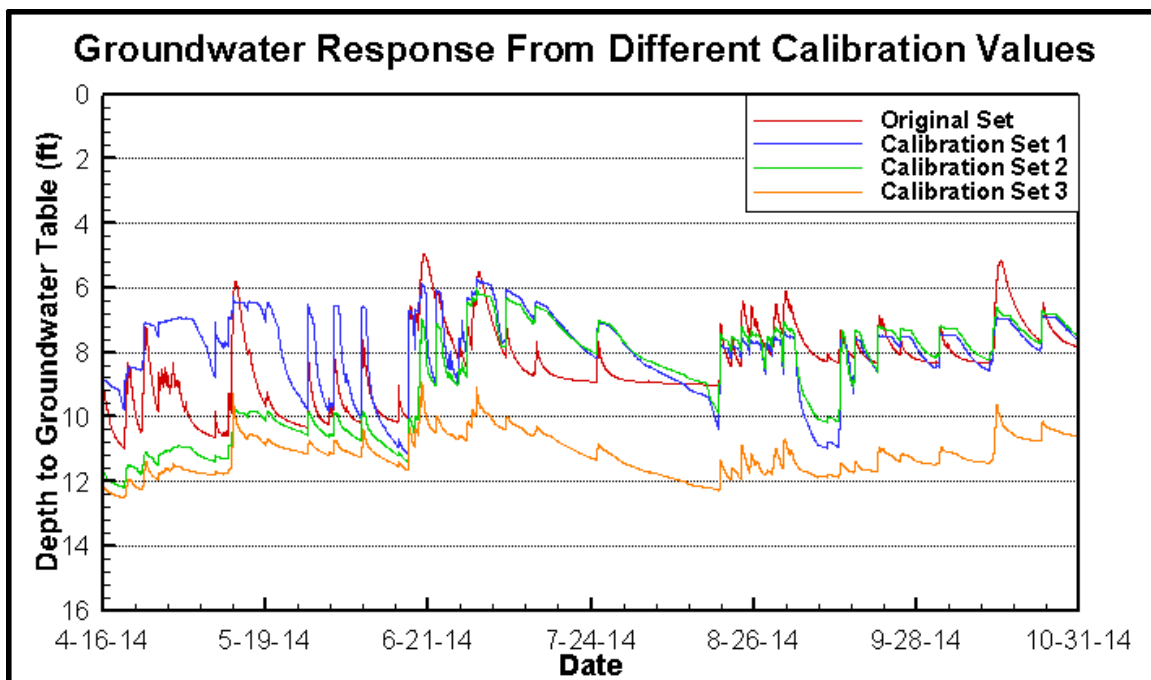


Figure 5.7: The simulated groundwater responses for the original  $\alpha$  and  $\beta$  values and the three calibration value sets.

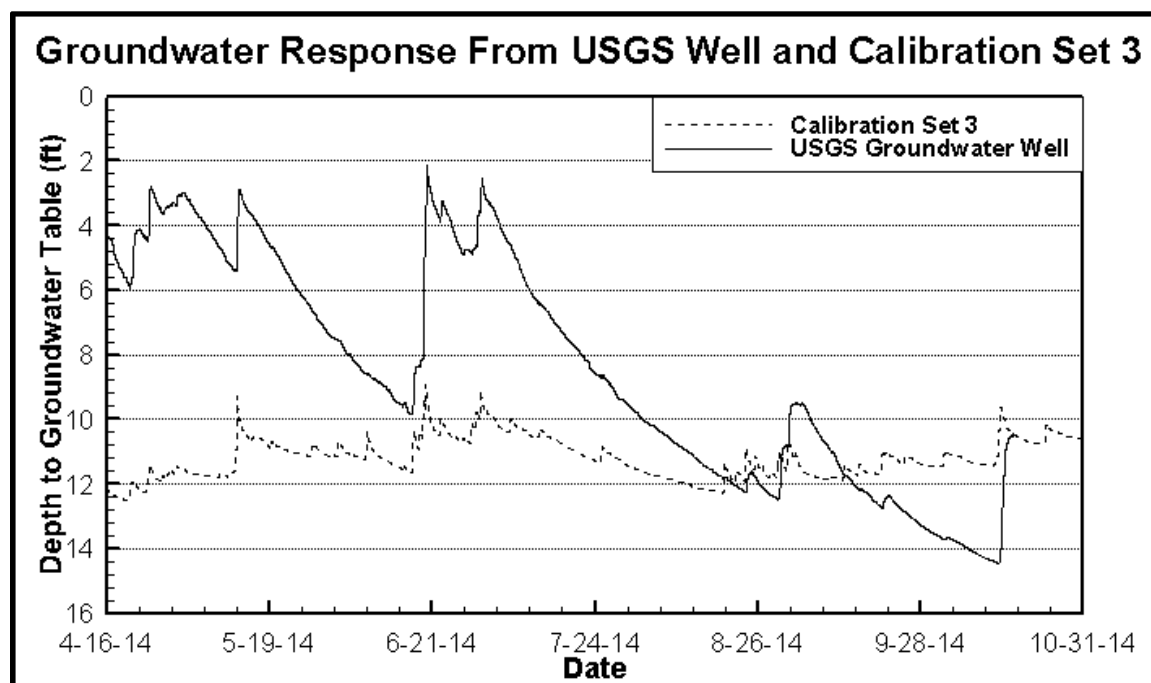


Figure 5.8: The simulated groundwater response using  $\alpha$  and  $\beta$  values from calibration set 3 and the data from the USGS groundwater well. The response from calibration set 3 is the closest to what is expected based on the data from the USGS groundwater well.

Table 5.3 shows the calibration ratios for the three different simulations. As with the figures, the ratios in this table are from the first year of the simulations. Although this did not represent a pseudo steady state, it was the most informative of the simulations years. Beyond this point the model stored too much water and greatly overshoot the discharge to precipitation ratio. The complete table of results for this calibration component can be found in Appendix A.

Table 5.3: Results from the calibration of Van Genuchten  $\alpha$  and  $\beta$  values. The most accurate groundwater response was observed using calibration set 3.

<b>Ratios</b>	<b>Target</b>	<b>Initial Values</b>	<b>Calibration Set 1</b>	<b>Calibration Set 2</b>	<b>Calibration Set 3</b>
Q/P	0.25	0.15	0.49	0.38	0.26
ET/P	0.75	0.08	0.34	0.38	0.45
E/ET	0.30	0.74	0.58	0.47	0.38
T/ET	0.70	0.26	0.42	0.53	0.62
Q <sub>b</sub> /Q	0.55	0.48	0.26	0.30	0.36
Q/Q <sub>r</sub> (Spillville)	1.00	0.54	1.75	1.36	0.94
Q/Q <sub>r</sub> (Otter Creek)	1.00	0.56	1.86	1.45	1.00

#### 5.4.2 Transpiration Limiting Saturations Parameters

As the name suggests the TLS parameters control the conditions under which transpiration is allowed to occur and therefore how much transpiration occurs. In Iowa, transpiration accounts for approximately 70% of total evapotranspiration; unless the correct amount of transpiration is achieved in the model it will not be possible to achieve the correct amount total evapotranspiration. Since the input for HGS is PET, the TLS parameters also control how much evaporation is allowed to occur because as transpiration is reduced there is more potential for evaporation. The four TLS parameters are: moisture content at the wilting point ( $\theta_{wp}$ ), moisture content at the field capacity ( $\theta_{fc}$ ),

moisture content at the oxic limit ( $\theta_o$ ), and moisture content at the anoxic limit ( $\theta_{an}$ ). HGS uses the Kristensen and Jensen (1975) approach to estimate actual transpiration ( $T_p$ ):

$$T_p = f_1(\text{LAI})f_2(\theta)\text{RDF}(E_p - E_{\text{can}})$$

where,

$f_1(\text{LAI})$  = Function of the leaf area index

$f_2(\theta)$  = Function of the water content as shown below

RDF = Root distribution function where  $E_p$  is the PET and  $E_{\text{can}}$  is the canopy evaporation

The water content function,  $f_2(\theta)$ , varies between 0 and 1 with the form:

$$f_2(\theta) = \begin{cases} 0; & \text{for } 0 \leq \theta \leq \theta_{\text{wp}} \\ 1 - \left( \frac{\theta_{\text{fc}} - \theta}{\theta_{\text{fc}} - \theta_{\text{wp}}} \right)^{C_3/E_p} & ; \text{for } \theta_{\text{wp}} < \theta \leq \theta_{\text{fc}} \\ 1; & \text{for } \theta_{\text{fc}} < \theta \leq \theta_o \\ 1 - \left( \frac{\theta_{\text{an}} - \theta}{\theta_{\text{an}} - \theta_o} \right)^{C_3/E_p} & ; \text{for } \theta_o < \theta \leq \theta_{\text{an}} \\ 0; & \text{for } \theta_{\text{an}} < \theta \end{cases}$$

The shape of the  $f_2(\theta)$  function is shown in Figure 5.9 using the values  $\theta_{\text{wp}}=0.20$ ,  $\theta_{\text{fc}}=0.32$ ,  $\theta_o=0.76$ ,  $\theta_{\text{an}}=0.90$ , and the transpiration fitting parameter  $C_3=2.31 \times 10^{-7}$  (Li et al. 2008). As the figure shows, the transitions between  $f_2(\theta)=0$  and  $f_2(\theta)=1$  are very distinct and occur at the field capacity and the oxic limit. The change is particularly abrupt because the transpiration fitting parameter ( $C_3$ ) is small, a larger  $C_3$  value would result in a more gradual transition.

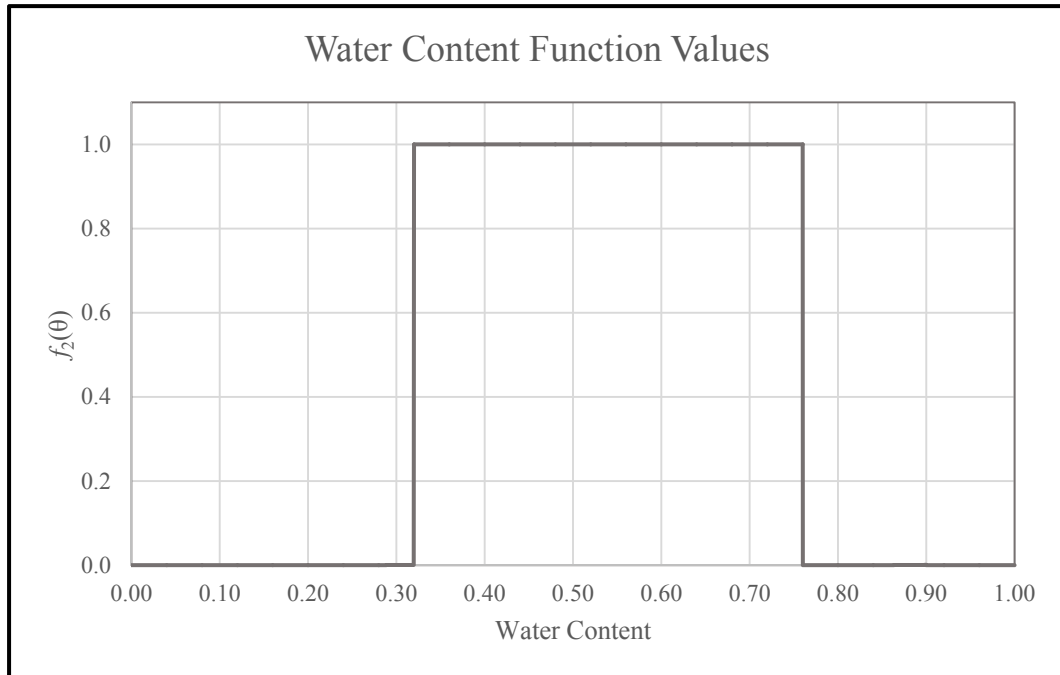


Figure 5.9: The plot of the water content function with  $\theta_{wp}=0.20$ ,  $\theta_{fc}=0.32$ ,  $\theta_o=0.76$ ,  $\theta_{an}=0.90$ , and the transpiration fitting parameter  $C_3=2.31 \times 10^{-7}$ .

Four different literature sources were reviewed to determine acceptable values for the TLS parameters. These sources and the values suggested by each are shown in Table 5.4.

Table 5.4: TLS values from literature sources. These values were used as a starting point for the TLS calibration simulations.

TLS Parameter	Li et al. (2008)	Sciuto and Diekkruger (2010)	Cornelissen et al. (2014)	Schilling et al. (2014)
Wilting Point ( $\theta_{wp}$ )	0.20	0.30		0.05
Field Capacity ( $\theta_{fc}$ )	0.32	0.40		0.15
Oxic Limit ( $\theta_o$ )	0.76	0.85	0.88-0.90	1
Anoxic Limit ( $\theta_{an}$ )	0.90	0.97	0.96-0.97	1.001

The TLS values which were used in the calibration process were based on these literature values but the values were adjusted as the outcomes of various calibration tests

were examined. Including the original values, there were six sets of TLS values used during the calibration process (Table 5.5).

Table 5.5: TLS value sets used in the calibration process.

<b>TLS Parameters</b>	<b>Original Set</b>	<b>Set 1</b>	<b>Set 2</b>	<b>Set 3</b>	<b>Set 4</b>	<b>Set 5</b>
Wilting Point ( $\theta_{wp}$ )	0.20	0.20	0.20	0.20	0.20	0.20
Field Capacity ( $\theta_{fc}$ )	0.32	0.32	0.32	0.32	0.32	0.32
Oxic Limit ( $\theta_o$ )	0.76	0.76	0.79	0.76	0.76	1.00
Anoxic Limit ( $\theta_{an}$ )	0.90	0.93	0.95	0.97	0.99	1.01

When these calibration simulations were run and the ratios were compared, it became apparent that the simulations improved as the anoxic limit increased and the best simulation was found with the oxalic limit of 1.00 and anoxic limit of 1.01. The ratios reported in Table 5.6 are from the fifth year of the simulation; although the simulations had not yet reach a pseudo steady state the information was sufficient to select a the preferred TLS values. The results from all simulated years can be found in Appendix A along with the percent change between years for the volume of each water balance component.

These high oxalic and anoxic limits ensures that transpiration is always active. Although this stretches the bounds of what is physically realistic, it produced the most accurate calibration ratios and outlet hydrograph (Figure 5.10); when lower anoxic limits were used the small peak in October was much too high and not enough water left the watershed through evapotranspiration.

Table 5.6: Results from the TLS calibration simulations. The calibration ratios are given for the 5 different TLS value sets tested along with the initial values. The results from calibration set 5 were deemed to be the best based on the ratios and comparisons of the plots. The reported ratios are from the fifth year of simulation and although the simulations had not yet achieved a pseudo steady state the information they provided was sufficient to pick a set of values for future simulations.

<b>Ratios</b>	<b>Target</b>	<b>Original Set</b>	<b>Calibration Set 1</b>	<b>Calibration Set 2</b>	<b>Calibration Set 3</b>	<b>Calibration Set 4</b>	<b>Calibration Set 5</b>
Q/P	0.25	0.72	0.70	0.67	0.62	0.51	0.36
ET/P	0.75	0.28	0.31	0.33	0.38	0.46	0.65
E/ET	0.30	0.73	0.67	0.61	0.53	0.43	0.29
T/ET	0.70	0.27	0.33	0.39	0.47	0.57	0.71
Q <sub>b</sub> /Q	0.55	0.27	0.27	0.27	0.27	0.30	0.30
Q/Q <sub>r</sub> (Spillville)	1.00	2.56	2.48	2.39	2.23	1.81	1.27
Q/Q <sub>r</sub> (Otter Creek)	1.00	2.56	2.47	2.38	2.20	1.80	1.21



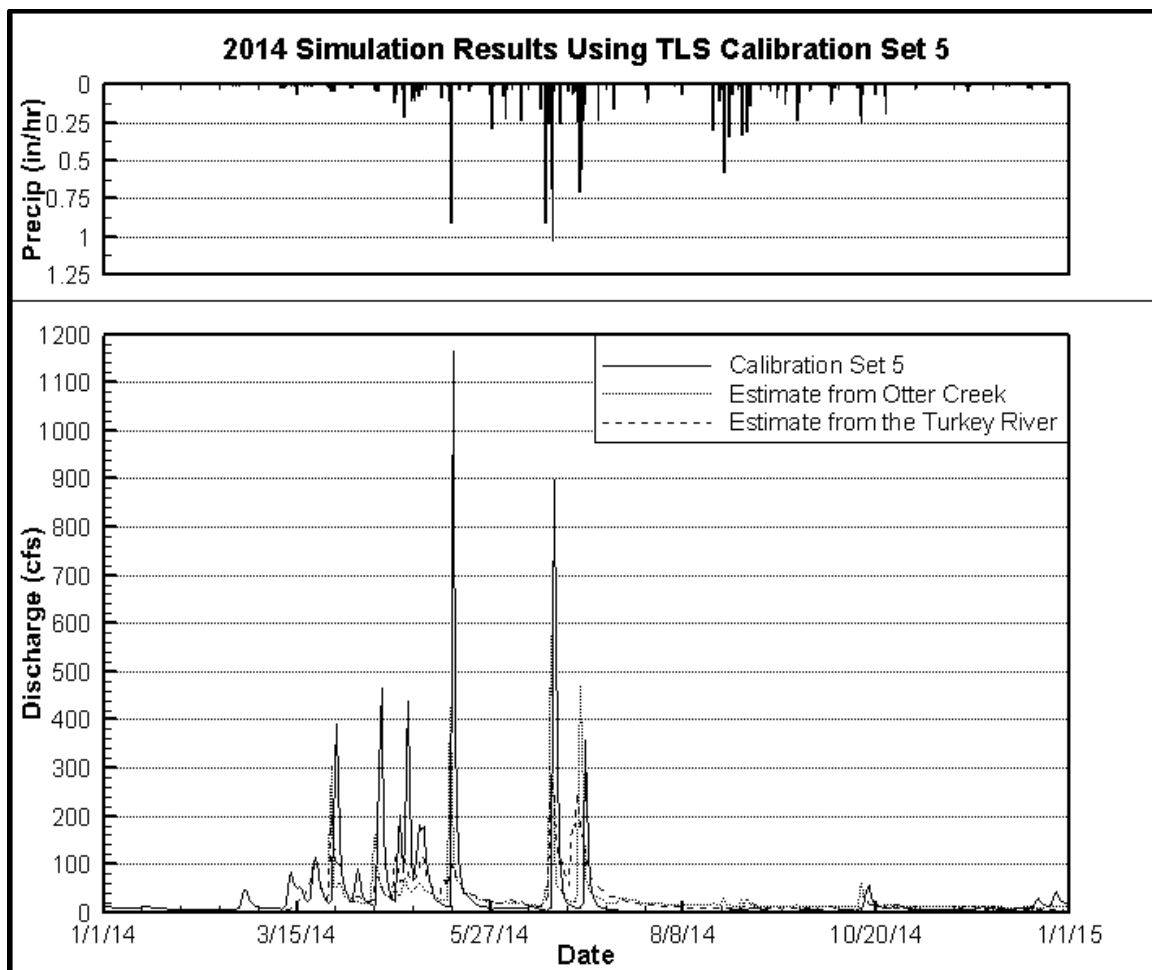


Figure 5.10: The discharge for 2014 using the TLS values from calibration set 5. These results were from the fifth simulated year with 2014 data and although it was not at a pseudo steady state it did provide enough information to determine that this set of TLS values were most appropriate.

#### 5.4.3 Tile Layer Hydraulic Conductivity

The tile layer was included over the entirety of the URC model but in reality drainage tiles are only located in agricultural fields where the owner or farmer believes that the soil does not drain adequately for maximum productivity. To account for this difference, the hydraulic conductivity of the tile layer was adjusted using an equation developed by Thomas (2015) which uses the Total Drainage Density (TDD) of an Iowa watershed to estimate the saturated hydraulic conductivity of the tile layer media. The equation is given as:

$$K_{s(\text{eq})} = 5242 \text{ TTD}^2 + 2295 \text{ TTD} + 1.4$$

where,

$K_{s(\text{eq})}$  = Saturated hydraulic conductivity of the tile layer in meters per day

TDD = Total Drainage Density in linear meters of drain tile per square meter of surface area

To determine the TDD, it was assumed that the drain tile is arranged in a regular rectangular pattern which means that the TDD is the inverse of the tile spacing. The tile spacing in URC was determined from the Iowa Drainage Guide based on the soil types within the watershed (Melvin et al. 2008). URC is primarily made up of well drained, silt loam soil with 70.8% of the watershed Fayette soil and 21.5% Downs soil. Based on the Iowa Drainage Guide, Fayette soil does not require drainage while it is recommended that Downs soil have a tile spacing of 70 to 90 feet (21.3 to 27.4 meters). Figure 5.11 shows the areas which would require tile drainage to achieve full productivity according to the Iowa Department of Natural Resources (Iowa Department of Natural Resources and Iowa Geological Survey 2003-2014). The use of drain tile can improve crop yields and as a result many farmers will install tile on land where it may not necessarily be required to ensure the best conditions possible (Schilling and Helmers 2008). For this reason it is likely that all of the Downs soil areas and some of the Fayette soil areas have drain tile installed.

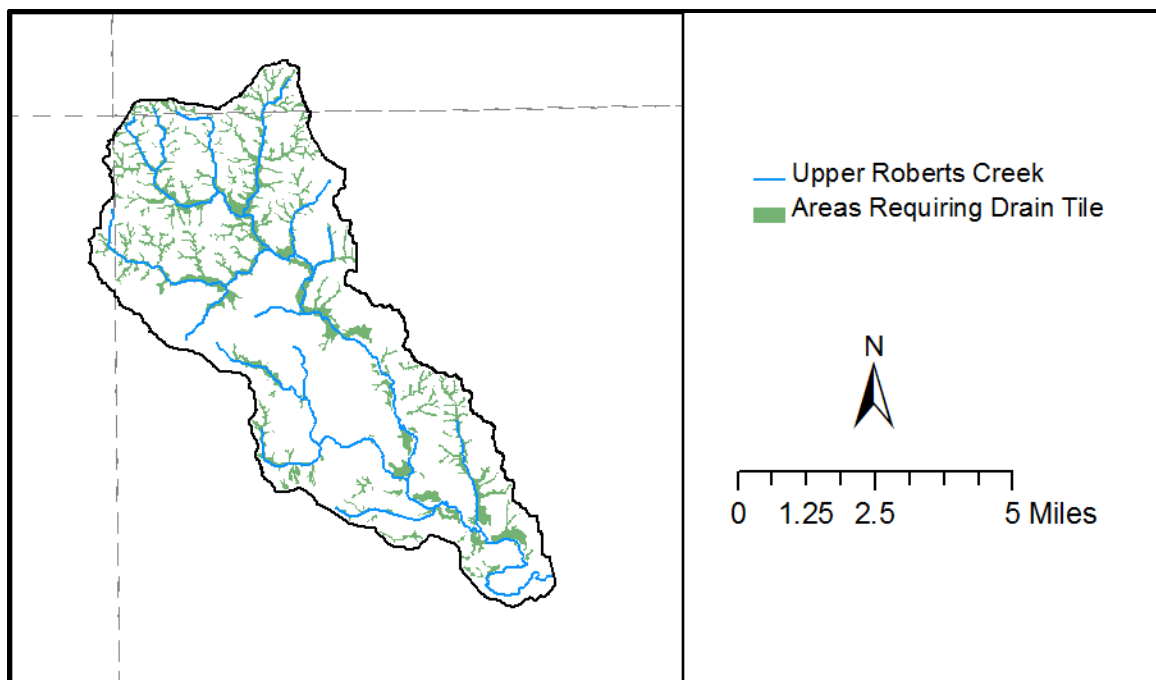


Figure 5.11: Areas within URC watershed requiring drainage tile to achieve full productivity. Drainage tile can be installed outside of this region if the farmer or landowner thinks that it will increase productivity.

To determine the best tile spacing estimate for the URC model, five different spacing values were simulated and the calibration target ratios were examined. Table 5.7 shows the different tile spacing values along with the equivalent hydraulic conductivities and Table 5.8 shows the ratio results. These ratio results are from the sixth simulated year at which time all of the simulations had reached a pseudo steady state. The results for all six simulated years are shown in Appendix A along with the percent change between years for the volume of each water balance component.

Table 5.7: Tile spacing and the equivalent hydraulic conductivity used in URC calibration simulations. Five different tile spacing options were simulated.

<b>Tile Spacing (meters)</b>	<b>Equivalent Hydraulic Conductivities</b>	
	<b>meters per day</b>	<b>meters per second</b>
10	283.32	0.0032792
15	177.70	0.0020567
20	129.26	0.0014960
25	101.59	0.0011758
30	83.72	0.00096903

Table 5.8: Results from tile spacing simulations. The calibration ratios are given for the five different tile spacing intervals along with the ratios for the simulation without tile. These ratios are from the sixth year of each simulation. The results of the simulation with 10 meter tile spacing were deemed to be the best in that the simulations using this value closely matched the target values.

<b>Ratios</b>	<b>Target</b>	<b>No Tile</b>	<b>10 Meters</b>	<b>15 Meters</b>	<b>20 Meters</b>	<b>25 Meters</b>	<b>30 Meters</b>
Q/P	0.25	0.36	0.36	0.36	0.36	0.36	0.36
ET/P	0.75	0.65	0.65	0.65	0.65	0.65	0.65
E/ET	0.30	0.29	0.29	0.29	0.29	0.29	0.29
T/ET	0.70	0.71	0.71	0.71	0.71	0.71	0.71
Q <sub>b</sub> /Q	0.55	0.30	0.68	0.60	0.55	0.51	0.48
Q/Q <sub>r</sub> (Spillville)	1.00	1.27	1.28	1.28	1.27	1.27	1.27
Q/Q <sub>r</sub> (Otter Creek)	1.00	1.22	1.21	1.21	1.21	1.21	1.21

The results show that as the tile density increases, the proportion of baseflow also increases without other major ratio impacts. As the baseflow increases, the event peaks are reduced and as such the tile spacing was a useful tool in reducing the peaks so they more closely matched the estimates based on Otter Creek at Elgin and the Turkey River at Spillville. Although the baseflow to total flow ratio was at the upper end of the reasonable range, it was determined that the 10 meter tile spacing was the most appropriate because the ratios were reasonable and the event peaks were the lowest of the spacing options tested. The simulated discharge is shown in Figure 5.12 along with the estimated discharges based on the USGS gauges Otter Creek at Elgin and the Turkey River at Spillville.

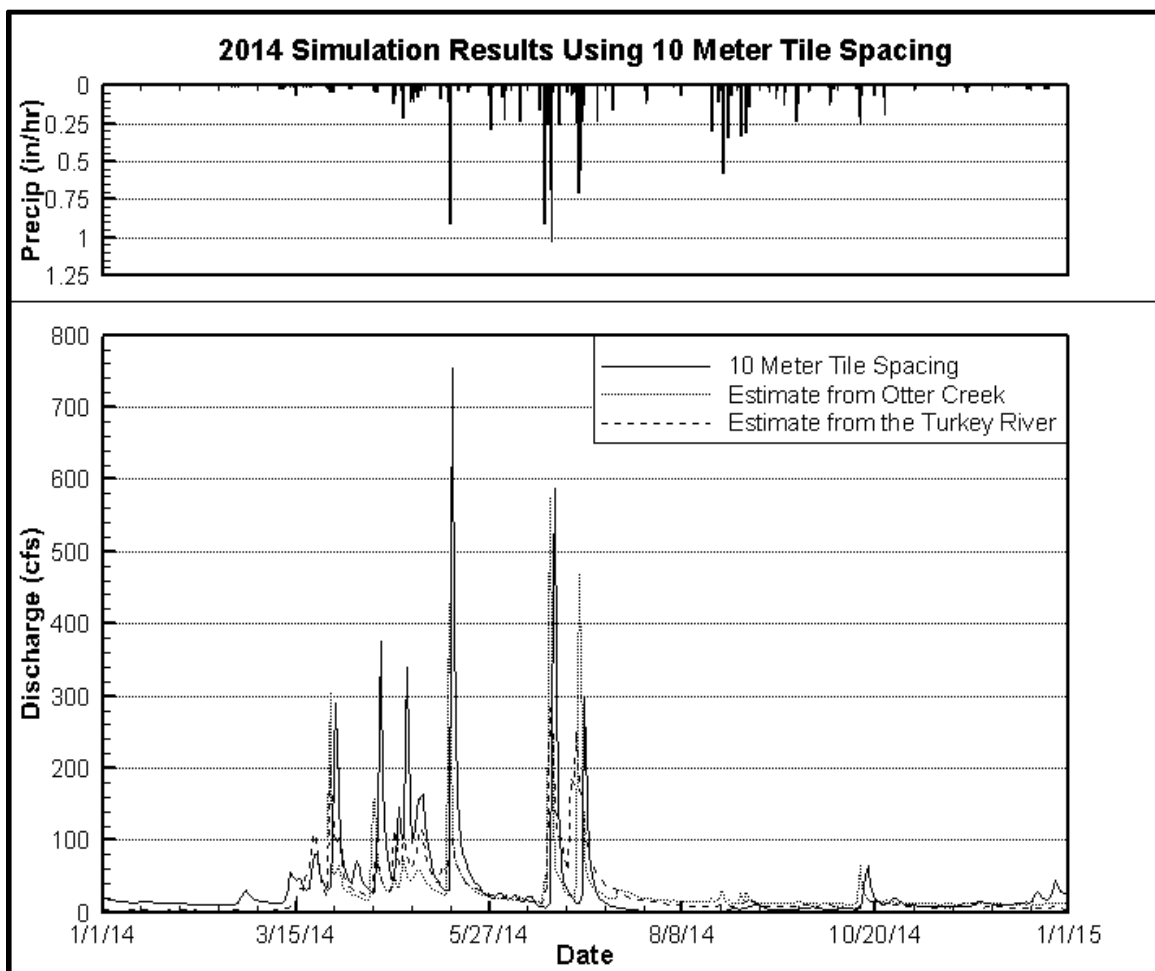


Figure 5.12: The discharge for the sixth year of 2014 simulation using the 10 meter tile spacing. This was the most accurate of tile spacing calibration simulations.

#### 5.4.4 Rill Storage

While the calibration of the tile layer conductivity was taking place, the value for the specified rill storage was also being calibrated. These rill storage calibration simulations did not include the tile layer and the preferred option from each of these last two calibration steps were combined in the final model. This approach broke from the previous steps which all built upon one another.

Rill storage is the depth of water required on the surface before water is allowed to run off the landscape. All previous simulations had specified the rill storage to be 0.002 meters but literature values up to 0.2 meters can be found (Frei and Fleckenstein 2014). The calibration of the URC model was performed within this range by testing rill storage values of 0.02 and 0.2 meters along with the initial value of 0.002 meters. The downside to increasing the rill storage depth is that it increases the required computing time. The impact was most significant with the rill storage of 0.2 meters where the simulation was stopped before one simulated year was complete because it was running prohibitively slow. The simulation with 0.02 meter rill storage was allowed to continue running but was approximately 45% slower than the simulations with the rill storage of 0.002 meters.

Table 5.9 contains the calibration ratios for the completed rill storage simulations in year 6 of the simulation when both simulations had reached a pseudo steady state. The calibration ratios and the percent volumetric change in each of the components of the hydrologic cycle can be found in Appendix A.

Table 5.9: Results from the rill storage calibration tests. These results are from the sixth year of the calibration test when both simulations had reached a pseudo steady state.

<b>Ratios</b>	<b>Target</b>	<b>0.002 Meter Rill Storage</b>	<b>0.02 Meter Rill Storage</b>
Q/P	0.25	0.36	0.36
ET/P	0.75	0.65	0.65
E/ET	0.30	0.29	0.31
T/ET	0.70	0.71	0.69
Q <sub>b</sub> /Q	0.55	0.30	0.26
Q/Q <sub>r</sub> (Spillville)	1.00	1.27	1.28
Q/Q <sub>r</sub> (Otter Creek)	1.00	1.22	1.22

Based on these results, it was deemed that the small changes in the calibration ratios were outweighed by the increase in simulation time so the smaller rill storage (0.002 meters) was selected as the preferred option for the final URC model.

### 5.5 Final Parameter Values

Once the calibration process was complete, the final set of parameter values was assembled. Since the change in the rill storage value caused the simulations to slow down and would not be used in the final model, the preferred tile layer hydraulic conductivity simulations combined the best options from the other calibration simulations and it was selected as the final model. Plots and ratios for this final model can be found in the previous section discussing the tile layer hydraulic conductivity calibration. Table 5.10 contains the final material property values, Table 5.11 contains the final overland property values, Table 5.12 contains the final evaporation property values, and Table 5.13 contains the transpiration property values. The final LAI time series for agricultural, grassy, and forested areas used to calculate the evapotranspiration in the model can be found in Appendix B. The LAI values for developed areas and the stream remained 1.0 and 0 respectively.



Table 5.10: Final material property values used in URC watershed model.

Soil Type	Horizontal Hydraulic Conductivity (m/s)	Porosity	$\alpha$	$\beta$
Silt Loam	$2.11 \times 10^{-6}$	0.439	0.41	2.80
Silt Clay	$1.11 \times 10^{-6}$	0.481	1.62	1.32
Loamy Sand	$4.43 \times 10^{-6}$	0.387	2.67	1.45
Loam	$1.39 \times 10^{-6}$	0.399	1.11	1.47
Rock Outcrop	$1.60 \times 10^{-6}$	0.400	2.70	4.00
Tile	$3.28 \times 10^{-3}$	0.439	1.12	1.47
Stream	$1.20 \times 10^{-3}$	0.440		

Table 5.11: Final overland property values used in URC watershed model.

Land Cover Type	X and Y Friction	Rill Storage	Coupling Length
Agricultural	0.07	0.002	0.01
Grass	0.07	0.002	0.01
Forest	0.12	0.002	0.01
Developed	0.10	0.002	0.01
Wet Areas	0.05	0.002	0.01
Stream	0.03	0.002	0.01
Overland (Other)	0.08	0.002	0.01

Table 5.12: Final evaporation property values used in URC watershed model.

Land Cover Type	Evaporation Depth	Evaporation Limiting Saturation		Canopy Storage Parameters	Initial Interception Storage
		Minimum	Maximum		
Agricultural	0.2	0.30	0.40	0.00005	0.0
Grass	0.2	0.30	0.40	0.00005	0.0
Forest	0.2	0.30	0.40	0.00005	0.0
Developed	0.2	0.30	0.40	0.00005	0.0
Stream	0.0	0.20	0.32	0.0	0.0

Table 5.13: Final transpiration property values used in URC watershed model.

Land Cover Type	Root Depth	TLS Parameters				Transpiration Fitting Parameters		
		Wilting Point	Field Capacity	Oxic Limit	Anoxic Limit	C1	C2	C3
Agricultural	1.00	0.20	0.32	1.00	1.01	0.30	0.2	2.31x10 <sup>-7</sup>
Grass	0.93	0.20	0.32	1.00	1.01	0.30	0.2	2.31x10 <sup>-7</sup>
Forest	2.00	0.20	0.32	1.00	1.01	0.30	0.2	2.31x10 <sup>-7</sup>
Developed	1.00	0.20	0.32	1.00	1.01	0.30	0.2	2.31x10 <sup>-7</sup>
Stream	0.00	0.29	0.30	0.31	0.32	0.00	1.0	0.0

### 5.6 Chapter Summary

As with all models, the URC model required calibration to ensure that the simulations were accurately representing what was naturally occurring. The initial conditions for the model were developed from a fully saturated state by allowing the model to drain with a small amount of continuously applied PET. The depth to the groundwater tables was monitored in six observation wells scattered in the watershed and the average depth to the water table in these wells was compared to the depth to water table in a nearby USGS groundwater well. The output file specifying the initial heads for the model was selected by choosing the output time where the average depth was in adequate agreement with the USGS well. This output file provided the starting condition for the simulations but the examination of the model performance primarily occurred once the model had reached a pseudo steady state where the annual volumetric change in the main components of the hydrologic cycle was less than 1%.

Once the initial conditions for the model were selected, calibration moved on to fitting the model parameters. Four different areas were examined during the calibration process: the Van Genuchten  $\alpha$  and  $\beta$  values, the TLS parameters, the tile layer hydraulic conductivity, and the rill storage value. Simulations were performed which examined the impacts these parameters had on the model. The results from these simulations were compared by looking at annual hydrologic ratios. The annual hydrologic ratios examined

were total discharge to precipitation ( $Q/P$ ), evapotranspiration to precipitation ( $ET/P$ ), evaporation to evapotranspiration ( $E/ET$ ), transpiration to evapotranspiration ( $T/ET$ ), baseflow to total discharge ( $Q_b/Q$ ), and total discharge to estimated total discharge based on the USGS gauges on Otter Creek at Elgin, Iowa and the Turkey River at Spillville, Iowa ( $Q/Q_r$ ). In addition to the ratios, the hydrograph at the watershed outlet was visually compared to the estimated discharges based on the USGS gauges on Otter Creek at Elgin, and the Turkey River at Spillville.

Through this calibration process, a single model was selected which most accurately represented what was naturally occurring. This final model will be used in the following chapter to examine different scenarios and determine the impact each may have on URC watershed.

## CHAPTER 6: SIMULATED SCENARIOS

### 6.1 Introduction

Once the calibration was complete, the final model was used to simulate different hypothetical conservation practice scenarios for URC watershed. The simulations were used to quantify the change in flow and nitrogen load which could be possible if the practices covered by each scenario were implemented. There were two conservation practices used in the scenarios, cover crops with no-till or strip-till practices on all cropland and the construction of eight nitrate removal wetlands. Figure 6.1 shows the cropland on which cover crops with conservation tillage practices would be used and the locations of the nitrate removal wetlands.

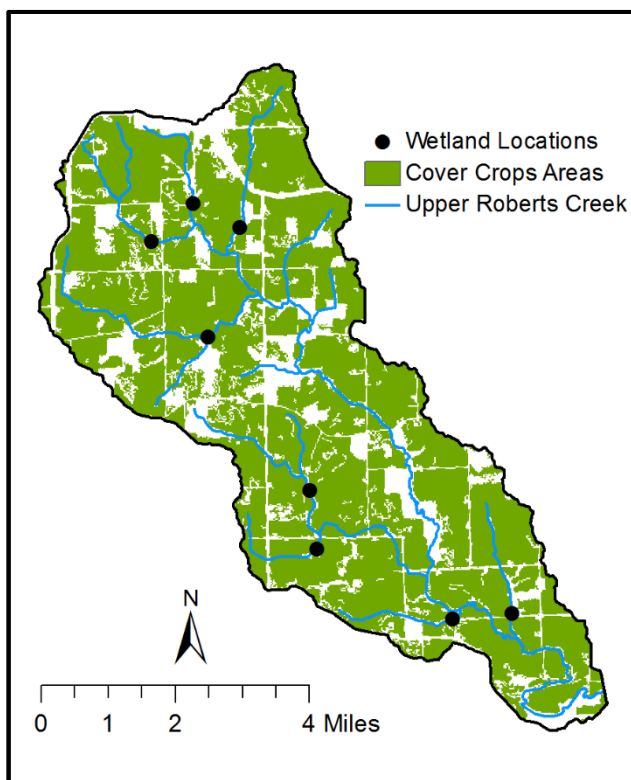


Figure 6.1: Locations of hypothetical conservation practice implementation in URC watershed.

Getting all farmers to use cover crops with no-till and strip-till practices on all their cropland would be very difficult and eight nitrate removal wetlands in URC watershed is a higher concentration than would likely be possible. As a point of reference, Rock Creek watershed in central Iowa is roughly twice the size of URC watershed and the watershed plan for Rock Creek only calls for seven nitrate removal wetlands (Keil and Sutphin 2014). The implementation of these practices at an unrealistic scale in URC watershed was used to quantify the maximum reductions in flow and nitrogen which could be observed in an ideal scenario.

Using these two conservation practices, three scenario groups were simulated; in the first group only cover crops with no-till and strip-till practices were simulated, in the second group only nitrate removal wetlands were simulated, and in the third group both cover crops with conservation tillage practices and nitrate removal wetlands were simulated. Each of these groups and the individual simulations which make up each group will be described in the rest of this chapter.

All of these simulations used the pseudo steady state flow field initial condition developed during the calibration process and nitrate concentration fields taken from previous simulations using the appropriate tile nitrate concentrations. These previous simulations showed that the nitrate field very quickly stabilized so only two consecutive years of 2014 data were run for each simulation with the results of the second year reported here.

## 6.2 Nitrate Modeling Using HydroGeoSphere

HGS lacks the biogeochemical modeling capabilities of other models such as the Root Zone Water Quality Model (RZWQM) or Agro-IBIS. Both of these models are capable of accounting for terrestrial nitrogen cycling and alternative practices such as tillage, crop rotation, and fertilizer application which could impact the runoff, subsurface drainage, and nitrogen or nitrate transported from a field (North Temperate Lakes 2015;

USDA 2014). Without these same capabilities, modeling nitrogen transport in HGS was performed through the application of a set concentration of a conservative tracer to all of the water which flowed through the tile layer. The concentration and load of that conservative tracer could then be monitored at the watershed outlet to estimate the nitrogen lost from the watershed. The imposed tile layer concentrations were adjusted between the different scenarios to reflect the conservation practices and the level of efficiency which was being modeled.

This use of the conservative tracer to model nitrate in the watershed is not reflective of how nitrogen interacts with the environment. In reality, tile layer nitrate is variable throughout the year with changes due to fertilizer application, growth cycle of the plants, and soil disturbance. Of particular concern, since almost all of the baseflow travels through the tile layer, is that all baseflow carries the tile layer concentration. This means that during dry periods of the year when baseflow is dominant the measured concentration at the outlet increases; the scenario results shown throughout this chapter and in Appendix C exhibit this response. However, based on the evaluation of measured concentration time series data, the opposite effect should occur. During extended dry periods the nitrate concentration in a stream or river decreases because rainfall is required to mobilize the nitrate in the soil. Although the nitrate load estimates shown within this chapter are adequate for this study, understanding these shortcomings within model and the conservative tracer methodologies used here are very important. The coupling of a powerful hydrologic model such as HGS and a model capable of simulating the biogeochemical processes within the soil would be a useful tool for these sorts of comparative watershed studies.

### 6.3 Baseline Scenario

Before the scenarios utilizing conservation practices could be run, a baseline needed to be established for comparison with the conservation practices. For the baseline

simulation a concentration of 25 mg/L of nitrate was assigned to the tile layer. The annual yield from the baseline simulation was 33.8 lbs./ac which is approximately 50% greater than the annual average of 22.3 lbs./ac which was measured at the USGS stream gauge location on the Turkey River at Garber, Iowa (USGS 05412500) from 2004 to 2008 (Garrett 2012). The Iowa Water Quality Information System (2015) reports that for 2014 at this same location the yield was 17.3 lbs./ac. The simulated baseline annual load, annual yield, and annual peak discharge are all shown in Table 6.1.

Table 6.1: Results from baseline scenario with tile concentration of 25 mg/L.

<b>Baseline Annual Load (lbs.)</b>	<b>Baseline Annual Yield (lbs./ac)</b>	<b>Baseline Annual Peak discharge (cfs)</b>
760,615	33.8	2,493

That the yield of the baseline simulation was larger than those observed in the Turkey River indicates that the tile nitrate concentration applied within the model was too large. This is not a serious concern as the modifications to that baseline which incorporate the conservation practices were done as percentages and the main goal was to simulate percent reductions in load which will remain unchanged, but it should be noted that the load estimates themselves are likely larger than those which are found in the watershed. Based on the data from the USGS gauge on the Turkey River at Garber, a better baseline tile nitrate concentration would have been around 12 mg/L which would have approximately halved the annual load and annual yield.

#### 6.4 Cover Crops with No-Till and Strip-Till Practices

The use of cover crops with no-till and strip-till practices produce several benefits including reduced soil erosion from wind and water, increased soil infiltration, increased soil organic matter, and decreased nitrate loss (Kladivko et al. 2014). Cover crops are

commonly planted in the fall after the harvest of the primary crop where they take up excess nitrate in the soil and prevent it from leaching into the streams. In the spring and summer as the cover crop residue breaks down, the nitrate is recycled into the soil where it can be taken up by the primary crop. Typical cover crops for Iowa include oats, wheat, rye, and triticale (Singer et al. 2005).

In the URC model, the use of cover crops with no-till and strip-till practices were simulated by changing the surface roughness, infiltration rate, and the nitrate concentration in the tile layer. Cover crops have been shown to increase the surface roughness because the plants on the surface offer more obstruction to the flow of water than a bare earth field. This is especially true when using no-till and strip-till practices where the crop residue further increases the surface roughness (Dabney 1998). The change in roughness was represented by increasing the Manning's n coefficient by 40% on agricultural land from 0.07 to 0.098. The increase of 40% was determined by comparing the Manning's n coefficient for fallow soils and those cultivated with residue (United States Department of Agriculture 1986).

Dabney (1998) and Folorunso et al. (1992) have shown that cover crops and conservation tillage practices can increase the infiltration rate of the soil between 30% and 100%. To account for the infiltration changes in the URC model, the vertical hydraulic conductivities of all the soil types in the watershed were increased by 40%. Table 6.2 shows the changes that were made to the hydraulic conductivity for all soil types.



Table 6.2: Vertical hydraulic conductivity changes used to account for the increased infiltration from the use of cover crops. The vertical hydraulic conductivity was increased 40% for all soils types.

<b>Soil Type</b>	<b>Baseline Vertical Hydraulic Conductivity (m/s)</b>	<b>Cover Crop Vertical Hydraulic Conductivity (m/s)</b>
Silt Loam	$2.11 \times 10^{-5}$	$2.95 \times 10^{-5}$
Silt Clay	$1.11 \times 10^{-5}$	$1.56 \times 10^{-5}$
Loamy Sand	$4.43 \times 10^{-5}$	$6.20 \times 10^{-5}$
Loam	$1.39 \times 10^{-5}$	$1.95 \times 10^{-5}$
Rock Outcrop	$1.60 \times 10^{-5}$	$2.24 \times 10^{-5}$
Tile	$1.39 \times 10^{-6}$	$1.39 \times 10^{-6}$
Stream	$1.20 \times 10^{-5}$	$1.74 \times 10^{-5}$

The third area of impact for cover crops is the reduced nitrate loss from fields, especially nitrate loss through drainage tiles, due to uptake by the cover crop. The potential reduction in annual nitrate loss has been shown to be 40% in the agricultural Midwest (Malone et al. 2014). HGS does not have the capability to account for nitrate removed through plant uptake. To account for the nitrate captured by cover crops, the tile nitrate concentration was reduced from the baseline condition by 20% (20 mg/L), 40% (15 mg/L), and 60% (10 mg/L). The 60% reduction in tile nitrate concentration is greater than the potential reduction shown by Malone et al. (2014); it was included as an upper limit for the scenarios. The scenario results reported in this chapter will include the 60% tile nitrate reduction but all figures and highlighted watershed changes will focus on the 40% tile nitrate reduction because it is the limit that has previously been shown in literature. The figures for all scenarios can be found in Appendix C. A summary of the changes to the URC model which account for the addition of cover crops and conservation tillage practices is found in Table 6.3.

Table 6.3: Changes to the URC model to account for cover crops and conservation tillage practices.

<b>Cover Crop Impact</b>	<b>Representation in the Model</b>	<b>Change to Model Input</b>	<b>Literature Source</b>
Increased surface roughness	Increase Manning's n coefficient on agricultural land	Increase Manning's n by 40% for agricultural land	Dabney (1998) United States Department of Agriculture (1986)
Increased infiltration	Increase the vertical hydraulic conductivity	Increase the vertical hydraulic conductivity by 40% for all soils	Dabney (1998) Folorunso et al. (1992)
Reduction of nitrate	Reduce the nitrate concentration in the tile layer	Reduce the baseline tile concentration (25 mg/L) by 20%, 40%, and 60%	Malone et al. (2014)

For each of the cover crop scenarios, the reduction in annual load and peak were calculated (Table 6.4 and Table 6.5). The load reduction was 35.3% with the 15 mg/L tile nitrate concentration and the peak reduction was approximately the same for all tile nitrate concentrations at 5.3%. The slight differences in the annual peak reductions are likely due to differences in the simulation time steps since the only change between these three simulations is the nitrate concentration which has no impact on the discharge. Figure 6.2 shows the annual simulation with the tile concentration of 15 mg/L and Figure 6.3 is the same simulation but focuses on the summer period from June 15, 2014 to July 9, 2014. Appendix C contains similar figures for the 20 mg/L and 10 mg/L tile concentrations.

Table 6.4: Load reductions from cover crop scenarios.

Scenario	Load Reduction (lbs.)	Percent Load Reduction	Annual Yield (lbs./ac)
Cover Crops and 20% Reduction in Tile Concentration	138,447	18.2%	27.6
Cover Crops and 40% Reduction in Tile Concentration	293,863	38.6%	20.7
Cover Crops and 60% Reduction in Tile Concentration	441,006	58.0%	14.2

Table 6.5: Peak reductions from cover crop scenarios. All of the scenarios had approximately the same peak discharge reduction.

Tile Concentration Reduction	Peak Discharge Reduction (cfs)	Percent Peak Discharge Reduction
20%	132	5.30%
40%	132	5.31%
60%	131	5.26%

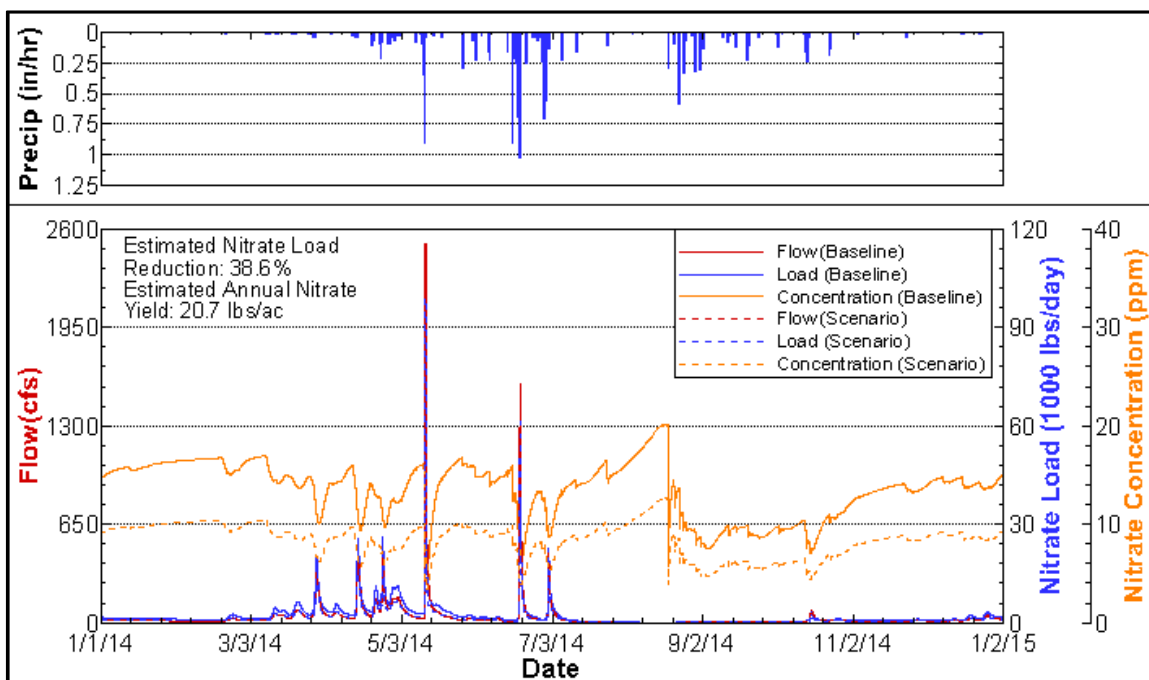


Figure 6.2: Annual cover crop simulation results with tile concentration reduction of 40% to 15mg/L.

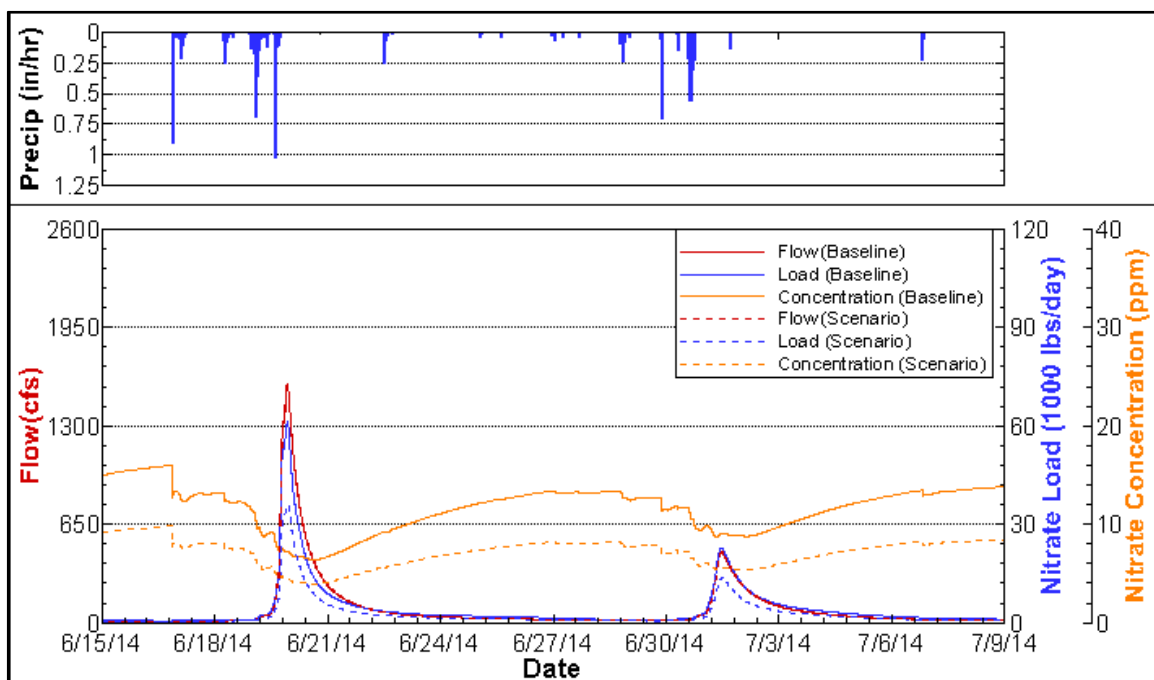


Figure 6.3: Cover crop simulation results from June 15 to July 9 with 40% reduction in the tile layer concentration of nitrate.

### 6.5 Nitrate Removal Wetlands

One of the large impacts that came about as a result of the transition from native prairies to agriculture was the removal and drainage of wetlands and one of the more promising ways to reduce the high levels of nitrate in streams which drain these agricultural areas is through the construction of new wetlands (Crumpton et al. 2006). Some studies have shown that wetlands can reduce the nitrate concentration in a stream by 40 to 90% (Iovanna et al. 2008). The Iowa Conservation Reserve Enhancement Program (CREP) has been working to establish wetlands in the 37 Iowa counties which use the most subsurface tile drainage with the goal of reducing the nitrate export and downstream impacts. URC watershed is not located in any of these counties but CREP served as a guide for the hypothetical URC wetlands.

To implement wetlands in the URC model, eight potential wetland locations were selected throughout the watershed. The location of each wetland was selected based on CREP guidelines and through visual inspection of aerial imagery and the watershed

DEM. CREP guidelines require that the wetlands must be located at a point which drains at least 500 acres of predominantly cropland, the wetland area should be between 0.5% and 2% of the drainage area flowing into it, 75% of the wetland must be less than 3 feet deep, and the wetlands must not prevent upstream land from draining properly (Crumpton et al. 2006). Sites were chosen which drained at least 500 acres and did not have a major impact on farm fields and property based on the aerial images. It was assumed that the correct wetland areas and depth would be achieved through the construction process and those criteria were not taken into account during site selection. Combined, the eight wetlands drain 49.2% of URC watershed. Figure 6.4 shows the numbering scheme which will be used to identify the wetland throughout the chapter and Table 6.6 shows the drainage area of each wetland.

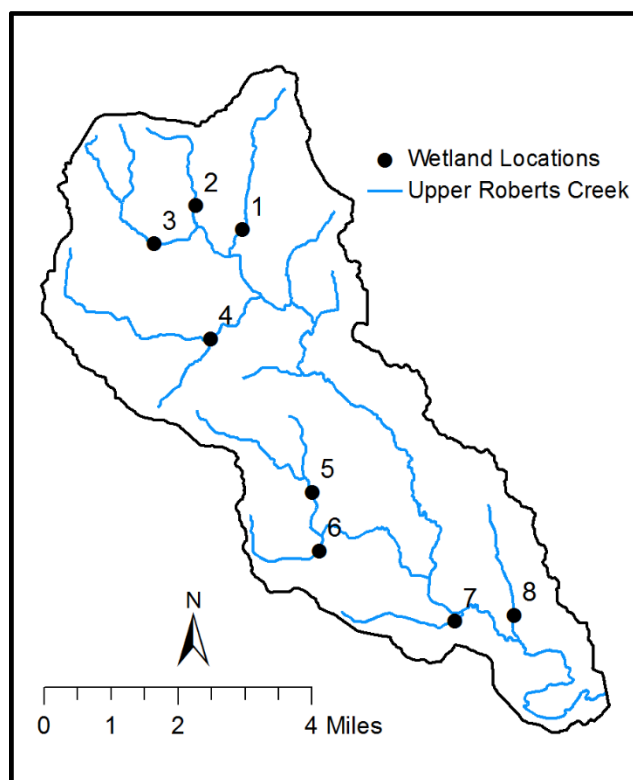


Figure 6.4: The numbering scheme for the hypothetical wetlands used in the URC model. The eight wetlands drain 49.2% of the watershed.

Table 6.6: The individual drainage areas and wetland surface areas for the hypothetical URC wetlands.

<b>Wetland Number</b>	<b>Drainage Area (acres)</b>	<b>Percent of Total Watershed</b>	<b>Wetland Surface Area - 0.5% of Drainage Area (acres)</b>	<b>Wetland Surface Area - 2.0% of Drainage Area (acres)</b>
1	1867.9	8.3%	9.3	37.4
2	528.7	2.3%	2.6	10.6
3	1624.7	7.2%	8.1	32.5
4	2777.4	12.3%	13.9	55.5
5	1470.9	6.5%	7.4	29.4
6	834.0	3.7%	4.2	16.7
7	742.5	3.3%	3.7	14.9
8	1235.3	5.5%	6.2	24.7
Sum	11081.6	49.2%		

With the wetland locations selected, the wetland weir heights needed to be chosen. CREP wetlands are designed with a single broadcrested weir outlet. Since they are designed for nitrate removal they do not provide significant flood storage and do not have an outlet pipe or alternate drain device which would lower the water level below the level of the weir. The weir heights which were modeled were determined from design plans obtained from the Natural Resources Conservation Service (NRCS) for seven CREP wetlands in Floyd County, Iowa. The average weir height on the seven wetlands was 1.86 meters so weir heights of 1 meter and 2 meters were selected for the model. In any individual simulation all of the wetlands were modeled with either a 1 meter weir or a 2 meter weir; there were no simulations where weir heights varied among the within the simulation.

To account for the weir height in the URC model, the rill storage was adjusted to match the desired height. The rill storage is the amount of water which is required on the surface before water is allowed to flow off of a given element. Although the rill storage of only a two elements was changed for each wetland, the site selection of the wetlands ensured that ponding occurred behind those elements to the level of the applied rill

storage. By modeling the wetlands through changes in the rill storage, physical changes to the elevations and the grid were avoided.

With the two weir heights selected, simulations were run to determine the volume of water the wetlands would store. This storage would later be used to ensure mass was conserved within the watershed and that there was balance between the simulations. The simulations used to determine the total storage in the wetlands were surface-only simulations so there was no infiltration or exfiltration. A baseline simulation was run without the wetlands where 5 inches of rain was applied over 20 days followed by 3 years of drainage without rainfall or PET. By the end of this simulation there was almost no discharge from the watershed and the volume of water remaining on the surface was calculated to determine the volume of water naturally stored within the depressions of the watershed. The same simulation was then run with the 1 meter and 2 meter wetlands in place. The difference between the volume of the water on the surface at the end of each of these simulations and the baseline condition was considered to be the total volume of the wetlands (Table 6.7).

Table 6.7: Storage in the hypothetical wetlands of URC. The volumes of all eight wetlands were combined in this storage calculation.

	<b>Baseline</b>	<b>1 Meter Wetland</b>	<b>2 Meter Wetland</b>
Volume Remaining on Surface (ac-ft)	148.4	193.8	277.3
Variation from Baseline – Wetland Volume (ac-ft)		46.1	129.7
Average Wetland Volume (ac-ft)		5.8	16.1

As in the baseline cover crop simulation, a tracer was applied to the tile in the wetland simulations at a concentration 25 mg/L. This continuity enabled the baseline cover crop simulation to be used as the baseline for the wetland simulations as well. As

mentioned in the cover crop section, HGS is able to model the movement of nitrate but is unable to model the uptake and storage of nitrate as it would occur in a wetland. However, with a known nitrate removal efficiency for the wetlands, the nitrate load output could be adjusted and quantify the impact of the wetlands.

Crumpton et al. (2006) have developed an equation to estimate the nitrate removal efficiency of CREP wetlands:

$$\text{Nitrate Removal Efficiency} = 103 \times \text{HLR}^{-0.33}$$

Where HLR is the annual hydraulic loading rate:

$$\text{HLR} = \frac{\text{Total Annual Discharge}}{\text{Surface Area}}$$

In the URC model, a hydrograph output location was placed at the downstream outlet point of each wetland. Using the discharge data from these points and the known surface area range of 0.5% to 2.0% of the total drainage area, the nitrate removal efficiency for each wetland in each simulation was calculated. The reduction in nitrate load from each of these wetlands could be combined to determine the reduction in nitrate load for the whole watershed. Table 6.8 shows the calculated wetland efficiencies and load reductions for the scenario with the 1 meter weir height and Table 6.9 shows the calculated wetland efficiencies and load reductions for the 2 meter weir height.



Table 6.8: Wetland efficiency and load reduction calculations for 1 meter wetland scenarios.

Wetland Number	Wetland Efficiency with Surface Area of 0.5% of Drainage Area	Wetland Efficiency with Surface Area of 2.0% of Drainage Area	Load Reduction with 0.5% Surface Area (lbs.)	Load Reduction with 0.5% Surface Area (lbs.)
1	26.17%	41.35%	15,458	24,425
2	26.32%	41.59%	4,464	7,053
3	26.41%	41.73%	13,565	21,435
4	25.95%	41.00%	25,215	39,842
5	25.83%	40.82%	13,176	20,819
6	26.52%	41.91%	6,830	10,792
7	26.21%	41.41%	6,347	10,029
8	26.10%	41.24%	11,178	17,663
<b>Total Watershed Load Reduction</b>			96,234	152,057

Table 6.9: Wetland efficiency and load reduction calculations for 2 meter wetland scenarios.

Wetland Number	Wetland Efficiency with Surface Area of 0.5% of Drainage Area	Wetland Efficiency with Surface Area of 2.0% of Drainage Area	Load Reduction with 0.5% Surface Area (lbs.)	Load Reduction with 0.5% Surface Area (lbs.)
1	25.07%	39.62%	16,942	26,770
2	26.48%	41.84%	4,401	6,954
3	26.43%	41.76%	13,547	21,405
4	26.01%	41.10%	25,019	39,532
5	25.58%	40.42%	13,428	21,217
6	26.83%	42.39%	6,697	10,582
7	26.43%	41.76%	6,185	9,773
8	26.28%	41.52%	11,011	17,399
<b>Total Watershed Load Reduction</b>			97,229	153,630

The calculated total watershed load reductions were used to modify the annual nitrate load at the outlet of the watershed to represent the load which would have been observed with the wetlands in place. From this new reduced watershed load, the annual watershed efficiency was calculated for each scenario and that efficiency was used to reduce the simulated load and concentration uniformly over the entire year. The

procedure is shown below and Table 6.10 contains the calculated annual watershed efficiencies.

$$\begin{aligned} & \text{Original Watershed Load} - \text{Total Watershed Load Reduction} \\ & = \text{Reduced Watershed Load} \end{aligned}$$

$$\begin{aligned} & \frac{\text{Original Watershed Load} - \text{Reduced Watershed Load}}{\text{Original Watershed Load}} \\ & = \text{Annual Watershed Efficiency} \end{aligned}$$

Table 6.10: Calculated annual watershed efficiencies for the wetland scenario simulations.

<b>Scenario</b>	<b>Annual Watershed Efficiency</b>
1 meter Wetland Weir with Surface Area 0.5% of Drainage Area	12.63%
1 meter Wetland Weir with Surface Area 2.0% of Drainage Area	19.97%
2 meter Wetland Weir with Surface Area 0.5% of Drainage Area	12.76%
2 meter Wetland Weir with Surface Area 2.0% of Drainage Area	20.16%

Since these wetlands were designed as nitrate removal wetlands, they are always full of water and therefore offered no flood storage or peak reduction. In fact, in both wetland cases the annual peak increased by about 1%. The results from the wetland only scenario group are shown in Table 6.11. The greatest annual nitrate load reduction was observed with the 2 meter wetland weir and a wetland surface area equal to 2.0% of the wetland drainage area.

Table 6.11: Results from the wetland scenario simulations. The simulation with the greatest load reduction was with the 2 meter wetland weir and a surface area which was 2.0% of the drainage area.

<b>Scenario</b>	<b>Load Reduction (lbs.)</b>	<b>Percent Load Reduction</b>	<b>Annual Yield (lbs./ac)</b>
1 meter Wetland Weir with Surface Area 0.5% of Drainage Area	95,269	12.5%	29.6
1 meter Wetland Weir with Surface Area 2.0% of Drainage Area	151,093	19.9%	27.1
2 meter Wetland Weir with Surface Area 0.5% of Drainage Area	95,929	12.6%	29.5
2 meter Wetland Weir with Surface Area 2.0% of Drainage Area	152,330	20.0%	27.0

The differences between the wetland with the 1 meter weir and the 2 meter weir are very small. In these scenarios, the wetland weir is built at the same location regardless of the size so the drainage area and the annual discharge from each wetland weir size should be the same. The only change in the calculation of the wetland efficiency, and therefore the nitrate load, is the surface area and it can be observed that the larger surface area does result in a greater overall watershed efficiency and nitrate load reduction. If wetland construction were to actually occur, the size of the weir would be based on the terrain and construction needs at the site and not on the targeted efficiency of the wetlands.

The complete annual simulation and the summer period from June 15 to July 9 for the scenario with the 2 meter wetland weir and wetland surface area equal to 2.0 percent of the total drainage area are shown in Figure 6.5 and Figure 6.6 respectively. Similar figures for the other scenarios can be found in Appendix C.

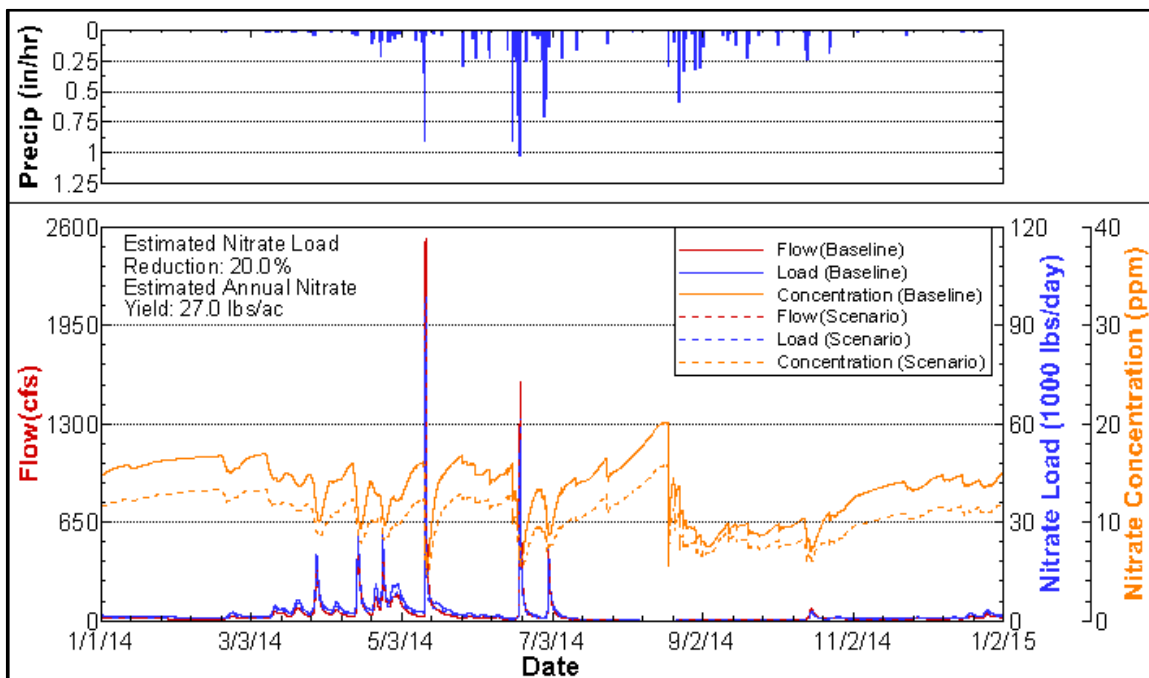


Figure 6.5: Annual simulation results from scenario with 2 meter wetland weir and a wetland surface area equal to 2.0% of total wetland drainage area. This scenario provided the greatest nitrate load reduction of wetland only scenario group.

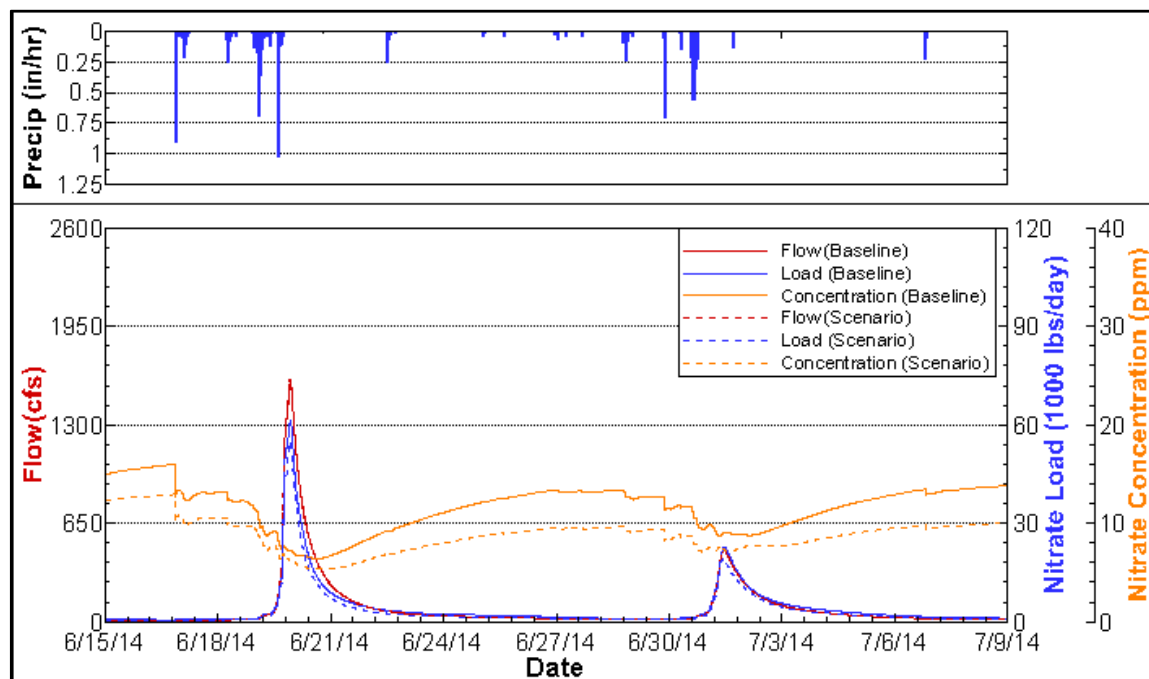


Figure 6.6: Simulation results from June 15 to July 9 from scenario with 2 meter wetland weir and a wetland surface area equal to 2.0% of total wetland drainage area.

The simulated percent load reductions were achieved with only 49.2% of the watershed draining through these wetlands. With that perspective, the impacts of these wetlands on the watershed are large and indicate that they could be an effective tool in reducing the nitrate load leaving the watershed. This would especially be true if the selection of locations ensured that a larger proportion of the watershed drained through the wetlands.

## 6.6 Combined Cover Crops with No-Till and Strip-Till

### Practices and Nitrate Removal Wetlands

The final scenario group incorporated both cover crops and wetlands. These combined practice scenarios offer the most potential to reduce nitrate below the level required in the Iowa Nutrient Reduction Strategy (Iowa Department of Agriculture and Land Stewardship et al. 2013). In these scenarios the tile nitrate concentrations were assigned at 20 mg/L, 15 mg/L, or 10 mg/L and the wetlands were assigned a weir height of 2 meters and surface areas of either 0.5% of the wetland drainage area or 2.0% of the wetland drainage area. The previous section showed that it was the wetland surface area and not the weir height that impacted the wetland efficiency; for this reason, only one wetland weir height was explored in the combined scenarios. In total there were six different scenarios tested in this scenario group.

The wetland efficiencies were calculated with the same methodology shown in the previous section. Table 6.12 shows the total watershed efficiencies for each of the scenarios.

Table 6.12: Watershed nitrate removal efficiencies for the combined practice scenarios.

<b>Scenario</b>	<b>Total Watershed Nitrate Removal Efficiency</b>
Cover Crops and 20% Reduction in Tile Nitrate Concentration and Wetland with Surface Area 0.5% of Drainage Area	12.72%
Cover Crops and 20% Reduction in Tile Nitrate Concentration and Wetland with Surface Area 2.0% of Drainage Area	20.09%
Cover Crops and 40% Reduction in Tile Nitrate Concentration and Wetland with Surface Area 0.5% of Drainage Area	12.72%
Cover Crops and 40% Reduction in Tile Nitrate Concentration and Wetland with Surface Area 2.0% of Drainage Area	20.10%
Cover Crops and 60% Reduction in Tile Nitrate Concentration and Wetland with Surface Area 0.5% of Drainage Area	12.69%
Cover Crops and 60% Reduction in Tile Nitrate Concentration and Wetland with Surface Area 2.0% of Drainage Area	20.05%

As mentioned in the previous section, the nitrate removal efficiencies are very similar between simulations with the wetland surface area equal to 0.5% of the wetland drainage area and between simulations with wetland surface area equal to 2.0% of the wetland drainage area because the flow through each wetland is approximately the same and the only change is in the surface area which changes the hydraulic loading rate and the nitrate removal efficiency of the wetland. The results for each of these simulations is shown in Table 6.13. The scenario with the 40% reduction in tile layer concentration and wetland surface area equal to 2.0% of wetland drainage area resulted in a watershed load reduction of 51.0%. The annual and summer plots for this scenario are shown in Figure 6.7 and 6.8 respectively.

Table 6.13: Results from the combined practice scenarios. The simulation with 40% reduction in tile nitrate concentration and wetland surface areas which are 2.0% of the wetland drainage areas showed a reduction in annual nitrate load of 51.0%.

<b>Scenario</b>	<b>Load Reduction (lbs.)</b>	<b>Percent Load Reduction</b>	<b>Annual Yield (lbs./ac)</b>
Cover Crops and 20% Reduction in Tile Nitrate Concentration and Wetland with Surface Area 0.5% of Drainage Area	217,134	28.5%	24.1
Cover Crops and 20% Reduction in Tile Nitrate Concentration and Wetland with Surface Area 2.0% of Drainage Area	263,063	34.6%	22.1
Cover Crops and 40% Reduction in Tile Nitrate Concentration and Wetland with Surface Area 0.5% of Drainage Area	353,121	46.4%	18.1
Cover Crops and 40% Reduction in Tile Nitrate Concentration and Wetland with Surface Area 2.0% of Drainage Area	387,566	51.0%	16.6
Cover Crops and 60% Reduction in Tile Nitrate Concentration and Wetland with Surface Area 0.5% of Drainage Area	481,344	63.3%	12.4
Cover Crops and 60% Reduction in Tile Nitrate Concentration and Wetland with Surface Area 2.0% of Drainage Area	504,893	66.4%	11.4

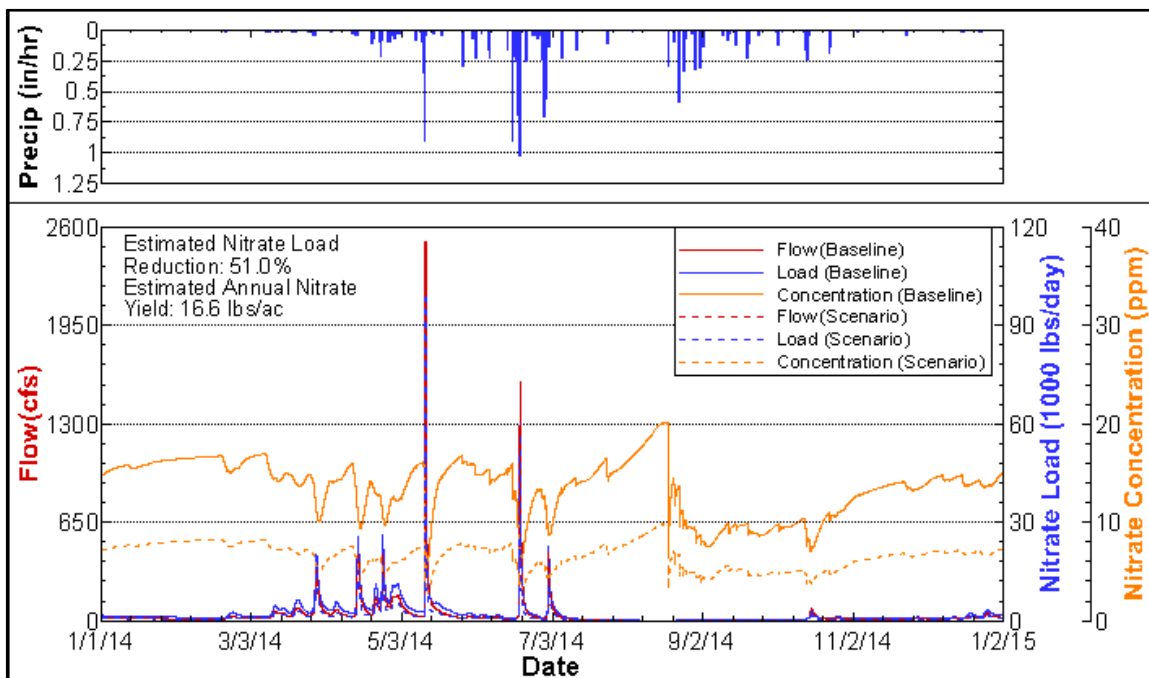


Figure 6.7: Annual simulation results for scenario with cover crops, 40% reduction in tile layer nitrate concentration, and a wetland surface area equal to 2.0% of the wetland drainage area.

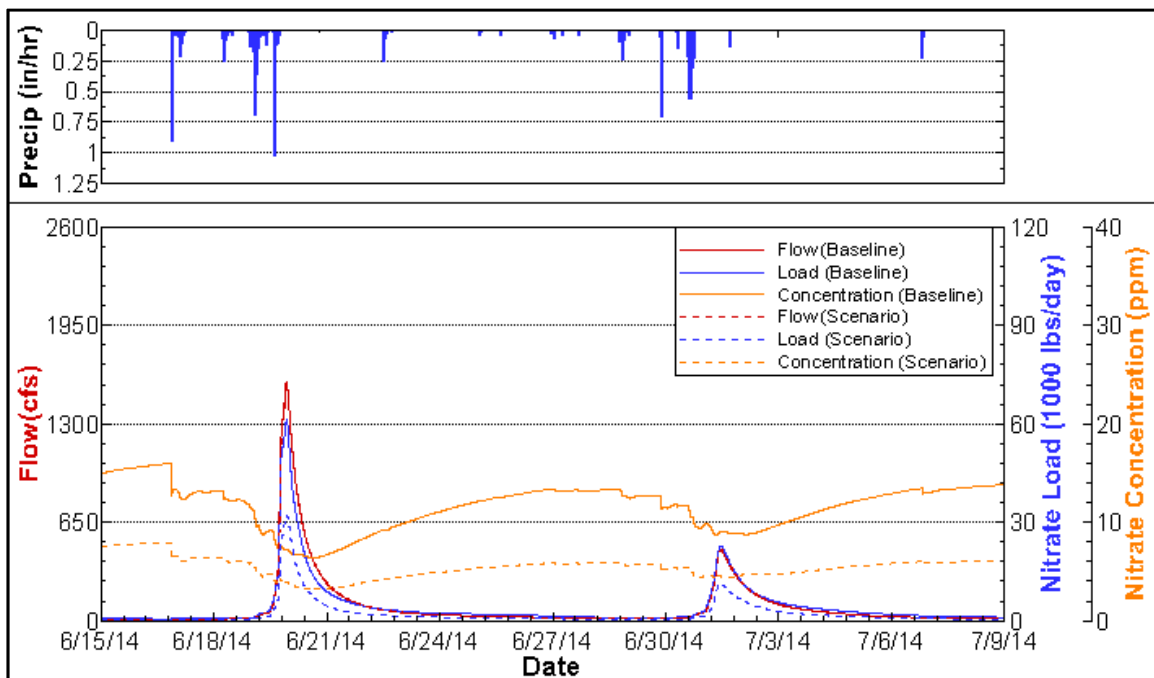


Figure 6.8: Simulation results from June 15 to July 9 for scenario with cover crops, 40% reduction in tile layer nitrate concentration, and a wetland surface area equal to 2.0% of the wetland drainage area.



All of the combined scenarios which used cover crops with the 40% or 60% reduction in tile nitrate concentration could have theoretically achieved the Iowa Nutrient Reduction Strategy goal of 41% nitrogen load reduction from non-point sources, regardless of the wetland design used.

### 6.7 Chapter Summary

With a calibrated model of URC, scenarios were tested to determine the possible nitrate load reduction from BMPs. There were two different conservation practices which were combined to form three scenario groups. The two conservation practices were the use of cover crops along with conservation tillage practices and the construction of eight wetlands in the watershed. The three scenario groups were each conservation practice on its own and the combination of the two as a combined practice scenario group.

Before any scenarios could be run, a baseline was established where the calibrated URC model was run with an assigned tile nitrate concentration of 25 mg/L. The result from this baseline test was an annual watershed nitrate yield of 33.8 lbs./ac which approximately 50% greater than the 22.3 lbs./ac measured for the Turkey River watershed.

With this baseline established, the scenarios were run. The within the cover crop scenario group the surface roughness and infiltration were increased with changes to Manning's n on agricultural lands and the vertical hydraulic conductivity on all soils. The tile nitrate concentration was reduced by 20%, 40%, or 60%, depending on the simulation, to account for the increased nitrate uptake from the cover crops. The nitrate load reduction from the cover crop scenario group was 38.6% with the 40% reduction in tile nitrate concentration.

The wetland scenarios looked at the construction of the wetlands and how efficient the wetlands would be at removing nitrate. It was assumed that any wetlands in the watershed would be constructed with a design similar to CREP wetlands. This means

that they would have a surface area of between 0.5% and 2.0% of the total wetland drainage area. Using the simulated flow through each wetland and the designed surface area range, a range of wetland efficiencies was developed and the simulation results were modified to show the nitrate removal possible through wetland construction. The constructed wetlands took four different forms based on two weir heights (1 meter and 2 meters) and the two surface area extremes. The greatest nitrate load reduction for the wetland scenarios was 20.0% from the wetlands with 2 meter weirs and wetland surface areas which were 2.0% of the wetland drainage area.

The final scenario group was the combination of the two individual practices. The nitrate load reduction from the combined scenario of cover crops with a tile nitrate concentration of 15 mg/L and wetlands with surface areas which were 2.0% of the total wetland drainage area was 51%. All of the combined scenarios which involved the 40% or 60% reduction in tile nitrate concentration exceeded the 41% non-point source nitrate reduction targeted in the Iowa Nutrient Reduction Strategy.

## CHAPTER 7: SUMMARY AND CONCLUSIONS

This Master's thesis set out to accomplish 3 goals:

- 1) Develop a hydrologic model for URC which reproduces observed annual water balance ratios.
- 2) Evaluate potential nitrate reduction benefits from the use of cover crops and CREP-style wetlands in URC.
- 3) Determine the combinations of conservation strategies and BMPs which may theoretically achieve the Iowa Nutrient Reduction Strategy goal of reducing the nitrogen load from non-point sources by 41%.

To accomplish these goals, a hydrologic model was developed using the modeling software HGS, calibrated with data inputs from gauges and instruments near the watershed, and used to evaluate the potential changes BMPs could have when compared against a baseline. In the end all three goals were achieved through the working hydrologic model of URC.

### 7.1 Development of the Upper Roberts Creek Model

The URC model was developed with HGS which is a three dimensional, surface/subsurface, distributed, physically-based hydrologic modeling program. HGS allows for the complete simulation of watershed processes and for the inclusion of nitrate transport within the model. An unstructured, triangular surface grid was developed based on the physical characteristics of the watershed which had 12,300 surface nodes and 24,316 two dimensional elements. This surface grid was layered 15 times from the surface to the bedrock with a greater density of layers near the surface of the model to allow for a quicker response to the soil moisture changes which occur there. The end result was a grid with 15 nodal layers and 14 elemental layers containing a total of 184,500 nodes and 340,424 three dimensional elements.

Material, overland flow, and evapotranspiration properties were all assigned to the model grid based on the physical characteristics present at each location with parameters assigned based on literature values. Material properties were assigned based on soil types from SSURGO data while overland flow and evapotranspiration properties were assigned based on NLCD data.

In addition to the physical information, inputs were also required to complete the URC model. Precipitation data was gathered from five IFC rainfall gauges in nearby Otter Creek. The average rainfall from these gauges supplied most of the rainfall data for 2014 with data from a climate station at Calmar, Iowa filling in information prior to the installation of the Otter Creek gauges. Evapotranspiration data was gathered from a site near Nashua, Iowa and was adjusted with a cropping coefficient based on corn as the predominant crop and land cover in URC watershed. The combination of this physical model information and the model inputs formed the complete URC model.

## 7.2 Calibration of the Upper Roberts Creek Model

With the model developed, calibration was needed to ensure that it was accurately simulating the watershed behavior. Four areas were examined during the calibration process: the Van Genuchten parameters, the TLS parameters, the hydraulic conductivity of the tile layer, and the rill storage value.

The predominant soil type in URC watershed is silt loam which covers over 98% of the watershed. Through the adjustment of the Van Genuchten  $\alpha$  and  $\beta$  values for silt loam, the simulated response of groundwater wells to rainfall events was calibrated to the observed response in nearby wells. Three different combinations of  $\alpha$  and  $\beta$  were tested before settling on  $\alpha=0.41$  and  $\beta=2.80$ .

The TLS parameters were adjusted to ensure that the simulated discharge peaks matched the estimated peaks used throughout the calibration process, especially those

peaks later in the year. Six different TLS value sets were tested with the most accurate set being that which allowed for the greatest amount of watershed transpiration.

The tile layer was modeled throughout the watershed so an equivalent hydraulic conductivity was needed to accurately represent the impact the tile layer would have on the landscape. Five different hydraulic conductivities were tested and the one that produced the most accurate response was the equivalent of drain tile lines spaced every 10 meters.

The final area explored during calibration was the value used for rill storage in the watershed. Three different rill storage values were tested; one was one order of magnitude larger than the original and the other was two orders of magnitude larger. The two larger values slowed down the simulation without major impacts to the calibration ratios so the original value was retained in the final model.

### 7.3 Use of the Upper Roberts Creek Model

The calibrated model was used to explore the impacts conservation practices and BMPs would have on URC watershed. To do this, simulations incorporating conservation practices were run with 2014 data and compared to a baseline simulation which did not include any conservation practices. Two main conservation practices were explored: the use of cover crops on all agricultural land in the watershed and the construction of eight CREP-style wetlands. These conservation practices were applied as part of three groups of simulations: those with only cover crops, those with only wetlands, and those with the combined practices of cover crops and wetlands.

#### 7.3.1 Simulated Peak Flow and Nitrate Load Reduction from Cover Crops

The use of cover crops in URC watershed was simulated through increasing the surface roughness on agricultural land by 40% to account for increased plant residue, increasing the hydraulic conductivity of all soils by 40% to account for increased

infiltration, and reducing the tile layer nitrate concentration by 20%, 40%, or 60% to account for the ability of the cover crops to take up nitrate from the soil. There was a 5.3% reduction in annual peak discharge as a result of the implementation of cover crops. The annual nitrate load reduction with the 40% reduction in tile nitrate concentration was 38.6%.

### 7.3.2 Simulated Nitrate Load Reduction from Constructed Wetlands

CREP wetland general guidelines were followed when choosing the locations for the eight wetlands in URC; additionally, locations were selected which limited the impact the wetlands would have on agricultural. There were two main components to the wetland design: the weir height and the surface area of the wetland. The two weir designs considered were 1 meter and 2 meters high and the two surface areas considered were the CREP design limits of 0.5% and 2.0% of the wetland drainage area. The nitrate removal efficiency was calculated for each wetland in each simulation based on the flow through the wetland and the surface area of each wetland. From those individual efficiencies, a total watershed efficiency was calculated and the outlet concentration was reduced to reflect the impact of the wetlands. The maximum annual nitrate load reduction for the wetland only scenarios was 20.0% which was achieved from the wetlands with the 2 meter weir and a surface area equal to 2.0% of the wetland drainage area.

### 7.3.3 Simulated Nitrate Load Reductions from Combined Scenarios

Neither one of the previous scenario groups on their own were able to theoretically achieve the 41% nitrate reduction goal outlined in the Iowa Nutrient Reduction Strategy. It is unlikely that a single practice would make the impact that is needed; equally unlikely is it that a single practice would be expected to reduce nitrogen loads to the levels targeted in the Iowa Nutrient Reduction Strategy. The combination of

multiple practices is a much more likely approach and is much more likely to succeed. With this in mind, the cover crops and wetland scenarios were combined in simulations to see what nitrate load reductions might be possible through the use of both practices.

In these scenarios, the tile nitrate concentration was reduced from its initial value by 20%, 40%, and 60% as was done in the cover crops scenarios and the wetland surface areas were set at at 0.5% or 2.0% of the wetland drainage area as was done in the wetland scenarios. The wetland weir heights were all set at 2 meters because the wetland only scenarios showed that the wetland weir height had very little impact on the wetland efficiency. The load reduction from the combination scenario of tile nitrate concentration reduction of 40% accompanied wetland surface areas which were 2.0% of the total drainage area was 51.0%. In fact, all of the combined scenarios involving the 40% or 60% reduction in tile nitrate concentration showed the potential to achieve the Iowa Nutrient Reduction Strategy goal of reducing non-point source nitrogen by 41%.

#### 7.4 Final Remarks

The few scenarios simulated within this thesis are by no means the only available nitrogen reduction strategies. As mentioned in the section discussing the combined practice scenarios, the solution to the excessive discharge of nitrogen from Iowa waters is not any single practice but the combination of practices which are each capable of making a small reduction to the larger problem. The reduction estimates reported within this thesis are based on the assumptions outline throughout the thesis and represent what is currently known about these practices. As the field evolves, the understanding of these practices and their impacts will change. Hydrologic models such as the one developed for URC offer the potential to simulate the reductions offered by these combinations of practices saving time and money from costly project construction and testing but only when accompanied by the most up to date information concerning nitrogen reduction practices. Hydrologic models such as this should not be static but should evolve along

with the science to ensure that the most accurate information is available to the policy and decision makers who need it.



## APPENDIX A: COMPLETE CALIBRATION RESULTS

This appendix contains the complete results from the simulations performed during the calibration process. The percentages reported are the volumetric changes which occurred between the simulation years.

Table A.1: The calibration ratios and volumetric changes for the Van Genuchten parameter calibration simulations. Five years of simulations were performed but a pseudo steady state with a 1% change criteria was not achieved.

Year	Ratios	Target	Initial Values		Calibration Set 1		Calibration Set 2		Calibration Set 3	
			Ratio Value	Percent Change	Ratio Value	Percent Change	Ratio Value	Percent Change	Ratio Value	Percent Change
1	Q/P	0.25	0.15		0.49		0.38		0.26	
	ET/P	0.75	0.08		0.34		0.38		0.45	
	E/ET	0.30	0.74		0.58		0.47		0.38	
	T/ET	0.70	0.29		0.42		0.53		0.62	
	Q <sub>b</sub> /Q	0.55	0.48		0.26		0.30		0.36	
	Q/Q <sub>r</sub> (Spillville)	1.00	0.54		1.75		1.36		0.94	
	Q/Q <sub>r</sub> (Otter Creek)	1.00	0.56		1.86		1.45		1.00	
2	Q/P	0.25	0.39	158.8%	0.69	39.8%	0.62	63.1%	0.52	95.5%
	ET/P	0.75	0.18	123.0%	0.28	-7.5%	0.31	-19.3%	0.37	-17.7%
	E/ET	0.30	0.62	85.3%	0.74	4.6%	0.65	11.1%	0.54	17.4%
	T/ET	0.70	0.38	232.0%	0.26	-48.3%	0.35	-46.6%	0.46	-39.1%
	Q <sub>b</sub> /Q	0.55	0.43	129.6%	0.26	35.4%	0.27	45.9%	0.30	61.8%
	Q/Q <sub>r</sub> (Spillville)	1.00	1.40		2.45		2.22		1.85	
	Q/Q <sub>r</sub> (Otter Creek)	1.00	1.41		2.47		2.25		1.88	

Table A.1 - continued

Year	Ratios	Target	Initial Values		Calibration Set 1		Calibration Set 2		Calibration Set 3	
			Ratio Value	Percent Change	Ratio Value	Percent Change	Ratio Value	Percent Change	Ratio Value	Percent Change
3	Q/P	0.25	0.66	69.1%	Only 2 years of simulations with calibration set 1 were performed.	0.71	13.8%	0.65	26.5%	
	ET/P	0.75	0.27	44.0%		0.28	-10.6%	0.31	-15.7%	
	E/ET	0.30	0.67	56.1%		0.74	2.0%	0.66	3.0%	
	T/ET	0.70	0.33	24.4%		0.26	-34.0%	0.34	-37.6%	
	Q <sub>b</sub> /Q	0.55	0.33	32.9%		0.26	10.9%	0.27	16.9%	
	Q/Q <sub>r</sub> (Spillville)	1.00	2.37			2.53		2.33		
	Q/Q <sub>r</sub> (Otter Creek)	1.00	2.34			2.53		2.34		
4	Q/P	0.25	0.71	6.9%		0.74	4.0%	0.70	7.3%	
	ET/P	0.75	0.28	7.2%		0.26	-4.2%	0.29	-5.8%	
	E/ET	0.30	0.66	6.2%		0.78	0.5%	0.71	1.0%	
	T/ET	0.70	0.34	9.2%		0.22	-17.9%	0.29	-18.9%	
	Q <sub>b</sub> /Q	0.55	0.33	6.2%		0.26	3.6%	0.27	5.7%	
	Q/Q <sub>r</sub> (Spillville)	1.00	2.53			2.63		2.50		
	Q/Q <sub>r</sub> (Otter Creek)	1.00	2.49		2.63		2.50			

Table A.1 - continued

Year	Ratios	Target	Initial Values		Calibration Set 1		Calibration Set 2		Calibration Set 3	
			Ratio Value	Percent Change	Ratio Value	Percent Change	Ratio Value	Percent Change	Ratio Value	Percent Change
5	Q/P	0.25	0.71	0.8%	Only 2 years of simulations with calibration set 1 were performed.	0.75	1.3%	0.72	2.4%	
	ET/P	0.75	0.29	1.4%		0.26	-1.5%	0.28	-2.6%	
	E/ET	0.30	0.66	0.9%		0.79	0.1%	0.73	0.3%	
	T/ET	0.70	0.34	2.4%		0.21	-7.5%	0.27	-9.7%	
	Q <sub>b</sub> /Q	0.55	0.33	1.3%		0.26	1.4%	0.27	2.2%	
	Q/Q <sub>r</sub> (Spillville)	1.00	2.55			2.66		2.56		
	Q/Q <sub>r</sub> (Otter Creek)	1.00	2.51			2.67		2.56		

Table A.2: The calibration ratios and volumetric changes for the TLS parameter calibration simulations. Six years of simulations were performed for calibration set 5 which was the only set tested to reach the pseudo steady state.

Year	Ratios	Target	Original Set		Calibration Set 1		Calibration Set 2		Calibration Set 3		Calibration Set 4		Calibration Set 5	
			Ratio Value	$\Delta\%$	Ratio Value	$\Delta\%$	Ratio Value	$\Delta\%$	Ratio Value	$\Delta\%$	Ratio Value	$\Delta\%$	Ratio Value	$\Delta\%$
1	Q/P	0.25	0.26		0.26		0.25		0.24		0.22		0.14	
	ET/P	0.75	0.45		0.45		0.46		0.47		0.50		0.60	
	E/ET	0.30	0.38		0.37		0.36		0.35		0.33		0.27	
	T/ET	0.70	0.92		0.63		0.64		0.65		0.67		0.73	
	Q <sub>b</sub> /Q	0.55	0.36		0.36		0.35		0.35		0.35		0.41	
	Q/Q <sub>r</sub> (Spillville)	1.00	0.94		0.92		0.90		0.86		0.78		0.49	
	Q/Q <sub>r</sub> (Otter Creek)	1.00	1.00		0.97		0.95		0.90		0.82		0.50	
2	Q/P	0.25	0.52	95.5%	0.50	95.3%	0.49	95.1%	0.47	93.8%	0.41	87.2%	0.26	90.3%
	ET/P	0.75	0.37	-17.7%	0.38	-16.2%	0.39	-14.6%	0.42	-11.1%	0.48	-3.1%	0.64	7.8%
	E/ET	0.30	0.54	17.4%	0.52	17.1%	0.50	16.7%	0.46	16.8%	0.40	15.8%	0.29	14.4%
	T/ET	0.70	0.46	-39.1%	0.48	-35.8%	0.50	-32.6%	0.54	-26.4%	0.60	-12.6%	0.71	5.3%
	Q <sub>b</sub> /Q	0.55	0.30	61.8%	0.30	62.3%	0.30	63.2%	0.30	64.4%	0.31	62.7%	0.34	58.3%
	Q/Q <sub>r</sub> (Spillville)	1.00	1.85		1.80		1.75		1.66		1.46		0.94	
	Q/Q <sub>r</sub> (Otter Creek)	1.00	1.88		1.83		1.78		1.68		1.46		0.90	

Table A.2 - continued

Year	Ratios	Target	Original Set		Calibration Set 1		Calibration Set 2		Calibration Set 3		Calibration Set 4		Calibration Set 5	
			Ratio Value	Δ%	Ratio Value	Δ%	Ratio Value	Δ%	Ratio Value	Δ%	Ratio Value	Δ%	Ratio Value	Δ%
3	Q/P	0.25	0.65	26.5%	0.64	26.0%	0.62	25.3%	0.58	24.2%	0.47	15.5%	0.33	27.3%
	ET/P	0.75	0.31	-15.7%	0.33	-13.8%	0.35	-11.3%	0.39	-7.5%	0.47	-2.0%	0.65	0.7%
	E/ET	0.30	0.66	3.0%	0.62	3.0%	0.58	3.0%	0.51	2.6%	0.41	1.7%	0.29	2.1%
	T/ET	0.70	0.34	-37.6%	0.38	-31.8%	0.42	-25.6%	0.49	-16.2%	0.59	-4.5%	0.71	0.2%
	Q <sub>b</sub> /Q	0.55	0.27	16.9%	0.28	16.9%	0.28	16.8%	0.28	16.3%	0.30	13.1%	0.30	13.8%
	Q/Q <sub>r</sub> (Spillville)	1.00	2.33		2.27		2.20		2.06		1.69		1.19	
	Q/Q <sub>r</sub> (Otter Creek)	1.00	2.34		2.27		2.19		2.05		1.65		1.14	
4	Q/P	0.25	0.70	7.3%	0.68	7.0%	0.66	6.8%	0.61	6.1%	0.46	-1.8%	0.33	-0.9%
	ET/P	0.75	0.29	-5.8%	0.31	-4.6%	0.34	-3.5%	0.38	-1.8%	0.46	-2.1%	0.65	0.1%
	E/ET	0.30	0.71	1.0%	0.65	0.9%	0.60	0.7%	0.53	0.7%	0.41	-3.2%	0.29	-0.1%
	T/ET	0.70	0.29	-18.9%	0.35	-13.5%	0.40	-9.2%	0.47	-4.4%	0.59	-1.3%	0.71	0.2%
	Q <sub>b</sub> /Q	0.55	0.27	5.7%	0.27	5.5%	0.27	5.2%	0.27	4.6%	0.32	5.9%	0.30	-2.9%
	Q/Q <sub>r</sub> (Spillville)	1.00	2.50		2.43		2.34		2.19		1.66		1.18	
	Q/Q <sub>r</sub> (Otter Creek)	1.00	2.50		2.42		2.33		2.17		1.60		1.16	

Table A.2 - continued

Year	Ratios	Target	Original Set		Calibration Set 1		Calibration Set 2		Calibration Set 3		Calibration Set 4		Calibration Set 5	
			Ratio Value	Δ%	Ratio Value	Δ%	Ratio Value	Δ%	Ratio Value	Δ%	Ratio Value	Δ%	Ratio Value	Δ%
5	Q/P	0.25	0.72	2.4%	0.70	2.2%	0.67	2.0%	0.62	1.6%	0.51	8.9%	0.36	7.3%
	ET/P	0.75	0.28	-2.6%	0.31	-1.8%	0.33	-1.4%	0.38	-0.6%	0.46	0.4%	0.65	0.1%
	E/ET	0.30	0.73	0.3%	0.67	0.5%	0.61	0.1%	0.53	0.1%	0.43	4.8%	0.29	0.5%
	T/ET	0.70	0.27	-9.7%	0.33	-6.0%	0.39	-3.7%	0.47	-1.5%	0.57	-2.7%	0.71	-0.1%
	Q <sub>b</sub> /Q	0.55	0.27	2.2%	0.27	2.0%	0.27	1.8%	0.27	1.4%	0.30	-0.4%	0.30	7.3%
	Q/Q <sub>r</sub> (Spillville)	1.00	2.56		2.48		2.39		2.23		1.81		1.27	
	Q/Q <sub>r</sub> (Otter Creek)	1.00	2.56		2.47		2.38		2.20		1.80		1.21	
6	Q/P	0.25	0.73	1.0%	0.70	0.8%	0.68	0.7%	0.63	0.6%	0.55	7.8%	0.36	0.6%
	ET/P	0.75	0.28	-0.6%	0.31	-0.2%	0.33	0.3%	0.38	0.4%	0.46	-0.5%	0.65	0.0%
	E/ET	0.30	0.74	1.3%	0.68	1.2%	0.62	1.5%	0.54	1.2%	0.44	1.3%	0.29	0.1%
	T/ET	0.70	0.26	-5.7%	0.32	-3.1%	0.38	-1.5%	0.46	-0.6%	0.56	-1.8%	0.71	0.0%
	Q <sub>b</sub> /Q	0.55	0.27	0.8%	0.27	0.5%	0.27	0.3%	0.27	0.2%	0.28	1.8%	0.30	0.6%
	Q/Q <sub>r</sub> (Spillville)	1.00	2.56		2.48		2.39		2.23		1.95		1.27	
	Q/Q <sub>r</sub> (Otter Creek)	1.00	2.58		2.49		2.39		2.21		1.91		1.22	

Table A.3: The calibration ratios and volumetric changes for the different tile layer hydraulic conductivity values tested in the calibration process. The different tile layer hydraulic conductivities represented potential tile spacing in the watershed. Six years of simulations were performed at which point all the simulations had reached a pseudo steady state.

Year	Ratios	Target	No Tile		10 Meter		15 Meter		20 Meters		25 Meters		30 Meters	
			Ratio Value	$\Delta\%$	Ratio Value	$\Delta\%$	Ratio Value	$\Delta\%$	Ratio Value	$\Delta\%$	Ratio Value	$\Delta\%$	Ratio Value	$\Delta\%$
1	Q/P	0.25	0.14		All tile simulations were run from the end of the second year of the no tile simulations.									
	ET/P	0.75	0.60											
	E/ET	0.30	0.27											
	T/ET	0.70	0.73											
	Q <sub>b</sub> /Q	0.55	0.41											
	Q/Q <sub>r</sub> (Spillville)	1.00	0.49											
	Q/Q <sub>r</sub> (Otter Creek)	1.00	0.50											
2	Q/P	0.25	0.26	90.3%										
	ET/P	0.75	0.64	7.8%										
	E/ET	0.30	0.29	14.4%										
	T/ET	0.70	0.71	5.3%										
	Q <sub>b</sub> /Q	0.55	0.34	58.3%										
	Q/Q <sub>r</sub> (Spillville)	1.00	0.94											
	Q/Q <sub>r</sub> (Otter Creek)	1.00	0.90											



Table A.3 - continued

Year	Ratios	Target	No Tile		10 Meter		15 Meter		20 Meters		25 Meters		30 Meters	
			Ratio Value	Δ%	Ratio Value	Δ%	Ratio Value	Δ%	Ratio Value	Δ%	Ratio Value	Δ%	Ratio Value	Δ%
3	Q/P	0.25	0.33	27.3%	0.35		0.35		0.34		0.34		0.34	
	ET/P	0.75	0.65	0.7%	0.65		0.65		0.65		0.65		0.65	
	E/ET	0.30	0.29	2.1%	0.29		0.29		0.29		0.29		0.29	
	T/ET	0.70	0.71	0.2%	0.71		0.71		0.71		0.71		0.71	
	Q <sub>b</sub> /Q	0.55	0.30	13.8%	0.69		0.60		0.55		0.51		0.48	
	Q/Q <sub>r</sub> (Spillville)	1.00	1.19		1.26		1.23		1.22		1.21		1.20	
	Q/Q <sub>r</sub> (Otter Creek)	1.00	1.14		1.18		1.16		1.15		1.15		1.15	
4	Q/P	0.25	0.33	-0.9%	0.36	1.1%	0.35	2.6%	0.35	3.4%	0.35	3.9%	0.35	4.2%
	ET/P	0.75	0.65	0.1%	0.65	0.1%	0.65	0.2%	0.65	0.3%	0.65	0.2%	0.65	0.3%
	E/ET	0.30	0.29	-0.1%	0.29	0.0%	0.29	-0.2%	0.29	0.2%	0.29	0.0%	0.30	0.8%
	T/ET	0.70	0.71	0.2%	0.71	0.2%	0.71	0.4%	0.71	0.3%	0.71	0.3%	0.70	0.1%
	Q <sub>b</sub> /Q	0.55	0.30	-2.9%	0.68	0.0%	0.60	1.8%	0.54	2.7%	0.51	3.3%	0.48	3.6%
	Q/Q <sub>r</sub> (Spillville)	1.00	1.18		1.27		1.26		1.26		1.26		1.26	
	Q/Q <sub>r</sub> (Otter Creek)	1.00	1.16		1.20		1.20		1.20		1.20		1.20	

Table A.3 - continued

Year	Ratios	Target	No Tile		10 Meter		15 Meter		20 Meters		25 Meters		30 Meters	
			Ratio Value	Δ%	Ratio Value	Δ%	Ratio Value	Δ%	Ratio Value	Δ%	Ratio Value	Δ%	Ratio Value	Δ%
5	Q/P	0.25	0.36	7.3%	0.36	0.8%	0.36	0.9%	0.36	1.1%	0.36	1.2%	0.36	1.2%
	ET/P	0.75	0.65	0.1%	0.65	0.1%	0.65	0.1%	0.65	0.0%	0.65	0.1%	0.65	0.1%
	E/ET	0.30	0.29	0.5%	0.29	-0.1%	0.29	0.2%	0.29	0.2%	0.30	0.5%	0.30	0.1%
	T/ET	0.70	0.71	-0.1%	0.71	0.2%	0.71	0.1%	0.71	0.0%	0.70	-0.1%	0.70	0.1%
	Q <sub>b</sub> /Q	0.55	0.30	7.3%	0.68	0.9%	0.60	1.1%	0.54	1.2%	0.51	1.3%	0.48	1.3%
	Q/Q <sub>r</sub> (Spillville)	1.00	1.27		1.27		1.26		1.26		1.26		1.26	
	Q/Q <sub>r</sub> (Otter Creek)	1.00	1.21		1.21		1.21		1.21		1.21		1.21	
6	Q/P	0.25	0.36	0.6%	0.36	0.3%	0.36	0.4%	0.36	0.3%	0.36	0.4%	0.36	0.4%
	ET/P	0.75	0.65	0.0%	0.65	0.1%	0.65	0.0%	0.65	0.1%	0.65	0.1%	0.65	0.0%
	E/ET	0.30	0.29	0.1%	0.29	0.2%	0.29	-0.2%	0.29	-0.3%	0.29	0.1%	0.29	-0.2%
	T/ET	0.70	0.71	0.0%	0.71	0.0%	0.71	0.1%	0.71	0.2%	0.71	0.2%	0.71	0.1%
	Q <sub>b</sub> /Q	0.55	0.30	0.6%	0.68	0.3%	0.60	0.4%	0.55	0.4%	0.51	0.5%	0.48	0.5%
	Q/Q <sub>r</sub> (Spillville)	1.00	1.27		1.28		1.28		1.27		1.27		1.27	
	Q/Q <sub>r</sub> (Otter Creek)	1.00	1.22		1.21		1.21		1.21		1.21		1.21	

Table A.4: The calibration ratios and volumetric changes for the two rill storage heights tested. Six years of simulations were performed and both simulations reached a pseudo steady state in year 6.

Year	Ratios	Target	0.002 Meter Rill Storage		0.02 Meter Rill Storage		
			Ratio Value	Percent Change	Ratio Value	Percent Change	
1	Q/P	0.25	0.14		The 0.02 meter rill storage simulations were run from the end of the second year of the 0.002 meter rill storage simulations.		
	ET/P	0.75	0.60				
	E/ET	0.30	0.27				
	T/ET	0.70	0.73				
	Q <sub>b</sub> /Q	0.55	0.41				
	Q/Q <sub>r</sub> (Spillville)	1.00	0.49				
	Q/Q <sub>r</sub> (Otter Creek)	1.00	0.50				
2	Q/P	0.25	0.26	90.3%			
	ET/P	0.75	0.64	7.8%			
	E/ET	0.30	0.29	14.4%			
	T/ET	0.70	0.71	5.3%			
	Q <sub>b</sub> /Q	0.55	0.34	58.3%			
	Q/Q <sub>r</sub> (Spillville)	1.00	0.94				
	Q/Q <sub>r</sub> (Otter Creek)	1.00	0.90				
3	Q/P	0.25	0.33	27.3%	0.32		
	ET/P	0.75	0.65	0.7%	0.65		
	E/ET	0.30	0.29	2.1%	0.30		
	T/ET	0.70	0.71	0.2%	0.70		
	Q <sub>b</sub> /Q	0.55	0.30	13.8%	0.27		
	Q/Q <sub>r</sub> (Spillville)	1.00	1.19		1.15		
	Q/Q <sub>r</sub> (Otter Creek)	1.00	1.14		1.12		
4	Q/P	0.25	0.33	-0.9%	0.35	8.5%	
	ET/P	0.75	0.65	0.1%	0.65	0.3%	
	E/ET	0.30	0.29	-0.1%	0.30	0.9%	
	T/ET	0.70	0.71	0.2%	0.70	0.0%	
	Q <sub>b</sub> /Q	0.55	0.30	-2.9%	0.26	7.2%	
	Q/Q <sub>r</sub> (Spillville)	1.00	1.18		1.25		
	Q/Q <sub>r</sub> (Otter Creek)	1.00	1.16		1.20		

Table A.4 - continued

Year	Ratios	Target	0.002 Meter Rill Storage		0.02 Meter Rill Storage	
			Ratio Value	Percent Change	Ratio Value	Percent Change
5	Q/P	0.25	0.36	7.3%	0.36	1.6%
	ET/P	0.75	0.65	0.1%	0.65	0.1%
	E/ET	0.30	0.29	0.5%	0.31	0.3%
	T/ET	0.70	0.71	-0.1%	0.69	0.0%
	Q <sub>b</sub> /Q	0.55	0.30	7.3%	0.26	1.2%
	Q/Q <sub>r</sub> (Spillville)	1.00	1.27		1.27	
	Q/Q <sub>r</sub> (Otter Creek)	1.00	1.21		1.21	
6	Q/P	0.25	0.36	0.6%	0.36	0.6%
	ET/P	0.75	0.65	0.0%	0.65	0.0%
	E/ET	0.30	0.29	0.1%	0.31	0.2%
	T/ET	0.70	0.71	0.0%	0.69	0.0%
	Q <sub>b</sub> /Q	0.55	0.30	0.6%	0.26	0.6%
	Q/Q <sub>r</sub> (Spillville)	1.00	1.27		1.28	
	Q/Q <sub>r</sub> (Otter Creek)	1.00	1.22		1.22	

## APPENDIX B: LEAF AREA INDEX TIME SERIES

Table B.1: LAI for agricultural areas in the URC model. These LAI values are adapted from Kim et al. (2012).

<b>Time (seconds)</b>	<b>LAI</b>
0	0
13132800	0
13478400	0.2
13910400	0.4
14342400	0.7
14774400	1.2
15206400	1.8
15638400	2
16070400	2.5
16502400	2.9
16934400	2.9
17366400	2.9
17884800	2.9
18316800	2.8
18748800	2.7
19180800	2.7
19612800	2.4
20044800	2
20476800	1.7
20908800	1.4
21340800	1
21772800	0.7
22204800	0.3
22723200	0
31536000	0

Table B.2: LAI for grassy areas in the URC model. These LAI values are adapted from Asner et al. (2003).

<b>Time (seconds)</b>	<b>LAI</b>
0	1
12096000	1
12960000	1.2
13824000	2
14688000	2.5
15552000	3.5
16416000	3.5
23328000	2.5
25920000	1
31536000	1

Table B.3: LAI for forested areas in the URC model. These LAI values are adapted from Breuer et al. (2003).

<b>Time (seconds)</b>	<b>LAI</b>
0	1
2628000	1
5256000	1
7884000	2
10512000	3
13140000	4
15768000	4.5
18396000	4.5
21024000	3.5
23652000	3
26280000	1.25
28908000	1
31536000	1

## APPENDIX C: ADDITIONAL SCENARIO FIGURES

The figures in this appendix supplement those shown in Chapter 6. They show the results of the scenarios which did not produce the greatest nitrate load reduction in each of their respective scenario groups.

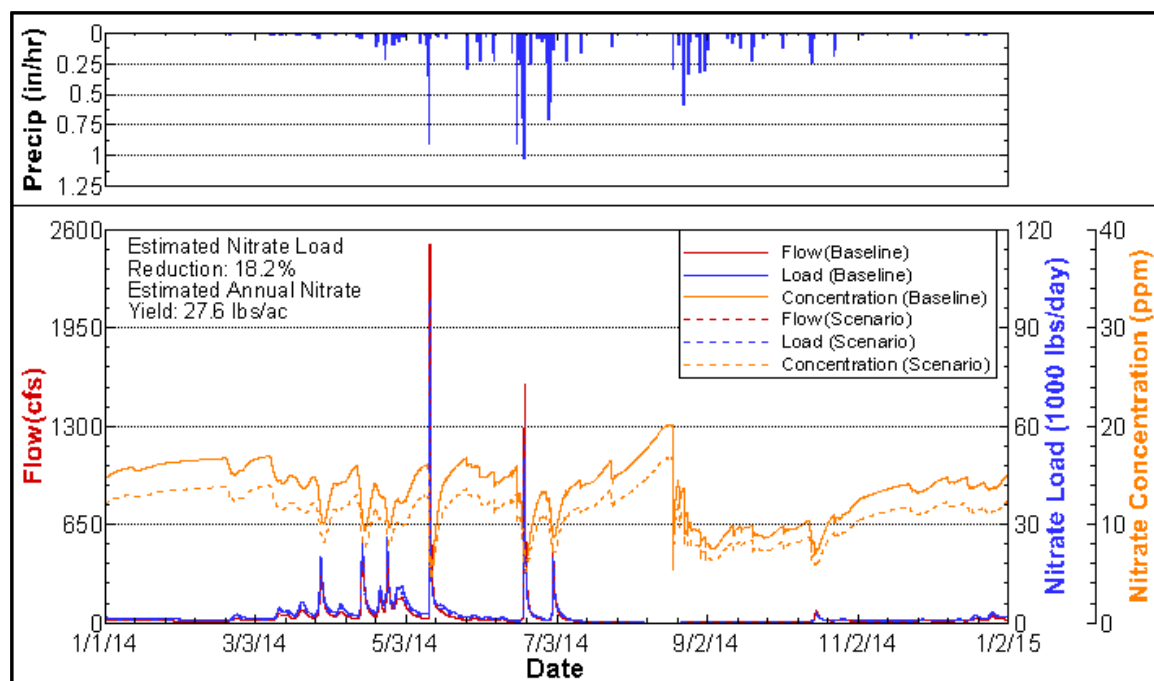


Figure C.1: Annual simulation results for scenario with cover crops and 20% reduction in tile nitrate concentration.

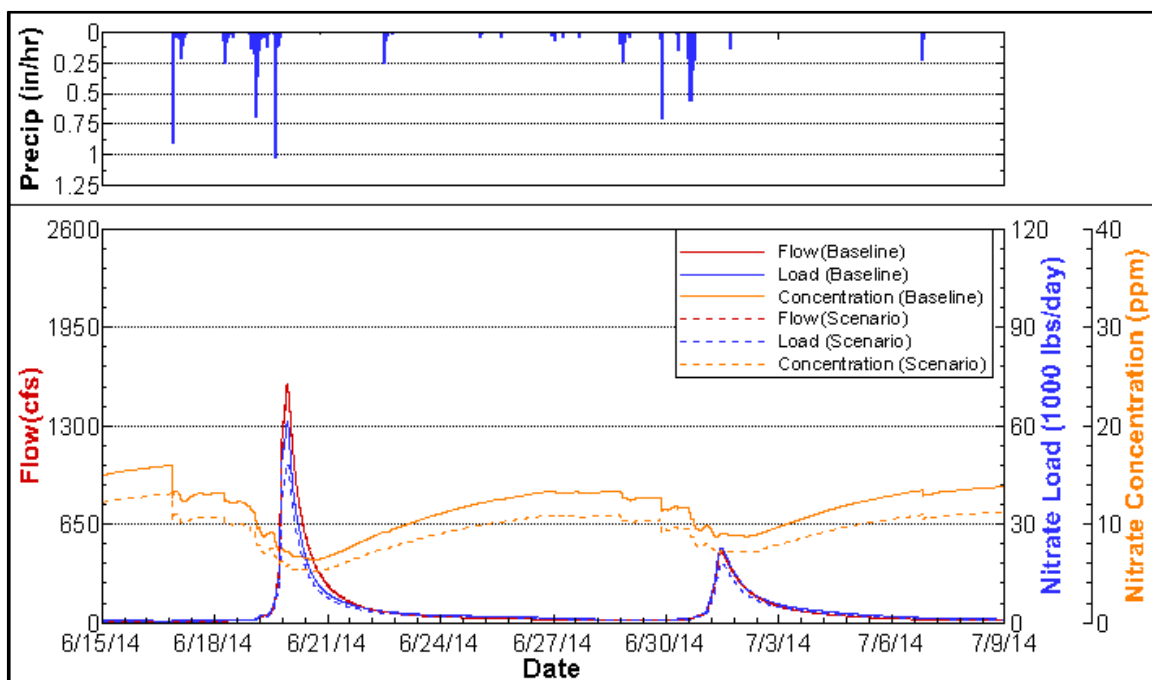


Figure C.2: Simulation results from June 15 to July 9 for scenario with cover crops and 20% reduction in tile nitrate concentration.

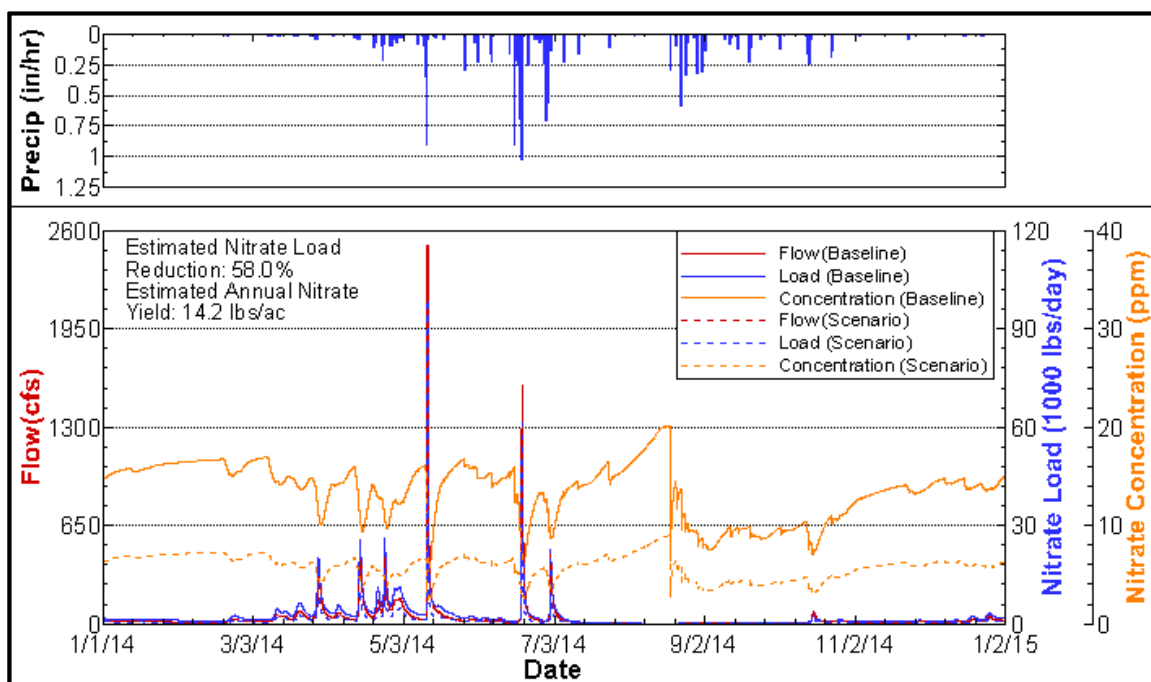


Figure C.3: Annual simulation results for scenario with cover crops and 60% reduction in tile nitrate concentration.



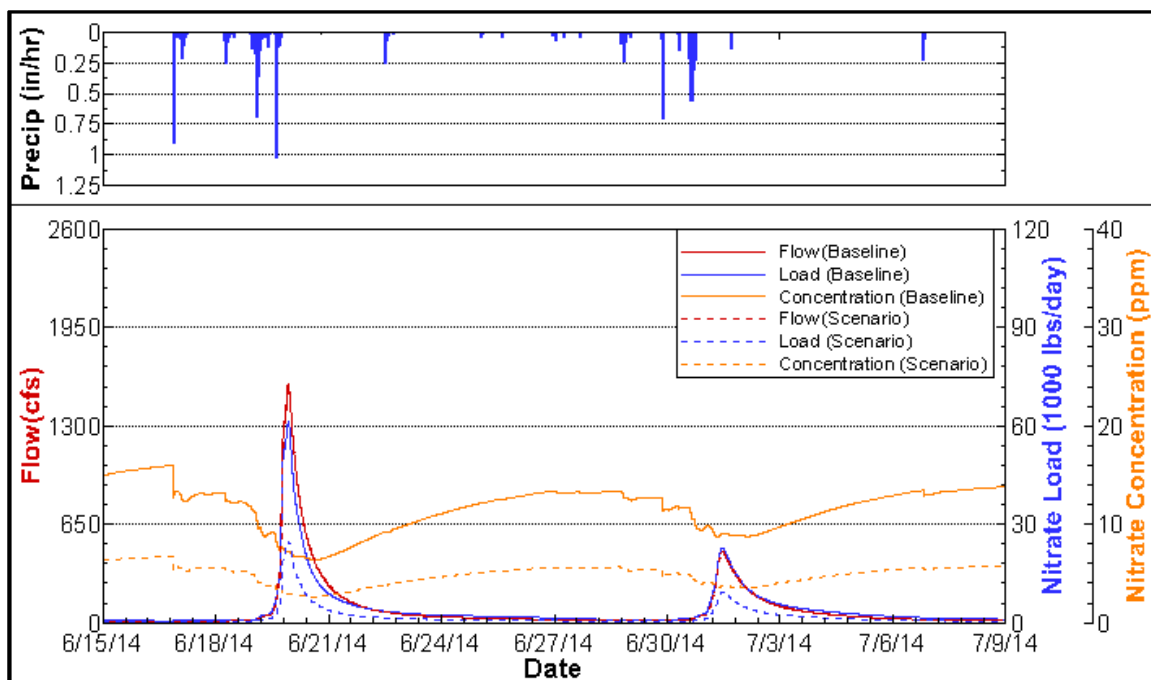


Figure C.4: Simulation results from June 15 to July 9 for scenario with cover crops and 60% reduction in tile nitrate concentration.

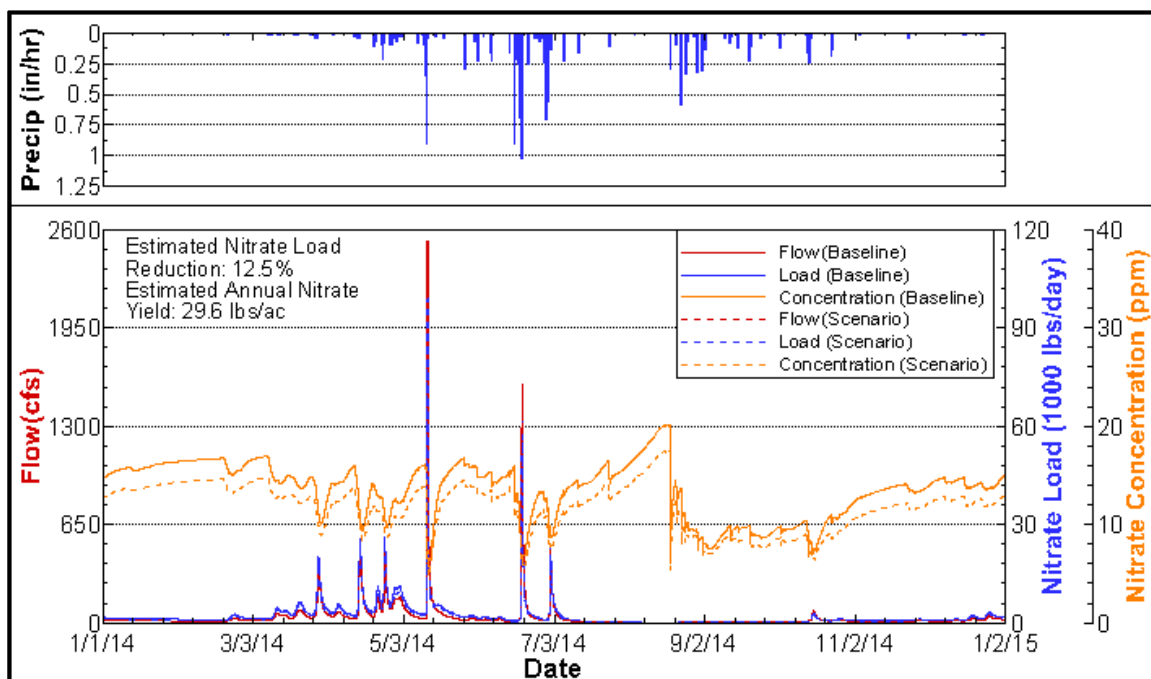


Figure C.5: Annual simulation results for scenario with 1 meter wetland weir and a surface area equal to 0.5% of the wetland drainage area.

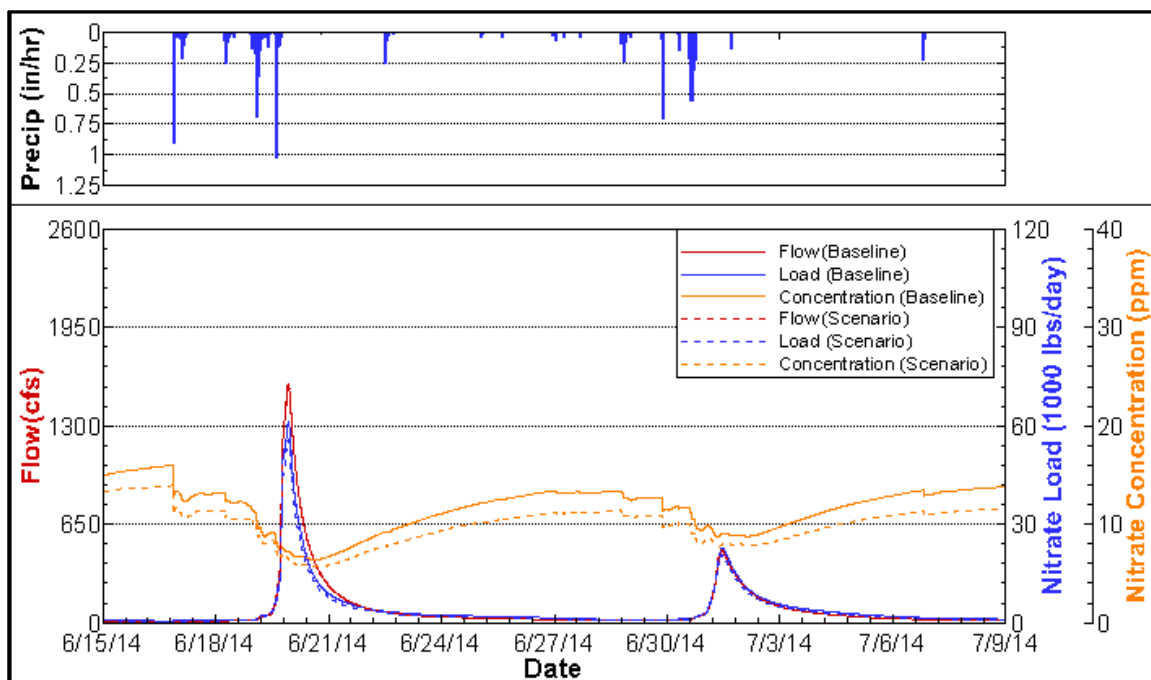


Figure C.6: Simulation results from June 15 to July 9 for scenario with 1 meter wetland weir and a surface area equal to 0.5% of the wetland drainage area.

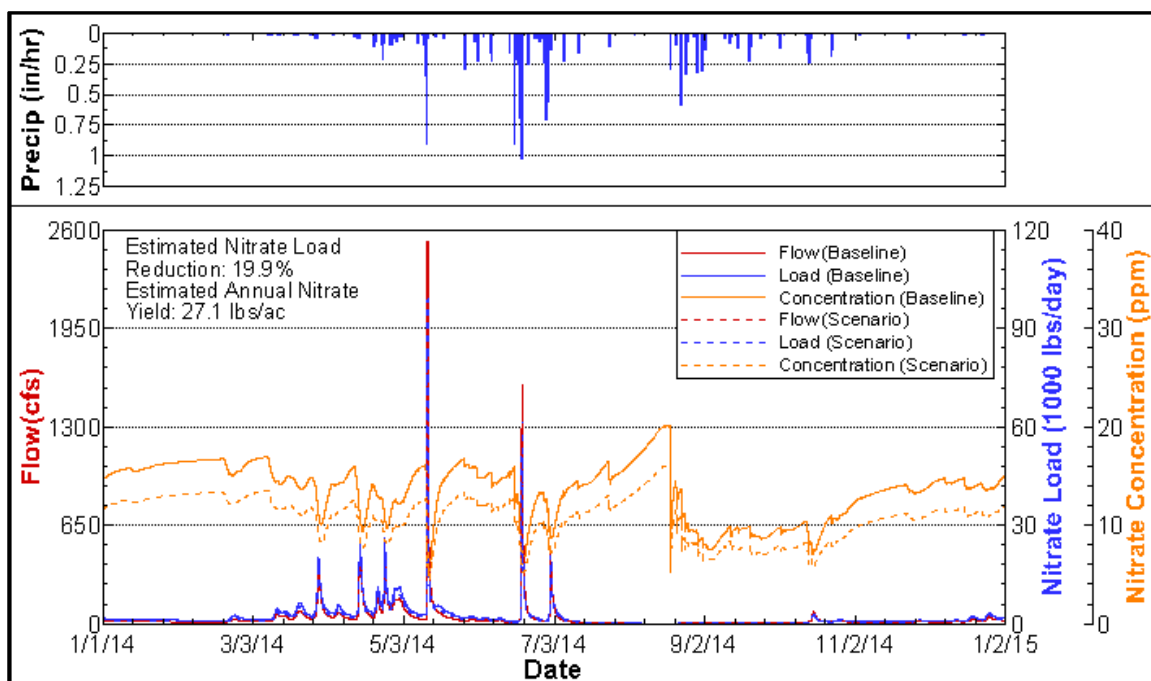


Figure C.7: Annual simulation results for scenario with 1 meter wetland weir and a surface area equal to 2.0% of the wetland drainage area.

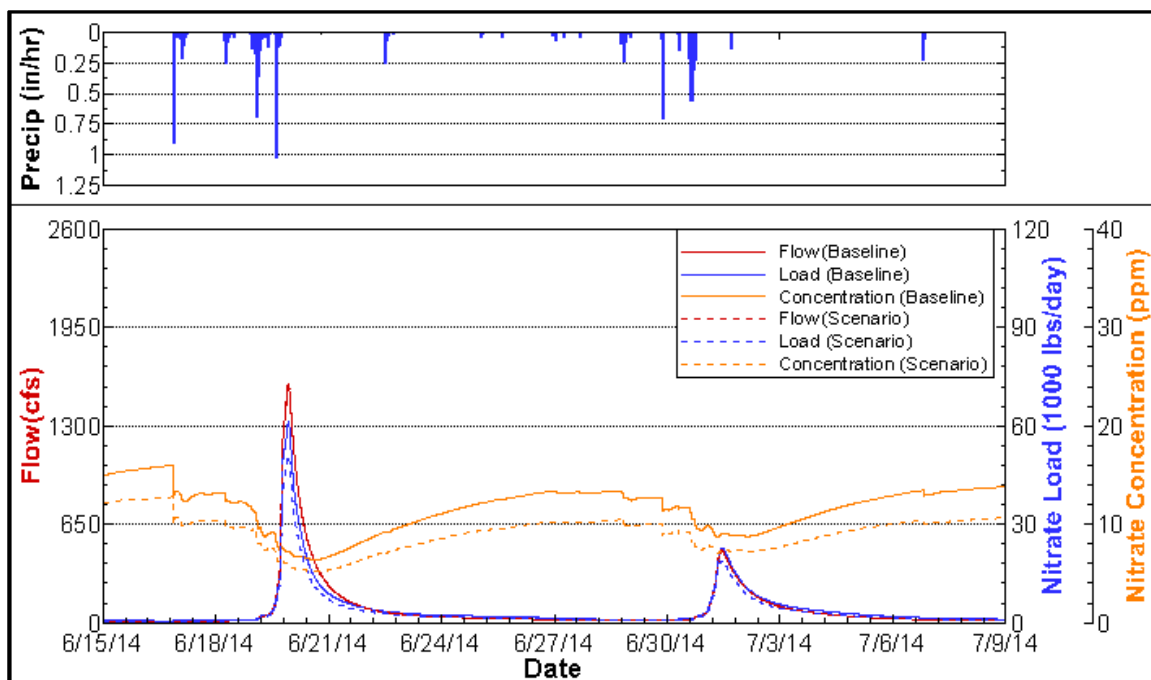


Figure C.8: Simulation results from June 15 to July 9 for scenario with 1 meter wetland weir and a surface area equal to 2.0% of the wetland drainage area.

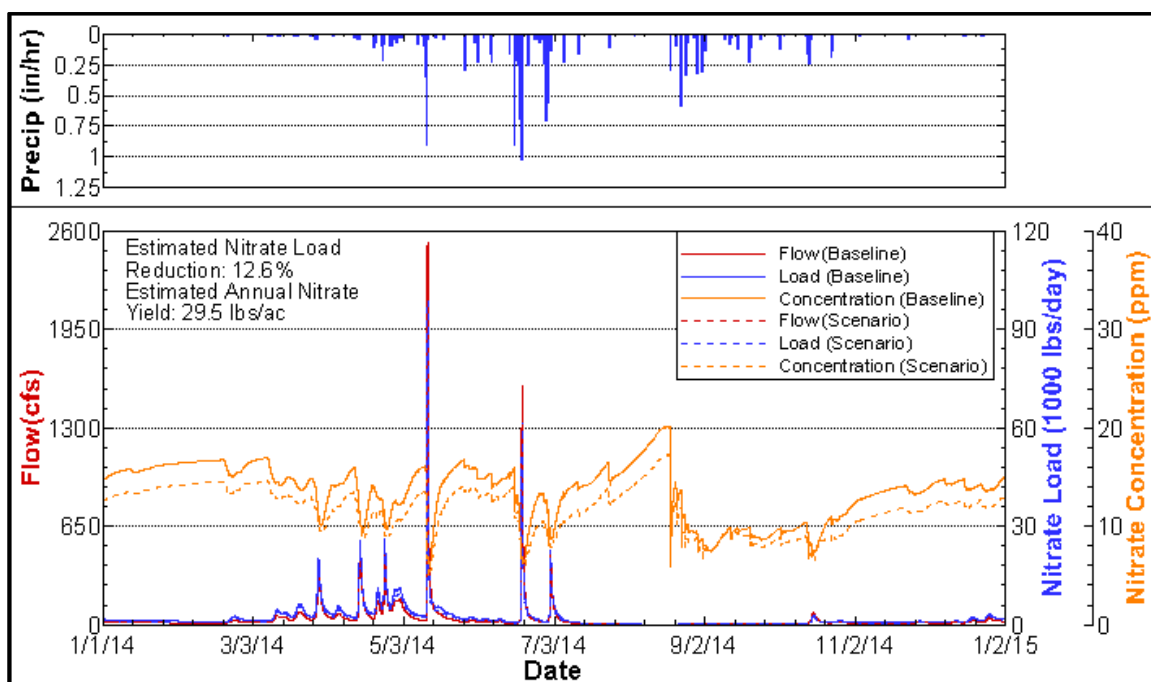


Figure C.9: Annual simulation results for scenario with 2 meter wetland weir and a surface area equal to 0.5% of the wetland drainage area.

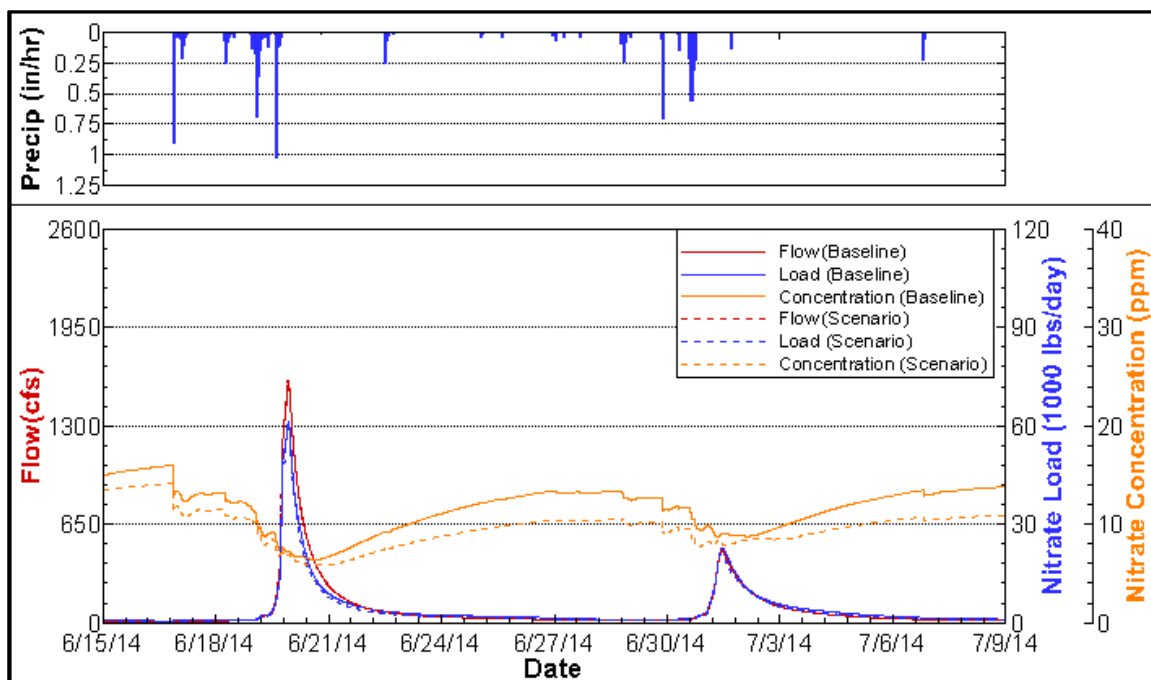


Figure C.10: Simulation results from June 15 to July 9 for scenario with 2 meter wetland weir and a surface area equal to 0.5% of the wetland drainage area.

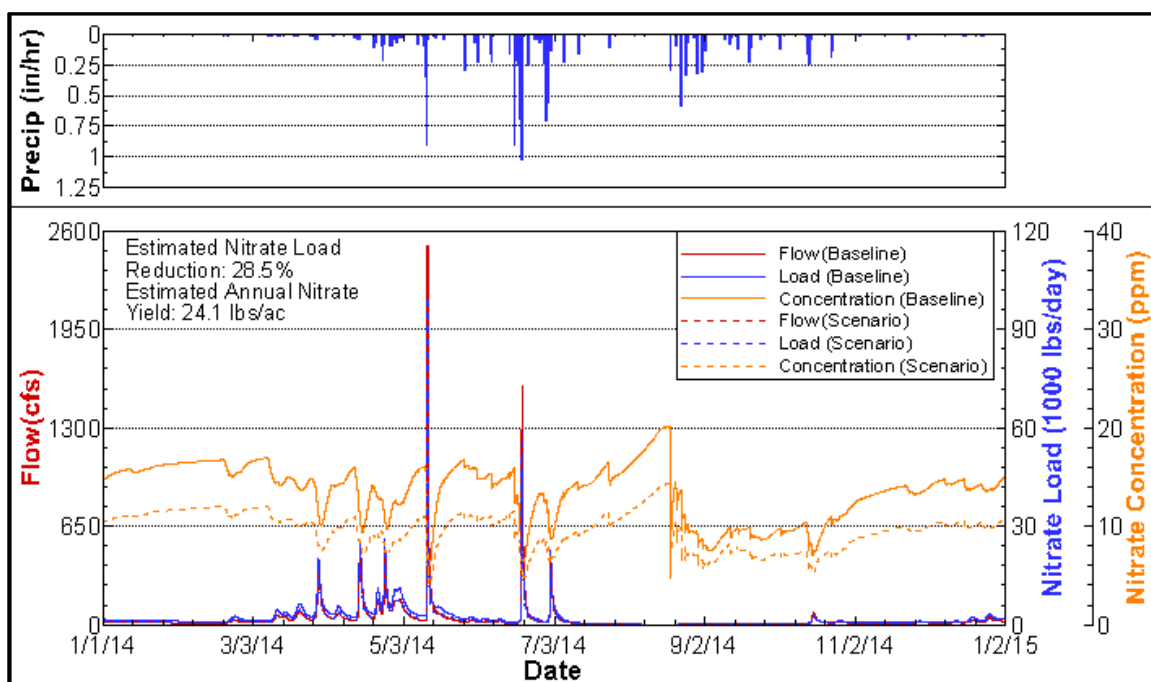


Figure C.11: Annual simulation results for scenario with cover crops, 20% reduction in tile layer nitrate concentration, and a wetland surface area equal to 0.5% of the wetland drainage area.

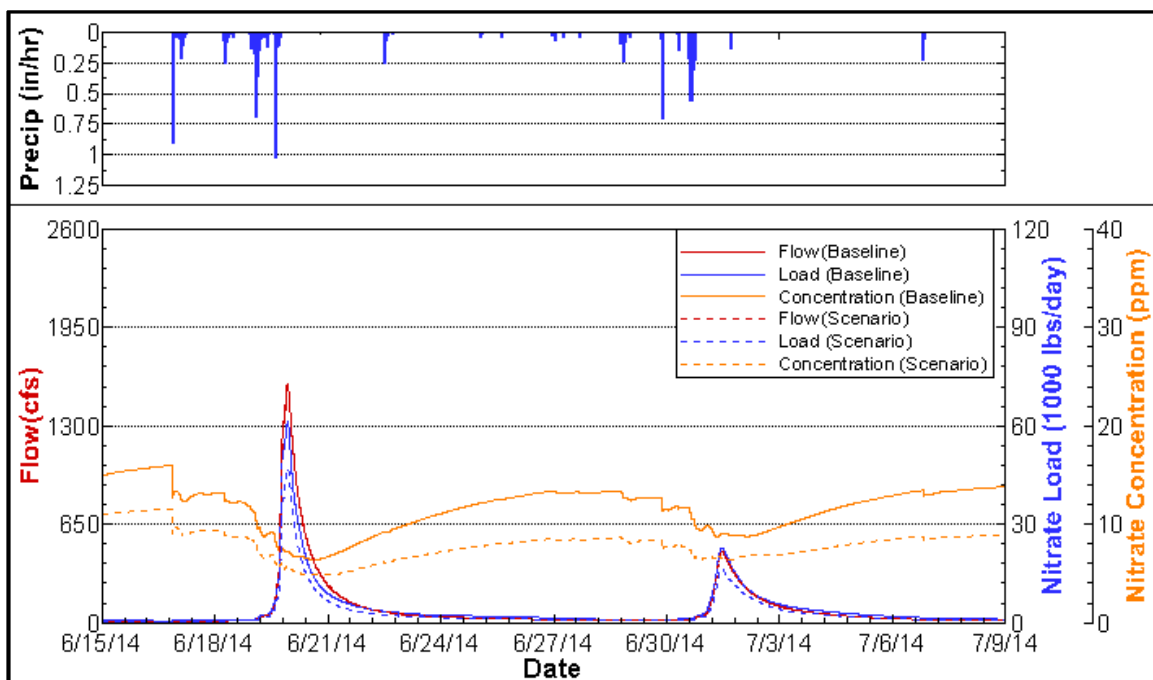


Figure C.12: Simulation results from June 15 to July 9 for scenario with cover crops, 20% reduction in tile layer nitrate concentration, and a wetland surface area equal to 0.5% of the wetland drainage area.

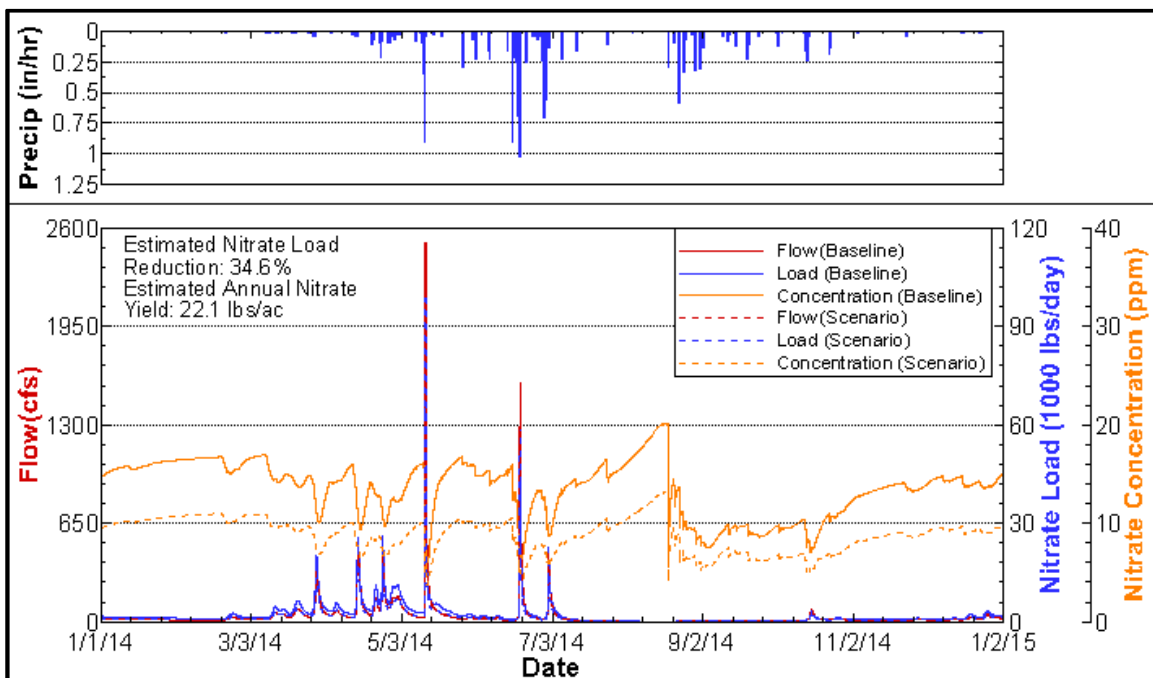


Figure C.13: Annual simulation results for scenario with cover crops, 20% reduction in tile layer nitrate concentration, and a wetland surface area equal to 2.0% of the wetland drainage area.

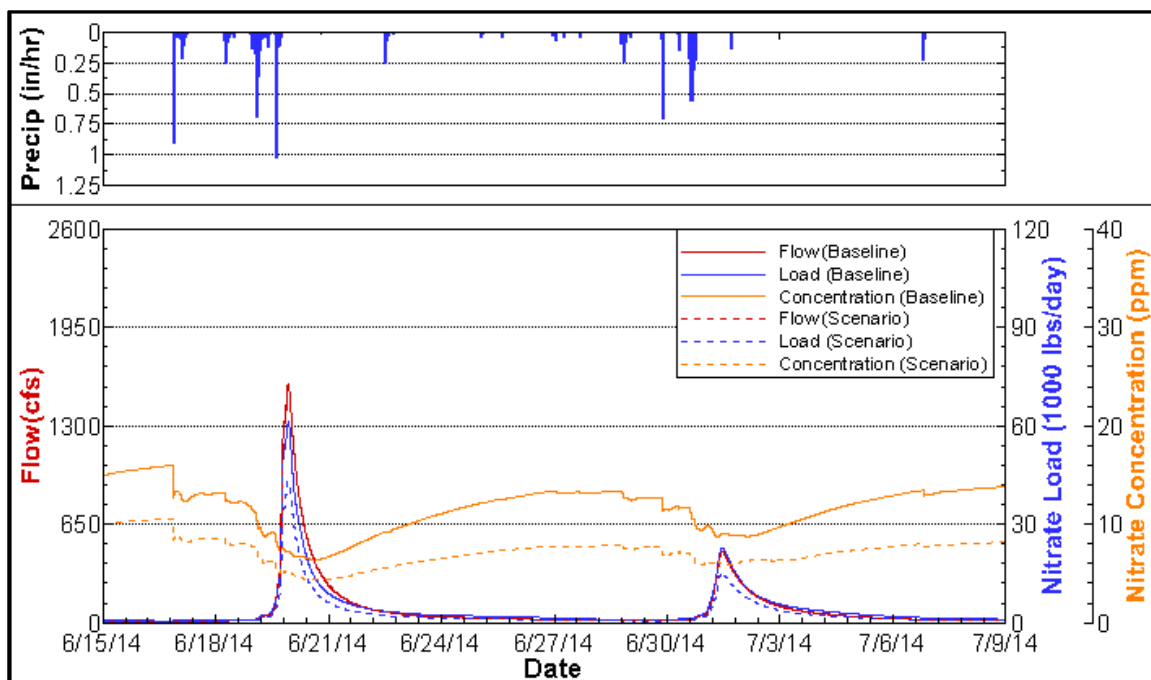


Figure C.14: Simulation results from June 15 to July 9 for scenario with cover crops, 20% reduction in tile layer nitrate concentration, and a wetland surface area equal to 2.0% of the wetland drainage area.

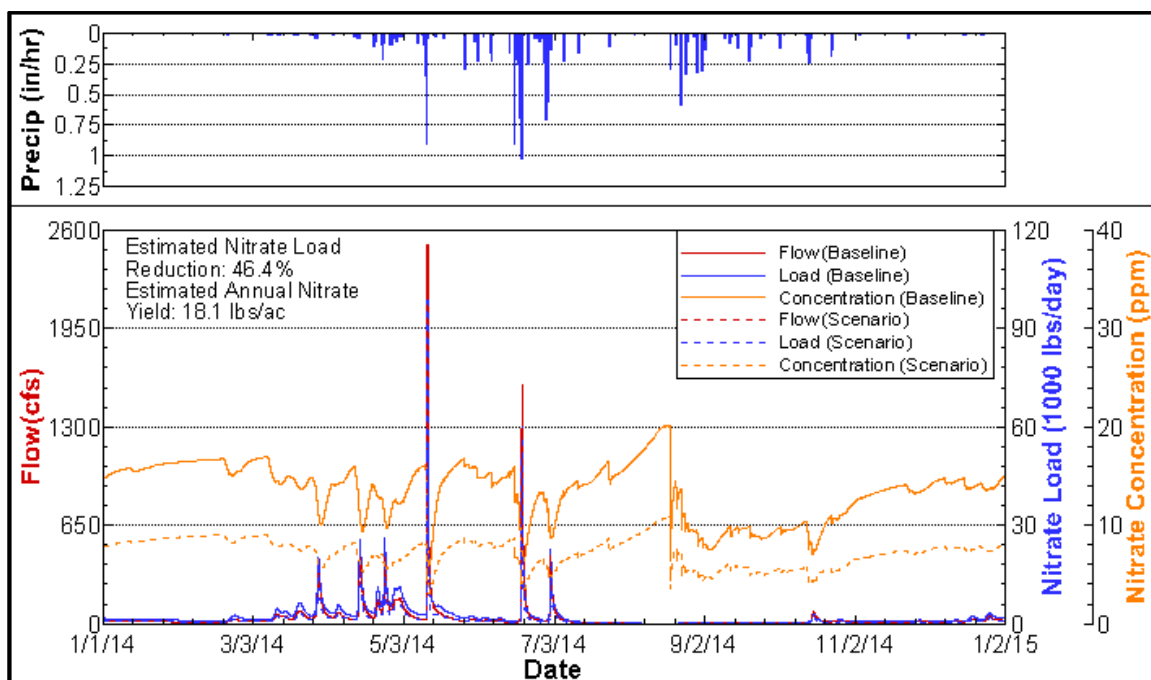


Figure C.15: Annual simulation results for scenario with cover crops, 40% reduction in tile layer nitrate concentration, and a wetland surface area equal to 0.5% of the wetland drainage area.

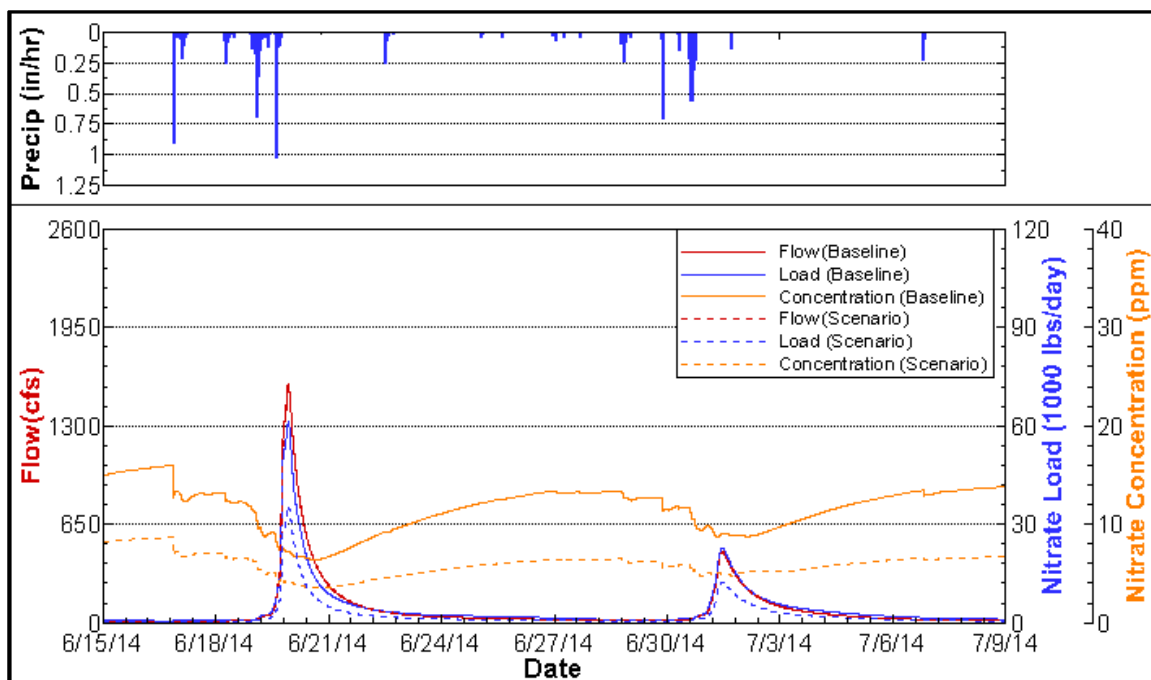


Figure C.16: Simulation results from June 15 to July 9 for scenario with cover crops, 40% reduction in tile layer nitrate concentration, and a wetland surface area equal to 0.5% of the wetland drainage area.

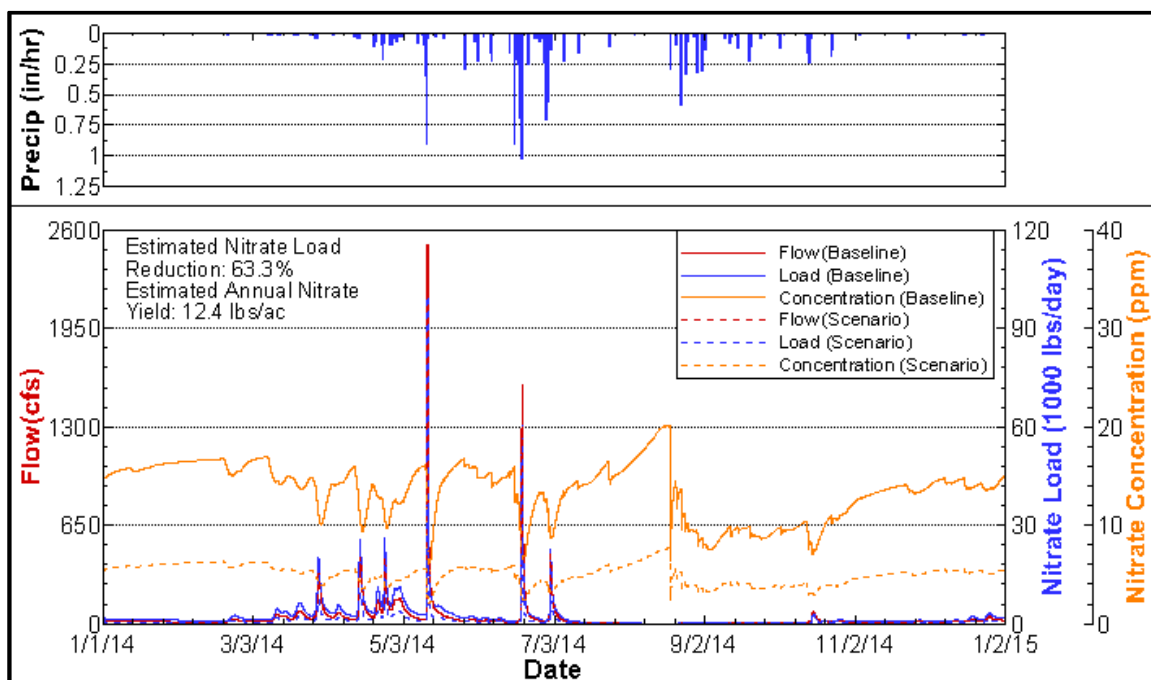


Figure C.17: Annual simulation results for scenario with cover crops, 60% reduction in tile layer nitrate concentration, and a wetland surface area equal to 0.5% of the wetland drainage area.

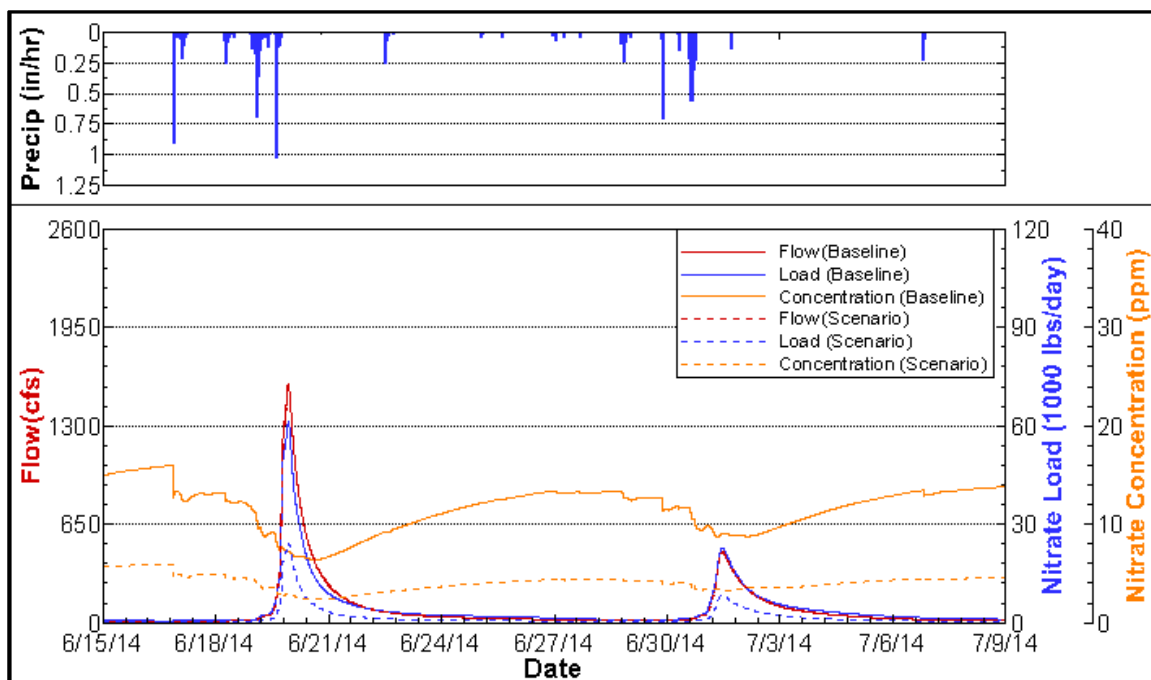


Figure C.18: Simulation results from June 15 to July 9 for scenario with cover crops, 60% reduction in tile layer nitrate concentration, and a wetland surface area equal to 0.5% of the wetland drainage area.

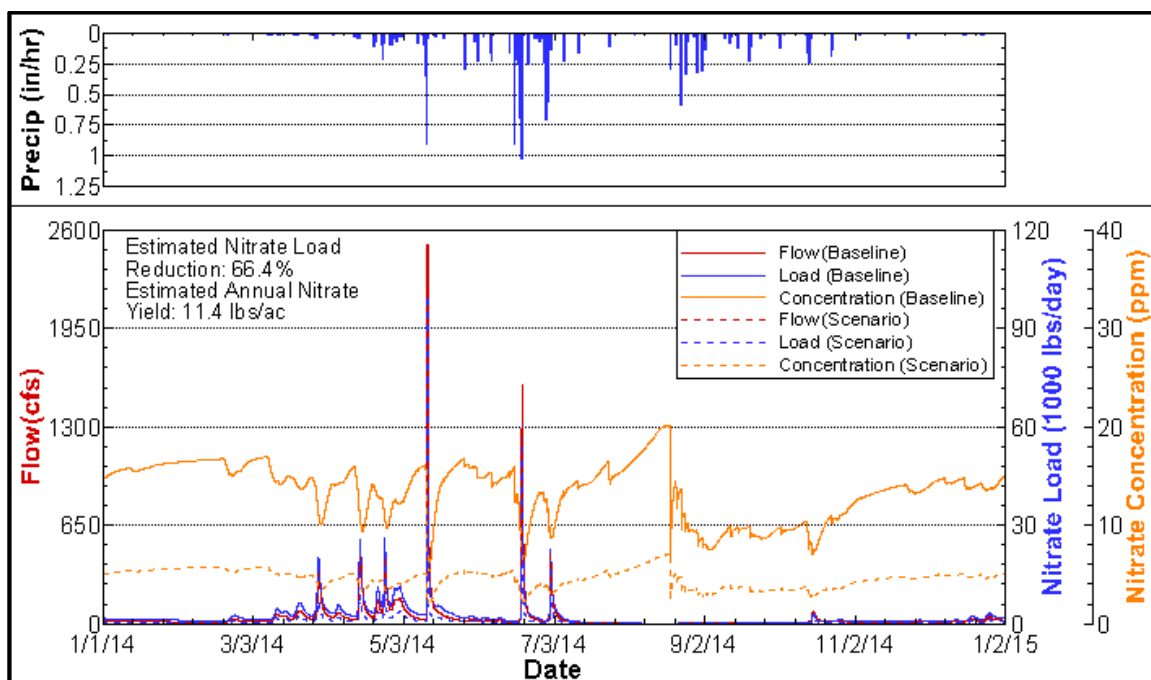


Figure C.19: Annual simulation results for scenario with cover crops, 60% reduction in tile layer nitrate concentration, and a wetland surface area equal to 2.0% of the wetland drainage area.



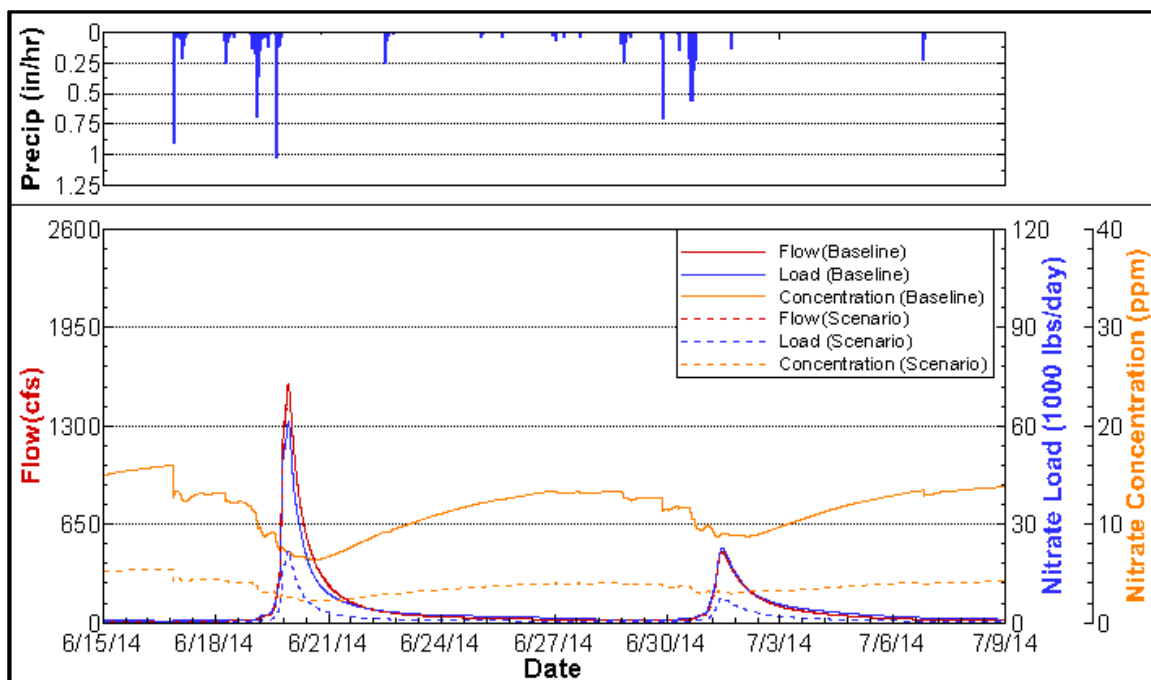


Figure C.20: Simulation results from June 15 to July 9 for scenario with cover crops, 60% reduction in tile layer nitrate concentration, and a wetland surface area equal to 2.0% of the wetland drainage area.

## REFERENCES

- Abbott, M. B., Bathurst, J. C., Cunge, J. A., Oconnell, P. E., and Rasmussen, J. (1986). "An Introduction to the European Hydrological System - Systeme Hydrologique Europeen, She .1. History and Philosophy of a Physically-Based, Distributed Modeling System." *J Hydrol*, 87(1-2), 45-59.
- Abdul, A. S. (1985). "Experimental and numerical studies of the effect of the capillary fringe on streamflow generation." Ph.D., University of Waterloo, Waterloo, Ontario, Canada.
- Ajami, H., McCabe, M. F., and Evans, J. P. (2015). "Impacts of model initialization on an integrated surface water-groundwater model." *Hydrol Process*, 29(17), 3790-3801.
- Aquanty Inc. (2013). "HydroGeoSphere User Manual." Waterloo, Ontario, 439.
- Asner, G. P., Scurlock, J. M. O., and Hicke, J. A. (2003). "Global synthesis of leaf area index observations: implications for ecological and remote sensing studies." *Global Ecol Biogeogr*, 12(3), 191-205.
- Babbar-Sebens, M., Barr, R. C., Tedesco, L. P., and Anderson, M. (2013). "Spatial identification and optimization of upland wetlands in agricultural watersheds." *Ecol Eng*, 52, 130-142.
- Babcock, B. A., and Kling, C. L. (2008). "Costs and Benefits of Fixing Gulf Hypoxia." *Iowa Ag Review*, Iowa State University Center for Agriculture and Rural Development, Ames, IA.
- Bradley, A. A., Jr., Ashok, K., Leach, N., and Tokuhisa, R. (2015). "Hydrologic modeling of the English River Watershed." IIHR - Hydroscience & Engineering, Iowa City, IA.
- Breuer, L., Eckhardt, K., and Frede, H. G. (2003). "Plant parameter values for models in temperate climates." *Ecol Model*, 169(2-3), 237-293.
- Brookfield, A., and Wilson, B. (2015). "Integrated groundwater/surface water model for the Lower Republican River basin, Kansas: A progress report." Kansas Geological Survey.
- Brunner, P., and Simmons, C. T. (2012). "HydroGeoSphere: A fully integrated, physically based hydrological model." *Ground Water*, 50(2), 170-176.
- Calder, I. R. (1993). "Hydrologic effects of land-use change." *Handbook of Hydrology*, D. R. Maidment, ed., McGraw-Hill.
- Chow, V. T. (1959). *Open-channel hydraulics*, McGraw-Hill, New York.
- Cornelissen, T., Diekkrüger, B., and Bogena, H. R. (2014). "Significance of scale and lower boundary condition in the 3D simulation of hydrological processes and soil moisture variability in a forested headwater catchment." *J Hydrol*, 516, 140-153.

- Crumpton, W. G., Stenback, G. A., Miller, B. A., and Helmers, M. J. (2006). "Potential benefits of wetland filters for tile drainage systems: Impact on nitrate loads to Mississippi River subbasins." U.S. Department of Agriculture, Ames, IA.
- Dabney, S. M. (1998). "Cover crop impacts on watershed hydrology." *J Soil Water Conserv*, 53(3), 207-213.
- De Schepper, G., Therrien, R., Refsgaard, J. C., and Hansen, A. L. (2015). "Simulating coupled surface and subsurface water flow in a tile-drained agricultural catchment." *J Hydrol*, 521(0), 374-388.
- Des Moines Water Works (2015). "High nitrate levels in Raccoon and Des Moines Rivers force Des Moines Water Works to start denitrification units." <http://www.dmww.com/about-us/news-releases/high-nitrate-levels-in-raccoon-and-des-moines-rivers-force-des-moines-water-works-to-start-denitrifi.aspx>. (May 26, 2015).
- Drake, C. W. (2014). "Assessment of flood mitigation strategies for reducing peak discharges in the Upper Cedar River watershed." M.S., The University of Iowa, Iowa City, IA.
- EPA Science Advisory Board (2007). "Hypoxia in the northern Gulf of Mexico: An update by the EPA Science Advisory Board." United States Environmental Protection Agency.
- Folorunso, O. A., Rolston, D. E., Prichard, T., and Louie, D. T. (1992). "Soil surface strength and infiltration-rate as affected by winter cover crops." *Soil Technol*, 5(3), 189-197.
- Frei, S., and Fleckenstein, J. H. (2014). "Representing effects of micro-topography on runoff generation and sub-surface flow patterns by using superficial rill/depression storage height variations." *Environmental Modelling & Software*, 52, 5-18.
- Fry, J. A., Xian, G., Jin, S., Dewitz, J. A., Homer, C. G., Yang, L., Barnes, C. A., Herold, N. D., and Wickham, J. D. (2011). "Completion of the 2006 National Land Cover Database for the conterminous United States." *PE&RS*, 77(9), 858-864.
- Garrett, J. D. (2012). "Concentrations, loads, and yields of select constituents from major tributaries of the Mississippi and Missouri Rivers in Iowa, water years 2004-2008." *Scientific Investigations Report*, U.S. Geological Survey, Reston, Virginia, 61.
- Gillham, R. W. (1984). "The Capillary-Fringe and Its Effect on Water-Table Response." *J Hydrol*, 67(1-4), 307-324.
- Goderniaux, P., Brouyere, S., Fowler, H. J., Blenkinsop, S., Therrien, R., Orban, P., and Dassargues, A. (2009). "Large scale surface-subsurface hydrological model to assess climate change impacts on groundwater reserves." *J Hydrol*, 373(1-2), 122-138.
- Hicks, M. J., and Burton, M. L. (2008). "Preliminary flood damage estimates for Iowa: Great flood of 2008." Ball State University.
- High Plains Regional Climate Center (2015). "Automated Weather Data Network." <http://www.hprcc.unl.edu/awdn.php>.

- Hoyt, W. G. (1936). *Studies of relations of rainfall and run-off in the United States*, U.S. Government Printing Office, Washington, D.C.
- IIHR - Hydroscience & Engineering/University of Iowa (2014). "HydroGeoSphere Watercycle." H. watercycle.fw, ed.
- Iovanna, R., Hyberg, S., and Crumpton, W. (2008). "Treatment wetlands: Cost-effective practice for intercepting nitrate before it reaches and adversely impacts surface waters." *J Soil Water Conserv*, 63(1), 14a-15a.
- Iowa Code § 466B.47 (2015). "Iowa nutrient research center - establishment and purpose."
- Iowa Department of Agriculture and Land Stewardship, Iowa Department of Natural Resources, and Iowa State University College of Agriculture and Life Sciences (2013). "Iowa Nutrient Reduction Strategy: A science and technology-based framework to assess and reduce nutrients to Iowa waters and the Gulf of Mexico." Iowa Department of Agriculture and Land Stewardship; Iowa Department of Natural Resources; Iowa State University College of Agriculture and Life Sciences, 26.
- Iowa Department of Natural Resources, and Iowa Geological Survey (2003-2014). "Natural resources geographic information system." IDNR - Iowa Geological Survey, Iowa City, IA.
- Iowa Environmental Council (2015). "Harmful algae blooms in Iowa lakes." <<http://www.iaenvironment.org/waterQuality/lakealgae.php>>. (7/29/2015).
- Iowa State University College of Agriculture and Life Sciences (2014). "Iowa nutrient research projects." <<https://www.cals.iastate.edu/nutrientcenter/project>>. (May 26, 2015).
- Iowa Water Quality Information System (2015). "Iowa Water Quality Information System."
- Islam, Z. (2011). "A review on physically based hydrologic modeling." University of Alberta, Edmonton, Alberta.
- Jones, J. P., Sudicky, E. A., and McLaren, R. G. (2008). "Application of a fully-integrated surface-subsurface flow model at the watershed-scale: A case study." *Water Resources Research*, 44(3), n/a-n/a.
- Kang, S., Gu, B., Du, T., and Zhang, J. (2003). "Crop coefficient and ratio of transpiration to evapotranspiration of winter wheat and maize in a semi-humid region." *Agricultural Water Management*, 59(3), 239-254.
- Keil, A., and Sutphin, T. (2014). "Watershed planning pays off in Rock Creek." *Advance*, Iowa Soybean Association Research Programs, Ankeny, IA.
- Kim, S.-H., Hong, S. Y., Sudduth, K., Kim, Y., and Lee, K. (2012). "Comparing LAI estimates of corn and soybean from vegetation indices of multi-resolution satellite images." *Korean Journal of Remote Sensing*, 28(6), 597-609.
- Kladivko, E. J., Kaspar, T. C., Jaynes, D. B., Malone, R. W., Singer, J., Morin, X. K., and Searchinger, T. (2014). "Cover crops in the upper midwestern United States: Potential

- adoption and reduction of nitrate leaching in the Mississippi River Basin." *J Soil Water Conserv*, 69(4), 279-291.
- Klingner, W. (2014). "The effects of increased infiltration and distributed storage on reducing peak discharges in an agricultural Iowa watershed: the Middle Racoon River." M.S., The University of Iowa, Iowa City, IA.
- Konrad, C. P. (2003). "Effects of urban development on floods." United States Geological Survey - Water Resources, Tacoma, WA.
- Krajewski, W. F., Lakshmi, V., Georgakakos, K. P., and Jain, S. C. (1991). "A monte-carlo study of rainfall sampling effect on a distributed catchment model." *Water Resources Research*, 27(1), 119-128.
- Kristensen, K. J., and Jensen, S. E. (1975). "A model for estimating actual evapotranspiration from potential evapotranspiration." *Nordic Hydrology*, 6(3), 170-188.
- Leavesley, G. H. (1994). "Modeling the effects of climate change on water resources - a review." *Climatic Change*, 28(1-2), 159-177.
- Li, Q., Unger, A. J. A., Sudicky, E. A., Kassenaar, D., Wexler, E. J., and Shikaze, S. (2008). "Simulating the multi-seasonal response of a large-scale watershed with a 3D physically-based hydrologic model." *J Hydrol*, 357(3-4), 317-336.
- Libra, R. D., Wolter, C. F., and Langel, R. J. (2004). "Nitrogen and phosphorus budgets for Iowa and Iowa watersheds." *Technical Information Series*, Iowa Geological Survey, 43.
- Linhart, S. M., Nania, J. F., Curtis L. Sanders, J., and Archfield, S. A. (2012). "Computing daily mean streamflow at ungaged locations in Iowa by using the Flow Anywhere and Flow Duration Curve Transfer statistical methods." *U.S. Geological Survey Scientific Investigations Report 2012-5232*, 50.
- Liu, H., Rowden, R. D., and Libra, R. D. (2000). "Groundwater and surface water monitoring in the Big Spring Basin 1996-1999: A summary review." *Technical Information Series*, Iowa Geological Survey, 121.
- Louisiana Universities Marine Consortium (2014). "Hypoxia Press Release 2014."
- Louisiana Universities Marine Consortium (2015). "Shelfwide Cruises." *Springer Ser Env Man*, <<http://www.gulfhypoxia.net/Research/Shelfwide%20Cruises/>>. (7/30/2015, 2015).
- Malone, R. W., Jaynes, D. B., Kaspar, T. C., Thorp, K. R., Kladvko, E., Ma, L., James, D. E., Singer, J., Morin, X. K., and Searchinger, T. (2014). "Cover crops in the upper midwestern United States: Simulated effect on nitrate leaching with artificial drainage." *J Soil Water Conserv*, 69(4), 292-305.
- Mattocks, C., and Forbes, C. (2008). "A real-time, event-triggered storm surge forecasting system for the state of North Carolina." *Ocean Modelling*, 25(3-4), 95-119.

- McDonald, J. E. (1961). "On the ratio of evaporation to precipitation." *Bulletin of the American Meteorological Society*, 42(3), 5.
- Melillo, J. M., Richmond, T., and Gary W. Yohe, E. (2014). "Climate change impacts in the United States: The third national climate assessment." U.S. Global Change Research Program, 841.
- Melvin, S. W., Seibel, D. C., Smith, V. H., Lucas, P. E., Frevert, W. D., and Nixon, J. R. (2008). "Iowa Drainage Guide." M. Helmers, ed., Iowa State Univeristy Extension and Outreach, Ames, Iowa, 97.
- Meselhe, E. A., Habib, E. H., and Ogden, F. L. (2004). "Performance evaluation of conceptual and physically based hyrdologic models." *24th Army Sciences Conference* Orlando Florida.
- Min, S. K., Zhang, X. B., Zwiers, F. W., and Hegerl, G. C. (2011). "Human contribution to more-intense precipitation extremes." *Nature*, 470(7334), 378-381.
- Mississippi River/Gulf of Mexico Watershed Nutrient Task Force (2008). "Gulf hypoxia action plan 2008 for reducing, mitigating, and controlling hypoxia in the northern Gulf of Mexico and improving water quality in the Mississippi River Basin." United State Environmental Protection Agency, 61.
- Mitsch, W. J., and Day, J. W. (2006). "Restoration of wetlands in the Mississippi-Ohio-Missouri (MOM) River Basin: Experience and needed research." *Ecol Eng*, 26(1), 55-69.
- Mulvany, T. J. (1850). "On the use of self-registering rain and flood gauges." *Proceedings of The Institution of Civil Engineers*, 4(2), 1-8.
- North Temperate Lakes (2015). "Agro-IBIS Model Development." <<https://lter.limnology.wisc.edu/project/agro-ibis>>.
- Penman, H. L. (1961). "Weather, plant and soil factors in hydrology." *Weather*, 16(7), 207-219.
- Perez, A. J. (2011). "Physics-based numerical modeling of groundwater flow and surface transport processes in the catchment areas." Doctor of Natural Sciences 6/24/2011, Eberhard Karls University, Tübingen, Baden-Württemberg, Germany.
- Price, K., Purucker, S. T., Kraemer, S. R., Babendreier, J. E., and Knightes, C. D. (2014). "Comparison of radar and gauge precipitation data in watershed models across varying spatial and temporal scales." *Hydrol Process*, 28(9), 3505-3520.
- Prior, J. C., and Iowa Department of Natural Resources (1991). *Landforms of Iowa*, University of Iowa Press for the Iowa Dept. of Natural Resources, Iowa City.
- PRISM Climate Group, and Oregon State University (2004). "30-yr normal precipitation: Annual (1981-2010)." <<http://www.prism.oregonstate.edu/normals/>>. (May 27, 2015).
- Refsgaard, J. C., and Knudsen, J. (1996). "Operational validation and intercomparison of different types of hydrological models." *Water Resources Research*, 32(7), 2189-2202.

- Rowden, R. D., Libra, R. D., and Hallberg, G. R. (1995). "Surface water monitoring in the Big Spring Basin 1986-1992: A summary review." *Technical Information Series*, Iowa Geological Survey, 109.
- Sanford, W. E., and Selnick, D. L. (2013). "Estimation of evapotranspiration across the conterminous United States using a regression with climate and land-cover data." *J Am Water Resour As*, 49(1), 217-230.
- Sauer, T. J., Alexander, R. B., Brahana, J. V., and Smith, R. A. (2008). "The importance and role of watersheds in the transport of nitrogen." *Nitrogen in the Environment: Sources, Problems, and Management*, J. L. Hatfield, and R. F. Follett, eds., Elsevier Inc., San Diego, CA.
- Schaap, M. G., Leij, F. J., and van Genuchten, M. T. (2001). "ROSETTA: a computer program for estimating soil hydraulic parameters with hierarchical pedotransfer functions." *J Hydrol*, 251(3-4), 163-176.
- Schilling, K. E. (2005). "Relation of baseflow to row crop intensity in Iowa." *Agriculture, Ecosystems & Environment*, 105(1-2), 433-438.
- Schilling, K. E., and Helmers, M. (2008). "Effects of subsurface drainage tiles on streamflow in Iowa agricultural watersheds: Exploratory hydrograph analysis." *Hydrol Process*, 22(23), 4497-4506.
- Schilling, K. E., Jha, M. K., Zhang, Y. K., Gassman, P. W., and Wolter, C. F. (2008). "Impact of land use and land cover change on the water balance of a large agricultural watershed: Historical effects and future directions." *Water Resources Research*, 44.
- Schilling, K. E., and Libra, R. D. (2003). "Increased baseflow in Iowa over the second half of the 20th century." *J Am Water Resour As*, 39(4), 851-860.
- Schilling, O. S., Doherty, J., Kinzelbach, W., Wang, H., Yang, P. N., and Brunner, P. (2014). "Using tree ring data as a proxy for transpiration to reduce predictive uncertainty of a model simulating groundwater-surface water-vegetation interactions." *J Hydrol*, 519, Part B, 2258-2271.
- Schlesinger, W. H., and Jasechko, S. (2014). "Transpiration in the global water cycle." *Agricultural and Forest Meteorology*, 189-190, 115-117.
- Schuermans, J. M., and Bierkens, M. F. P. (2007). "Effect of spatial distribution of daily rainfall on interior catchment response of a distributed hydrological model." *Hydrol Earth Syst Sc*, 11(2), 677-693.
- Sciuto, G., and Diekkruger, B. (2010). "Influence of soil heterogeneity and spatial discretization on catchment water balance modeling." *Vadose Zone J*, 9(4), 955-969.
- Seck, A., Welty, C., and Maxwell, R. M. (2015). "Spin-up behavior and effects of initial conditions for an integrated hydrologic model." *Water Resources Research*, 51(4), 2188-2210.
- Singer, J., Kaspar, T., and Pedersen, P. (2005). "Small grain cover crops for corn and soybean." Iowa State University Extension, Ames, Iowa.

- Singh, V. P., and Woolhiser, D. A. (2002). "Mathematical modeling of watershed hydrology." *J Hydrol Eng*, 7(4), 270-292.
- Thomas, N. (2015). "Discussions on HydroGeoSphere." K. Brauer, ed.
- United States Department of Agriculture (1986). "Urban hydrology for small watersheds (TR-55)." Natural Resources Conservation Service, Conservation Engineering Division.
- United States Geological Survey (2015). "National Water Information System data available on the World Wide Web (Water Data for the Nation)." <<http://waterdata.usgs.gov/nwis/>>. (May, 29, 2015).
- USDA (2014). "Agricultural Systems Research Unit: RZWQM." <<http://www.ars.usda.gov/Research/docs.htm?docid=17740>>.
- USDA (2014). "National Agricultural Statistics Service." <[http://www.nass.usda.gov/Statistics\\_by\\_State/Iowa/Publications/County\\_Estimates/](http://www.nass.usda.gov/Statistics_by_State/Iowa/Publications/County_Estimates/)>. (9/9/2015, 2015).
- Van Genuchten, M. T. (1980). "A closed-form equation for predicting the hydraulic conductivity of unsaturated soils." *Soil Sci Soc Am J*, 44(5), 892-898.
- Varvel, G. E., Vogel, K. P., Mitchell, R. B., Follett, R. F., and Kimble, J. M. (2008). "Comparison of corn and switchgrass on marginal soils for bioenergy." *Biomass Bioenerg*, 32(1), 18-21.
- Wang, L., Niu, S., Good, S. P., Soderberg, K., McCabe, M. F., Sherry, R. A., Luo, Y., Zhou, X., Xia, J., and Caylor, K. K. (2013). "The effect of warming on grassland evapotranspiration partitioning using laser-based isotope monitoring techniques." *Geochimica et Cosmochimica Acta*, 111, 28-38.
- Wang, Y., He, B., and Takase, K. (2009). "Effects of temporal resolution on hydrological model parameters and its impact on prediction of river discharge." *Hydrolog Sci J*, 54(5), 886-898.
- Woltemade, C. J., and Woodward, J. (2008). "Nitrate removal in a restored spring-fed wetland, Pennsylvania, USA." *J Am Water Resour As*, 44(1), 222-234.